NATIONAL TECHNICAL UNIVERSITY OF ATHENS
SCHOOL OF NAVAL ARCHITECTURE AND MARINE ENGINEERING
LABORATORY FOR SHIP AND MARINE HYDRODYNAMICS
Inter- Departmental Postgraduate Program: Marine Technology and Science

MASTER'S THESIS

«Numerical Investigation of the Wave Resistance of Catamaran Ships using Potential Solvers»

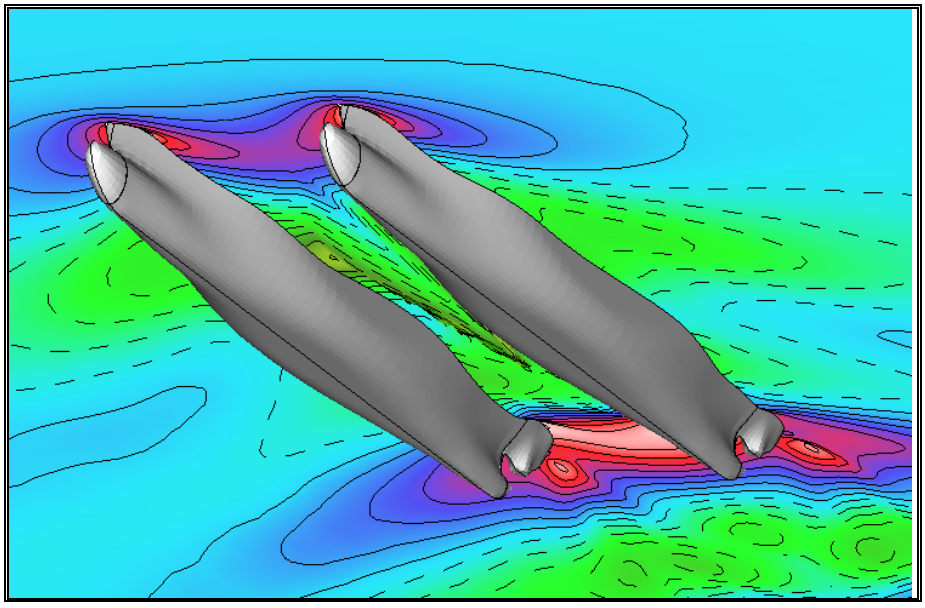

Stylianos P. Polyzos

Athens, July 2010

Supervising Professor
George Tzabiras

Examination Committee
Prof. G, Tzabiras, Prof. G. Grigoropoulos, Ass. Prof. G. Zarafonitis

ABSTRACT

Systematic numerical experiments were conducted to evaluate the use of the potential free-surface flow solver *catamaran.f*, developed at the *Laboratory of Ship and marine Hydrodynamics* of the *National Technical University of Athens* (N.T.U.A.) by *Professor George Tzabiras*, for predicting the wave resistance coefficient C_W, as well as the dynamic *sinkage*, *trim* and free-surface for a catamaran ship.

The potential solver adopts an iterative method for the calculation of the free-surface. At an intermediate iteration the free-surface is considered known and the direct potential problem is solved by implementing the kinematic boundary condition on constant source triangular or quadrilateral panels covering the submerged portion of the hull and the free-surface.

The pressure calculated on the free-surface does not satisfy the dynamic boundary condition and is introduced as a source term to calculate the correct vertical velocity on the free surface by solving the corresponding inviscid momentum equation. The above equation is numerically solved by applying the control volume method while the first order upstream difference scheme is adopted for the calculation of the convective coefficients.

Then the free surface is updated in two steps using the corrected vertical velocity. Convergence is achieved when both dynamic and kinematic boundary conditions are satisfied. By integrating the pressure on the hull, new values for sinkage and trim may be calculated. The wave resistance R_W is considered equal to the pressure resistance, since the potential theory is unable to predict any other resistance component (viscous pressure and frictional).

For the panel generation, the hull is divided into up to five regions. Each region is described by a number of 2D transverse sections which in turn are analytically described using the conformal mapping technique. The solver may model various different hull features such as bulbous bows, bulbous sterns and cruiser type or transom sterns. The transom may be modeled as “wet” or “dry”. The solver can also handle asymmetric demi-hulls.

Using the above solver, systematic numerical experiments were conducted for a total of thirteen hull shapes. Each hull was tested in two loading conditions, design and partial, in a speed range of 10-20 knots. For each test case data concerning C_W, sinkage, trim, wetted surface and wave pattern were acquired and are presented herein. The numerical results were compared with those acquired with another potential flow solver, *Shipflow*. It was concluded that sinkage, trim, wetted surface and wave pattern can be accurately predicted and that although the predictions for the wave resistance aren’t accurate enough, both solvers rank the hulls in the same order. Hence potential solvers may be used with confidence in optimizing the hull shape with respect to the wave resistance.

ACKNOWLEDGMENTS

The author would like to thank first of all, his *family and friends* for their support during this latest and all his previous undertakings.

The author can't thank enough Professor *George Tzabiras*, for providing his invaluable knowledge, experience and expertise and of course for his patience.

The author would also like to thank *Assistant Professor George Zarafonitis* as well as *Mr. Dimitris Mourkogiannis* for providing the hull shapes and the numerical results acquired by means of the Potential Solver "*Shipflow*".

Last but of course not least, the author would like to thank *Lloyd's Register Educational Trust* (*LRET*), since his Phd studies are supported by *LRET*.

The *Lloyd's Register Educational Trust* is an independent charity working to achieve advances in transportation, science, engineering and technology education, training and research worldwide for the benefit of all.

CONTENTS

1. INTRODUCTION

The flow around a ship traveling on the free water surface is described by the non-linear partial differences *Navier-Stokes* equations plus the *Continuity* equation, which cannot be solved analytically. Therefore in order to predict the flow characteristics for a ship, one must ether resort to experiments or solve the flow equations numerically. Furthermore one may choose to solve the *Navier-Stokes* equations or some simpler derivative. If the fluid is considered incompressible and inviscid then the original equations are simplified into a form of *Eulerian* equation. If fluid is also considered irrotetional then the field may be described by a *Laplace* equation for the potential φ. Then the direct problem where all boundaries are known in advance can be easily solved. The potential theory can describe a variety of flow fields, although the neglect of viscosity, vorticity and compressibility must not invalidate the results. The free-surface around a ship, poses further problems since the boundaries are not a priori known. To overcome this inherent problem, suitable techniques must be employed.

In this investigation we made use of the potential free-surface flow solver *catamaran.f*, developed at the *Laboratory of Ship and marine Hydrodynamics* by *George Tzabiras, Professor* at the *School* of *Naval Architecture and Marine Engineering* of the *National Technical University of Athens* (*N.T.U.A.*). The scope of this work was to evaluate the use of the above program for the prediction of the wave resistance coefficient C_W, as well as the dynamic *sinkage*, *trim* and free-surface for a catamaran vessel.

The above potential solver adopts an iterative method for the calculation of the free-surface. At an intermediate iteration the free-surface is considered known and the *direct potential problem* is solved by implementing the *kinematic* boundary condition on constant source triangular or quadrilateral panels covering the submerged portion of the hull and the free-surface.

The pressure calculated on the free-surface does not satisfy the *dynamic* boundary condition and is introduced as a source term to calculate the correct vertical velocity u_Z* on the free surface, by solving the corresponding inviscid momentum equation. The above equation is solved by applying the control volume method while the first order upstream difference scheme is adopted for the calculation of the convective coefficients. Then the free surface is updated in two steps using the corrected vertical velocity u_Z*. Convergence is achieved when both dynamic and kinematic boundary conditions are satisfied.

By integrating the pressure on the hull, new values for sinkage and trim may be calculated. The wave resistance R_W is considered equal to the pressure resistance, since the potential theory is unable to predict any other resistance component.

For the panel generation, the hull is divided into up to five regions. Each region is described by a number of 2D transverse sections, which in turn are analytically described using the conformal mapping technique. The solver may model various different hull features such as bulbous bows, bulbous sterns and cruiser type or transom sterns. The transom may be modeled as “wet” or “dry”. The solver can also handle asymmetric demi-hulls.

Using the above solver, systematic numerical experiments were conducted for a total of thirteen hull shapes. Each hull was tested in two loading conditions, design and partial, in a speed range of 10-20 knots. For each test case data concerning C_W, sinkage, trim, wetted surface and wave pattern were acquired and are presented herein. The program proved very stable and capable of predicting the flow characteristics for a variety of hull shapes.

The numerical results were compared with those acquired with another potential flow solver, *Shiplow*. The comparison between the two programs showed that although the results differed substantially, they were in good qualitative agreement. It was concluded that sinkage, trim and wetted surface can be accurately predicted even when using relatively coarse discretization. Furthermore the prediction of the wave patterns is accurate except near and abaft the stern, were viscous effects are dominant. Finally, although the predictions for the wave resistance are not accurate enough due mainly to the viscous effects at the stern of the ship, potential solvers may be used with confidence in optimizing the hull shape with respect to the wave resistance since both programs rank the hulls in the same order.

2. NUMERICAL METHOD

The numerical method adopted in this investigation, aims at predicting the pattern of the free surface about a catamaran ship as well as the wave component of the ship's resistance. The method is realized by means of the computer program *catamaran.f* written in *Fortran* and developed at the *Laboratory of Ship and marine Hydrodynamics* by *Professor George Tzabiras*. The flow field is considered potential and incompressible. The potential solver is based on the formulation of Hess & Smith (1966), while an iterative procedure, developed in-house, is adopted in order to calculate the exact shape of the free surface (Tzabiras, 2008).

Two Cartesian coordinates' systems are introduced, i.e. the ship reference system which is employed to construct the panels using the conformal mapping representation (see 2.4), having z=0 on the height of the deck and the absolute system on the undisturbed free surface where all the flow equations refer to (Fig. 2.1).

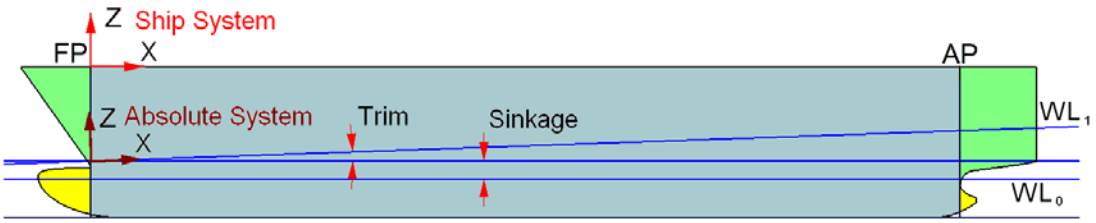

Figure 2.1 Definition of the ship reference and the absolute coordinates' system.

2.1 The Potential Solver

2.1.1 *The Potential Flow and its Applications*

In this investigation, the fluid is considered incompressible, inviscid and irrotational. Let $\boldsymbol{U}$ denote the fluid velocity at any point, p the fluid pressure, ρ the fluid density, μ the dynamic and ν the kinematic viscosity. In the following, symbols in bold denote vectors. For an incompressible and inviscid fluid ρ is constant and $\mu = \nu = 0$, hence the general *Navier-Stokes* equations (2.1.1) reduce to the *Eulerian* equation of motion (2.1.2).

$$\left.\begin{aligned}\frac{\partial \rho u_x}{\partial t}+\operatorname{div}(\rho u_x \boldsymbol{U}) &= -\frac{\partial p}{\partial x}+\operatorname{div}(\mu\ \operatorname{grad} u_x)+S_{M_x}\\ \frac{\partial \rho u_y}{\partial t}+\operatorname{div}(\rho u_y \boldsymbol{U}) &= -\frac{\partial p}{\partial y}+\operatorname{div}(\mu\ \operatorname{grad} u_y)+S_{M_y}\\ \frac{\partial \rho u_z}{\partial t}+\operatorname{div}(\rho u_z \boldsymbol{U}) &= -\frac{\partial p}{\partial z}+\operatorname{div}(\mu\ \operatorname{grad} u_z)+S_{M_z}\end{aligned}\right\} \tag{2.1.1}$$

$$\left.\begin{aligned}\frac{\partial u_x}{\partial t}+\operatorname{div}(u_x \boldsymbol{U}) &= -\frac{1}{\rho}\frac{\partial p}{\partial x}\\ \frac{\partial u_y}{\partial t}+\operatorname{div}(u_y \boldsymbol{U}) &= -\frac{1}{\rho}\frac{\partial p}{\partial y}\\ \frac{\partial u_z}{\partial t}+\operatorname{div}(u_z \boldsymbol{U}) &= -\frac{1}{\rho}\frac{\partial p}{\partial z}\end{aligned}\right\} \tag{2.1.2a}$$

$$\frac{\partial \boldsymbol{U}}{\partial t}+(\boldsymbol{U}\cdot\operatorname{grad})\boldsymbol{U}=-\frac{1}{\rho}\operatorname{grad} p \tag{2.1.2b}$$

The equation of continuity (2.1.3) simplifies to (2.1.4).

$$\frac{\partial \rho}{\partial t} + \mathrm{div}(\rho \boldsymbol{U}) = 0 \tag{2.1.3}$$

$$\mathrm{div}(\boldsymbol{U}) = 0 \tag{2.1.4}$$

In Equations (2.1.1) and (2.1.2) all body forces (such as gravity) have been assumed to be conservative, and their potentials have been absorbed in the pressure. Equations (2.1.2) and (2.1.4) hold in the field of flow, that is, the region exterior to the boundary surfaces, in our case, the immersed portion of the two hulls and the surrounding water surface.

In order to solve the above equations, certain boundary conditions must be added. The method adopted (Hess, 1966) can solve the direct problem of fluid dynamics. That is, the locations of all boundary surfaces are assumed known, possibly as functions of time, and the normal component of fluid velocity is prescribed on these boundaries. In our case though the boundaries are not a priori known, since neither the shape of the free surface, nor the attitude of the ship (dynamic sinkage and trim) are known in advance. In order to overcome this problem, an iterative procedure is adopted where the shape of the free surface is assumed, then the potential flow field is calculated and the free surface is updated (see 2.2) (Tzabiras, 2008).

The boundary condition will be written for the entire boundary *S* as

$$\boldsymbol{U} \cdot \boldsymbol{n}|_S = \boldsymbol{F} \tag{2.1.5}$$

where $\boldsymbol{n}$ is the unit outward normal vector at a point of *S*, and $\boldsymbol{F}=\boldsymbol{F}(\boldsymbol{x},\boldsymbol{t})$ is a known function of position on *S* and possibly also a known function of time. In our problem the boundaries at every step of the iterative procedure are considered static, hence

$$\boldsymbol{U} \cdot \boldsymbol{n}|_S = 0 \tag{2.1.6}$$

Furthermore a regularity condition at infinity must be imposed.

The above equations define an incompressible and inviscid flow, but not a potential flow. In a potential flow the velocity vector is equal to the negative gradient of a scalar potential function, the velocity potential φ.

$$\boldsymbol{U} = -\nabla \varphi \tag{2.1.7}$$

From vector calculus it is known that the curl of a gradient is equal to zero:

$$\nabla \times \nabla \varphi = 0 \tag{2.1.8}$$

Subsequently the vorticity of a potential flow field is zero:

$$\nabla \times \boldsymbol{U} = 0 \tag{2.1.9}$$

This implies that a potential flow is an irrotational flow.

Here, a slightly more general class of flows will be considered, according to the formulation of Hess (1966). The velocity field $\boldsymbol{U}$ is expressed as the sum of two velocities:

$$\boldsymbol{U} = \boldsymbol{U}_\infty + \boldsymbol{u} \tag{2.1.10}$$

The vector $\boldsymbol{U}_\infty$ is the velocity of the onset flow, which is defined as the velocity field that would exist in the fluid if all boundaries ceased to exist, here is equal to the negative of the ship's speed. The vector $\boldsymbol{u}$ is the disturbance velocity field due to the presence of boundaries. The velocity $\boldsymbol{u}$ is assumed to be irrotational, but $\boldsymbol{U}_\infty$ is not so restricted. Accordingly, $\boldsymbol{u}$ may be expressed as the negative gradient of a potential function φ, that is,

$$\boldsymbol{u} = -\mathrm{grad}\varphi \tag{2.1.11}$$

Since $\boldsymbol{U}_\infty$ is the velocity of an incompressible flow, it satisfies the continuity equation (2.1.4), and thus $\boldsymbol{u}$ does also; that is,

$$\mathrm{div}(\boldsymbol{u}) = 0 \tag{2.1.12}$$

Using $\boldsymbol{u}$ from (2.1.11) in (2.1.12) we derive to the expected result: the potential φ satisfies *Laplace* equation:

$$\nabla^2\varphi = 0 \tag{2.1.13}$$

The boundary conditions on φ arise from (2.1.6), (2.1.10) and (2.1.11) in the form:

$$\mathrm{grad}\varphi \cdot \boldsymbol{n}|_S = \left.\frac{\partial\varphi}{\partial n}\right|_S = \boldsymbol{U}_\infty \cdot \boldsymbol{n}|_S \tag{2.1.14}$$

The regularity condition at infinity is:

$$|\mathrm{grad}\varphi| \to 0 \tag{2.1.15}$$

Equations (2.1.13), (2.1.14), and (2.1.15) comprise a well-set problem for the potential φ, and it is this problem that the present method is designed to solve.

The onset flow $\boldsymbol{U}_\infty$ must be such that the disturbance velocity $\boldsymbol{u}$ is a potential flow. In our case $\boldsymbol{U}_\infty$ is also a potential flow and the above condition is obviously satisfied.

The essential simplicity of potential flow derives from the fact that the velocity field is determined by the equation of continuity (2.1.12) and the condition of irrotationality (2.1.11). Thus the equation of motion (2.1.2) is not used, and *the velocity may be determined independently of the pressure*.

Also time, *t*, enters only as a parameter in (2.1.14); therefore the instantaneous velocity is obtained from the instantaneous boundary condition; that is, *all problems are essentially steady with respect to determination of the velocity*. In our case, the equation of motion (2.1.2) can be integrated to give the *Bernoulli's* equation:

$$p - p_\infty = \frac{1}{2}\rho(|\boldsymbol{U}_\infty|^2 - |\boldsymbol{U}|^2) \tag{2.1.16}$$

(2.1.16) can be written in terms of the pressure coefficient C_P as

$$C_p = \frac{p - p_\infty}{\frac{1}{2}\rho|U|^2} = 1 - \frac{|U|^2}{|U_\infty|^2} \tag{2.1.17}$$

where p_∞ (=0) is the pressure at infinity.

The potential theory can describe a variety of flow fields, although the neglect of viscosity, vorticity and compressibility must not invalidate the results.

The neglect of viscosity is justified except in regions of rapid variations of speed, such as boundary layers and at points in or very near regions of catastrophic separation, for example wakes. In those regions, vorticity is also known to be important; hence the potential flow theory fails to provide reasonable predictions of the flow. Obviously, drag forces are never predicted correctly.

The neglect of compressibility is justified for all flows where the local Mach number does not exceed a value of approximately one-half. In the case of flow around ships, the Mach number is sufficiently low.

In our case, the aim is firstly to calculate the pattern of the free surface around catamaran ships, secondly the wave component of the ships resistance and finally the dynamic sinkage and trim. As for the free surface the potential theory is expected to provide good results except in areas were viscocity becomes very important such as the stern and wake of the ship. The wave resistance is considered to be equal to the calculated pressure resistance, since no other form of resistance (viscous pressure or frictional) can be predicted by means of the potential theory. Finally the sinakge and trim can be calculated by integrating the pressure on the hull.

2.1.2 *Numerical Formulation of the Potential Flow*

The exact solution of the direct problem of potential flow can be approached in a variety of ways, all of which must finally become numerical in order to be solved on a computing machine. The present method is based on an integral equation for a source-density distribution on the surface of the hulls and water, about which the flow is being computed.

The problem considered is that defined by (2.1.13), (2.1.14), and (2.1.15). Consider a unit point source located at a point q whose Cartesian coordinates are x_q, y_q, z_q. At a point P whose coordinates are x, y, z the potential due to this source is

$$\varphi = \frac{1}{r(P,q)} \tag{2.1.18}$$

where $r(P, q)$ is the distance between P and q, namely,

$$r(P,q) = \sqrt{(x - x_q)^2 + (y - y_q)^2 + (z - z_q)^2} \tag{2.1.19}$$

The designation “source” is employed in accordance with customary fluid dynamics usage. The potential (2.1.18) gives rise to a velocity radially outward in all directions

from the point *q*, and thus the point *q* may be thought of as the location of a "source" of fluid.

According to the present method, the solution is built up of elementary potentials of the form (2.1.18). Each potential satisfies (2.1.13) and (2.1.15) at all points except the point *q*. Because of the linearity of the problem, the potential due to any ensemble of such sources or any continuous distribution of them that lies upon the boundary surface *S* satisfies equations (2.1.13) and (2.1.15) in the region exterior to *S*.

Consider a continuous source distribution on the surface *S*. If the local intensity of the distribution is $\sigma(q)$, where the source point *q* is a general point of the surface *S*, then the potential of the distribution is

$$\varphi = \oiint_S \frac{\sigma(q)}{r(P,q)}\,dS \tag{2.1.20}$$

It is shown (Kellogg, 1929), that under very general conditions the disturbance potential of a body in potential flow can indeed be represented in the form (2.1.20).

Regardless of the nature of the function $\sigma(q)$, the disturbance potential as given by (2.1.20) satisfies two of the three equations of the direct problem of potential flow. The $\sigma(q)$ function is then determined from the requirement that the potential must also satisfy the third equation, (2.1.14), which expresses the normal-velocity boundary condition on the surface *S*.

The disturbance potential as given by (2.1.20) is differentiated, and the boundary condition (2.1.14) applied to it by allowing the point *P* to approach a point *p* on the surface *S*. The result is the following integral equation for the source-density distribution $\sigma(p)$:

$$2\pi\sigma(p) - \oiint_S \frac{\partial}{\partial n}\frac{1}{r(p,q)}\sigma(q)\,dS = \boldsymbol{n}(p)\cdot\boldsymbol{U}_\infty \tag{2.1.21}$$

In this equation, $\partial/\partial n$ denotes differentiation in the direction of the outward normal to the surface *S* at the point *p*, and the unit outward normal vector has been written $\boldsymbol{n}(p)$ to show explicitly its dependence on location. The solution of (2.1.21) is the central problem of the present method.

Equation (2.1.21) is a Fredholm integral equation of the second kind over the boundary surface *S*. The term $2\pi\sigma(p)$ arises from the delta function that is brought in by the limiting process of approaching the boundary surface. The kernel of the integral equation is the outward normal velocity at the point *p* due to a unit point source at the point *q*. This kernel depends only on the geometry of the surface *S*. The specific boundary conditions, that is, onset flow, enters (2.1.21) only on the right side.

The theory of the solution of (2.1.21) and fundamental existence and uniqueness theorems are beyond the scope of the present work and can be found in the potential flow literature.

The conditions under which a solution can be obtained are very general. For the problem of flow exterior to a given surface, *S* may consist of several disjoint surfaces. The right side is likewise practically unrestricted. Since only $\boldsymbol{U}_\infty$ enters (2.1.21), it is

not essential that this velocity field be derivable from a potential function, although of course the disturbance velocity field must be a potential flow. Furthermore $\boldsymbol{U}_\infty$ may vary with position.

There is one restriction on (2.1.21). The existence proof requires that the prescribed boundary value, that is, the right side of (2.1.21), be a continuous function of position on the surface. Because of the presence of $\boldsymbol{n}(p)$, this means that the surface S must have a continuous normal vector, thus boundaries with corners are excluded from the existence proof. In practice, however, it has been found that the present method does give correct results near convex corners. For concave corners the method has difficulty, but concave corners are rarely encountered on ship hulls.

For a known boundary surface S, the kernel of (2.1.21) can be calculated in a straightforward manner, and the equation is a linear one for the unknown function σ.

Furthermore, for three-dimensional bodies, (2.1.21) is a two-dimensional integral equation. This feature accounts for the efficiency of the integral-equation methods since the dimensionality of the problem is reduced by one.

Equation (2.1.21) is an integral equation of the second kind, for which the unknown function appears outside the integral as well as inside. Numerically, integral equations of the second kind are rather easily tractable since the integral equation is approximated by a set of linear algebraic equations, and the presence of the term outside the integral insures that in general the diagonal entries of the resulting coefficient matrix will be much larger than any off-diagonal entries. This feature is very important numerically, since it ensures the stability of iterative matrix-solution methods.

The two terms on the left side of (2.1.21) have a simple interpretation. The term $2\pi\sigma(p)$ is the contribution to the outward normal velocity at a point p on the boundary of the source density in the immediate neighborhood of p. The integral term represents the contribution of the source density on the remainder of the boundary surface to the outward normal velocity at p.

2.1.3 *The Numerical Method of Solution*

The approach adopted consists of approximating (2.1.21) by a set of linear algebraic equations. This is accomplished in the following manner. The boundary surface S (hull and water surface) about which the flow is to be computed, is approximated by a number of surface elements or panels, whose characteristic dimensions are small compared to those of S. Obviously the water surface should extent to infinity. Since that is impossible in the present method, only a portion of the free surface, around the hulls, is modeled (see 2.4.5, Figure 2.12). It should also be mentioned that since the problem is symmetric about x-axis, only one hull and one half of the water surface is modeled. Over each surface element the value of the surface source density is assumed constant. This reduces the problem of determining the continuous source density function σ to that of determining a finite number of values of σ, one for each of the surface elements.

The contribution of each element to the integral in (2.1.21) can be obtained by taking the constant but unknown value of σ on that element out of the integral and then performing the indicated integration of known geometric quantities over the element. Requiring (2.1.21) to hold at one point of the approximate body surface, that is, requiring the normal velocity to take on its prescribed value at one point, gives a linear relation between the values of σ on the elements. On each element a control point is selected where (2.1.21) is required to hold. This gives a number of linear equations equal to the number of unknown values of σ. The coefficient matrix consists of the normal velocities induced by the elements at each other's control points for unit values of source density. Once the linear equations have been solved, flow velocities and potential may be calculated at any point by summing the contributions of the surface elements and that of the onset flow.

Usually, velocities and pressures on the body surface are of greatest interest. Because of the manner in which the solution has been formulated, these must be evaluated at the control points, that is, at the same points where the normal velocity was made to take its prescribed value.

The basic input to the computer program consists of the specification of the hull surface about which the flow is to be computed, the free water surface around the hull and the onset flow (a uniform stream). The hull and water surface are specified by means of the coordinates of a set of points distributed over both of them (see 2.3). Because the input points are used to form the approximating surface elements, their distribution and total number determine the accuracy of the resulting calculations.

The input points are associated in groups of four and used to form plane quadrilateral surface elements or elements. The plane of the element is equidistant from the four input points used to form it, and its unit normal vector $\boldsymbol{n}$ is the normalized cross-product of two "tangential" vectors each of which is obtained by subtracting the coordinates of two of the four input points. The corners of the quadrilateral are projections of the four input points into the plane of the element. In order to model surfaces that end at a single point (bow, bulb, stern hub or stern without transom), the program can use triangular elements, by simply joining two of the four corner points. This is only necessary for the last row of elements.

Figure 2.2 shows the surface elements used on the hull and water surface for the Test Case *D354* (see 3.1), at V_S=15 kn, *Fn*=0.279, design displacement condition. The total number of elements used was 22,062.

On each element a control point is selected at which the normal velocity boundary condition is to be satisfied. The proper choice of the control point is not at all obvious. In this investigation, the location of the control point coincides with the location of the point, where the tangential to the element speed becomes zero. The later point is called a Null point (Hess, 1966).

It should be emphasized that for all body geometries the surface elements are simply devices for effecting the numerical solution of the integral equation (2.1.21). They essentially define integration increments and normal directions at points of the surface and have no direct physical significance. It is only at the control points that the normal velocity assumes its prescribed value. For example, if the normal velocity is prescribed as zero, it is in general nonzero at all points of the element except the

control point; that is, the element "leaks". At the edges of the elements the velocity approaches infinity because of the discontinuity of the source density and/or the discontinuity in slope. The computed flow has significance only at the control points themselves and at points off the body surface.

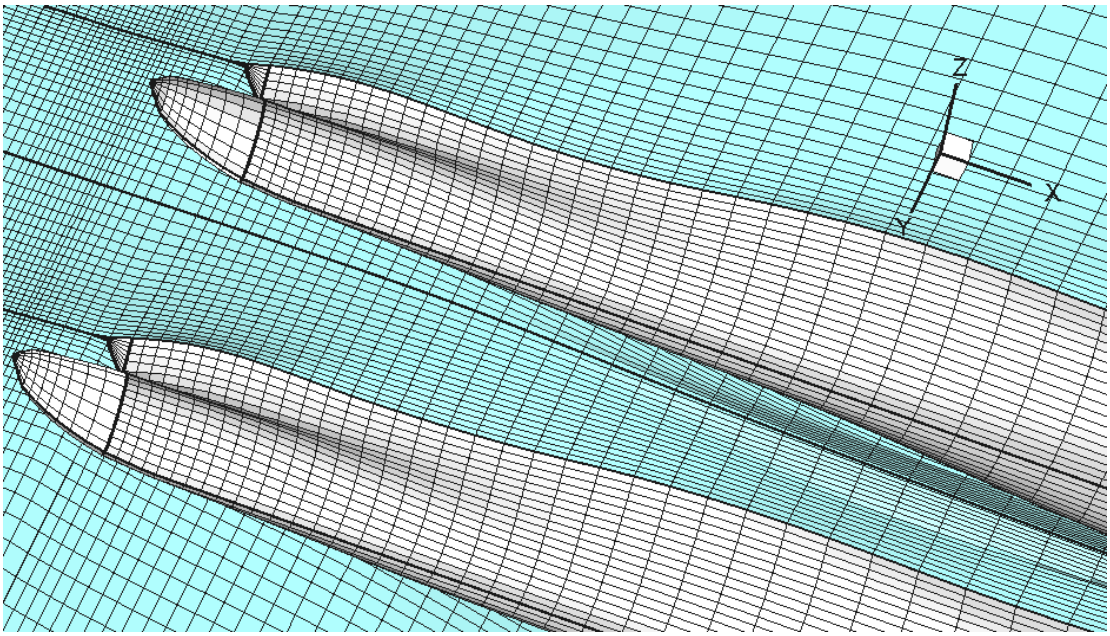

Figure 2.2 Panels on the water surface and hulls. Test case *D354*, design displacement condition, V_S=15 kn, *Fn*=0.279. Total Number of panels 22,062 (run d354a15a).

The accuracy of the calculation is determined by the number and distribution of the elements. In order to achieve a reasonable level of accuracy a total number of elements in the order of 5,000 would be sufficient. The present method though requires a significantly larger amount of elements on the free surface, in order to calculate its shape (see 2.2). In practice a total number of elements in the order of 20,000, is found to yield results of adequate accuracy.

In order to reduce the computational effort, the solution may start with a coarse grid which is successively refined to the maximum number of panels according to a sequel defined in the input data. Apart from the necessary geometrical interpolations, there is no difficulty to pass from the one grid resolution to another due to the steady-state decomposition which is followed.

Once the hull and water surfaces have been approximated by elements of the appropriate type, the elements are ordered sequentially and numbered from 1 to *N*, where *N* is the total number of elements. The exact order of the sequence is immaterial. It is simply a logical device for keeping track of the elements during the computational procedure. Reference will accordingly be made to the *ith* and the *jth* element, where the integers *i* and *j* denote the positions of the elements in the sequence.

Assume for the moment that the surface source density on the *jth* element has the constant value of unity. Denote by Φ_{ij} and $\boldsymbol{U}_{ij}$ the potential and velocity, respectively, that are induced at the control point of the *ith* element by a unit source density on the *jth* element. The formulas for the induced potential and velocity form

the basis of the present method of flow calculation. They are obtained by integrating over the element in question the formulas for the potential and velocity induced by a unit point source and thus depend on the location of the point at which the potential and velocity are being evaluated and also on the geometry of the element. Since there is no restriction on the location of the control point of the *ith* element with respect to the *jth* element, the formulas for Φ_{ij} and $\boldsymbol{U}_{ij}$ are those for the potential and velocity induced by an element at an arbitrary point in space.

For the plane quadrilateral elements used, the unit-point-source formulas for potential and velocity can be integrated analytically over an element. This is most conveniently done by using a coordinate system in which the element itself lies in a coordinate plane, and thus coordinates of points and components of vectors must be transformed between the reference coordinate system in which the body surface is input and an "element coordinate system" based on the element in question. The analytic integration over the element produces rather lengthy formulas, whose evaluation is time consuming. To conserve computing time, the effect of an element at points sufficiently far from the element is calculated approximately. This is accomplished by means of a multipole expansion. In fact, if the point in question is farther from the centroid of the element than four times the maximum dimension of the element, the quadrilateral source element may be replaced by a point source of the same total strength located at its centroid. With the accuracy criteria adopted, errors due to the use of the multipole expansion or point-source formulas are apparently small compared with those arising from the basic approximation of the body surface by plane elements having constant values of source density. The use of these alternative formulas therefore involves no loss of accuracy at all in the overall calculation.

When this phase of the calculation has been completed, the result consists of the *N*x*N* matrices Φ_{ij} and $\boldsymbol{U}_{ij}$ that give the potentials and velocities induced by the elements at each other's control points for a unit source density. The vector matrix $\boldsymbol{U}_{ij}$ is

$$\boldsymbol{U_{ij}} = X_{ij} \cdot \vec{i} + Y_{ij} \cdot \vec{j} + Z_{ij} \cdot \vec{k} \tag{2.1.22}$$

where *i, j, k* are the unit vectors along the axes of the reference coordinate system in which the body surface is input, and the scalar matrices X_{ij}, Y_{ij}, Z_{ij} are simply the components of $\boldsymbol{U}_{ij}$. The normal velocity induced at the control point of the *ith* element by a unit source density on the *jth* element is

$$A_{ij} = \boldsymbol{n}_i \cdot U_{ij} \tag{2.1.23}$$

where $\boldsymbol{n}_i$ is the unit normal vector to the *ith* element. The five matrices Φ_{ij}, X_{ij}, Y_{ij}, Z_{ij}, and A_{ij} do not necessarily have any zero entries. As mentioned above, the number of elements used is large enough for the handling of the amount of numerical data represented by these matrices to be a considerable problem.

It should be mentioned that the *i=j* case does not require special handling. Because the integration over an element is done analytically, problems of infinite integrands or principal-value integrals, fail to materialize. The velocity induced by an element at its own control point has a magnitude of 2π and is directed along the element's normal vector.

Above we calculated the matrix A_{ij}, whose entries are the normal velocities induced by the elements at each other's control points for unit values of source density. To obtain actual normal velocities, the entries of A_{ij} must be multiplied by the proper values of the source density σ. In particular, the quantity

$$\sum_{j=1}^{N} A_{ij} \cdot \sigma_j \tag{2.1.24}$$

is the normal velocity at the control point of the *ith* element due to the complete set of surface elements. Clearly, (2.1.24) is the approximation of the normal velocity associated with the disturbance potential of the body surface. To obtain the prescribed normal velocities at the control points of all elements, (2.1.24) must be set equal to the proper value as given by (2.1.14) for every value of *i*. The result is

$$\sum_{j=1}^{N} A_{ij} \cdot \sigma_j = -\boldsymbol{n_i} \cdot \boldsymbol{U}_{\infty,i} \; i = 1,2,\dots,\mathrm{N} \tag{2.1.25}$$

Equation (2.1.25) is a set of linear algebraic equations for the values of source density on the surface elements. This set of linear algebraic equations is the desired approximation of the integral equation (2.1.21). The method adopted for solving (2.1.21) is the iterative *Gauss-Seidel*.

Once the values of the source density σ_j have been obtained as the solution of (2.1.25), all other flow quantities of interest can be obtained by relatively rapid direct calculation. Flow quantities on the hull and water surfaces are computed only at the control points of the elements. Specifically, the potential and velocity at a control point on the surface are calculated from

$$\left.\begin{aligned} \varphi_i &= \sum_{j=1}^{N} \Phi_{ij} \cdot \sigma_j \\ \boldsymbol{U}_i &= \sum_{j=1}^{N} \boldsymbol{V}_{ij} \cdot \sigma_j + \boldsymbol{U}_{\infty,i} \end{aligned}\right\} i = 1,2,\dots,\mathrm{N} \tag{2.1.26}$$

The velocity $\boldsymbol{U_i}$ at each control point is given in terms of its components along the axes of the reference coordinate system in which the body is input.

$$\left.\begin{aligned} u_{x,i} &= \sum_{j=1}^{N} \boldsymbol{X}_{ij} \cdot \sigma_j + u_{\infty,x,i} \\ u_{y,i} &= \sum_{j=1}^{N} \boldsymbol{Y}_{ij} \cdot \sigma_j + u_{\infty,y,i} \\ u_{z,i} &= \sum_{j=1}^{N} \boldsymbol{Z}_{ij} \cdot \sigma_j + u_{\infty,z,i} \end{aligned}\right\} i = 1,2,\dots,\mathrm{N} \tag{2.1.27}$$

Notice that σ is the perturbation potential due to the body surface, and $\boldsymbol{U_i}$, is the total velocity, including the effects of the onset flow. The components of $\boldsymbol{U_i}$ are used to compute velocity magnitude and then pressure coefficient from (2.1.17). Flow quantities may also be computed at points off the body surface.

The pressure at each control point may then be calculated from the *Bernoulli's* equation (2.1.16) while the local value of the pressure coefficient C_P can be calculated from (2.1.17).

2.2 Calculation of the Free Surface

As mentioned in the previous paragraph, the potential solver used here, can attack only the direct problem of fluid dynamics, that is, the locations of all boundary surfaces are assumed known. In our case though the boundaries are not a priori known since neither the shape of the free surface nor the attitude of the ship (dynamic sinkage and trim) are known in advance. In order to overcome this problem, an iterative procedure is adopted (Tzabiras, 2008).

Assuming that at an intermediate step the free-surface geometry is known, the panels on the hull and water surface are directly constructed by finding analytically the intersection of the free-surface and the transverse sections (Fig.2.1). The points on a transverse cut of the free surface are found by interpolation (spline or linear) following an exponential arrangement. Then, the potential problem is solved by setting the normal velocity on the control point of each panel equal to zero (*kinematic condition*, see 2.1). After the calculation of the panel sources, the velocity components u_x, u_y, u_z, are calculated on the control points of the surface panels and the total pressure p^* is derived from the *Bernoulli's* equation (2.1.16).

In any intermediate step the *dynamic condition* is not satisfied, that is the pressure p^* is different than the sum of the ambient p_S (=0) plus the hydrostatic pressure ρgz. This difference is introduced as a source term to calculate the correct vertical velocity u_Z^* on the free surface by solving the corresponding inviscid momentum equation:

$$\rho\left[\frac{\partial u_x u_z^*}{\partial x}+\frac{\partial u_y u_z^*}{\partial y}+\frac{\partial u_z u_z^*}{\partial z}\right]=-\frac{\partial p^*}{\partial z} \tag{2.2.1a}$$

$$\rho \mathrm{div}(u_z^* \boldsymbol{U})=-\frac{\partial p^*}{\partial z} \tag{2.2.1b}$$

Equation (2.2.1) is solved numerically by applying the control volume method. The control volumes are defined by the panel surface (1234) and a suitably selected height δz^* (Fig.2.3). Equation (2.2.1) is then integrated in the control volume, after applying *Gauss' divergence theorem*.

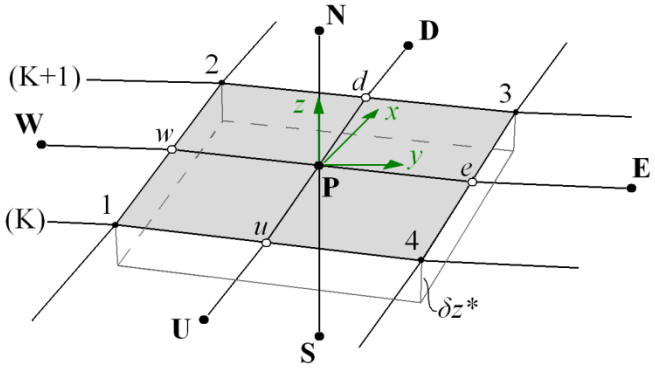

Figure 2.3 Control Volume for the calculation of the free surface.

$$\int_{CV} \mathrm{div}(a)dV = \int_A n \cdot a \, dA \tag{2.2.2}$$

$$\int_{CV} \rho \mathrm{div}(u_z^* \boldsymbol{U})dV = -\int_{CV} \frac{\partial p^*}{\partial z} dV \Rightarrow$$

$$\rho \int_A \boldsymbol{n} \cdot (u_z^* \boldsymbol{U})dA = -\int_{CV} \frac{\partial p^*}{\partial z} dV \Rightarrow \mathrm{I} = \mathrm{II} \tag{2.2.3}$$

where A is the surface of the control volume CV and $\boldsymbol{n}$ is the unit outward normal vector at a point of A.

$$\mathrm{I} = \rho \int_A \boldsymbol{n} \cdot (u_z^* \boldsymbol{U})dA =$$

$$= \rho \int_{(e)} \boldsymbol{n} \cdot (u_z^* \boldsymbol{U})dA + \rho \int_{(w)} \boldsymbol{n} \cdot (u_z^* \boldsymbol{U})dA + \rho \int_{(n)} \boldsymbol{n} \cdot (u_z^* \boldsymbol{U})dA +$$

$$+\rho \int_{(s)} \boldsymbol{n} \cdot (u_z^* \boldsymbol{U})dA + \rho \int_{(u)} \boldsymbol{n} \cdot (u_z^* \boldsymbol{U})dA + \rho \int_{(d)} \boldsymbol{n} \cdot (u_z^* \boldsymbol{U})dA \Rightarrow$$

$$\mathrm{I} = \mathrm{I}_e + \mathrm{I}_w + \mathrm{I}_n + \mathrm{I}_s + \mathrm{I}_u + \mathrm{I}_d \tag{2.2.4}$$

where *e*, *w*, *n*, *s*, *u*, *d* are the east, west, north, south, upstream and downstream faces of A respectively.

By considering $\boldsymbol{U}$, $\boldsymbol{n}$ and u_z^* constant over each face, Eq. (2.2.4) is approximated:

$$\left.\begin{aligned}
\mathrm{I}_d &= \rho \int_{(d)} u_{x,d} \cdot u_{z,d}^* dA = (23)_{pr} \cdot \delta z^* \cdot \rho \cdot u_{x,d} \cdot u_{z,d}^* \\
\mathrm{I}_u &= \rho \int_{(u)} -u_{x,u} \cdot u_{z,u}^* dA = -(14)_{pr} \cdot \delta z^* \cdot \rho \cdot u_{x,u} \cdot u_{z,u}^* \\
\mathrm{I}_e &= \rho \int_{(e)} u_{y,e} \cdot u_{z,e}^* dA = (34)_{pr} \cdot \delta z^* \cdot \rho \cdot u_{y,e} \cdot u_{z,e}^* \\
\mathrm{I}_w &= \rho \int_{(w)} -u_{y,w} \cdot u_{z,w}^* dA = -(12)_{pr} \cdot \delta z^* \cdot \rho \cdot u_{y,w} \cdot u_{z,w}^* \\
\mathrm{I}_n &= \rho \int_{(n)} u_{z,p} \cdot u_{z,p}^* dA = (E_{1234}) \cdot \rho \cdot u_{z,p} \cdot u_{z,p}^* \\
\mathrm{I}_s &= \rho \int_{(s)} u_{z,p} \cdot u_{z,p}^* dA = -(E_{1234}) \cdot \rho \cdot u_{z,p} \cdot u_{z,p}^* = -\mathrm{I}_n
\end{aligned}\right\} \tag{2.2.5}$$

Furthermore II is approximated:

$$\mathrm{II} = -\int_{CV} \frac{\partial p^*}{\partial z} dV = -(E_{1234}) \cdot (p_p^* - \rho g z_p) \tag{2.2.6}$$

In equations (2.2.5) and (2.2.6) the subscript P denotes values at the control point of the panel, while subscripts *e*, *w*, *n*, *s*, *u*, *d* denote values at the middle of the corresponding face of the panel. Furthermore (E_{1234}) is the area of the projection $(1234)_{pr}$ of the panel (1234) on the *xy*-plane (horizontal). Finally $(12)_{pr}$, $(34)_{pr}$, $(23)_{pr}$,

$(14)_{pr}$, are the lengths of the projections of the corresponding faces of $(1234)_{pr}$ on x and y-axis respectively.

In equation (2.2.5) $u_{x,d}$, $u_{x,u}$, $u_{y,e}$, $u_{y,w}$, are the exact velocity components at the middle of the corresponding face of the panel, as calculated by the potential theory and $u_{z,P}$, is the exact vertical velocity component at the control point of the panel, as calculated by the potential theory. Finally, $u_{z,d}$*, $u_{z,u}$*, $u_{z,e}$*, $u_{z,w}$* are the unknown values of u_z* at the middle of the corresponding face of the panel and are approximated by the first order upstream difference scheme:

$$\left.\begin{array}{ll} u^*_{z,d} = u^*_{z,P} & \\ u^*_{z,u} = u^*_{z,U} & \\ u_{y,e} > 0, & u^*_{z,e} = u^*_{z,P} \\ u_{y,e} < 0, & u^*_{z,e} = u^*_{z,E} \\ u_{y,w} > 0, & u^*_{z,w} = u^*_{z,W} \\ u_{y,w} < 0, & u^*_{z,w} = u^*_{z,P} \end{array}\right\} \qquad (2.2.7)$$

where the subscripts E, W, U, D denote values at the neighboring control points.

Due to the nature of the problem, $u_{x,d}$, $u_{x,u}$, are always positive, hence there is no need to check the values of $u_{x,d}$, $u_{x,u}$. Equations (2.2.5) and (2.26) after applying (2.2.7) are cast in the common form:

$$A_P u^*_{z,P} = A_E u^*_{z,E} + A_W u^*_{z,W} + A_U u^*_{z,U} + A_D u^*_{z,D} + (E_{1234})(p^*_P - \rho g z_P) \qquad (2.2.8)$$

As was mentioned before, δz* is the height of the control volume and acts as an arbitrary parameter that controls the convergence of the procedure. It is involved in the convective terms A_i of (2.2.8), but essentially determines the influence of the pressure gradient.

Since the convective coefficients are approximated by the first order upstream difference scheme, only one sweep of the computational domain is needed to solve for the vertical velocity component.

Although the corresponding solution is related only to the free-surface renewal, the disadvantage of the first order approximation is that necessitates fine discretizations to obtain satisfactory results. The calculated vertical velocity components are used to calculate a new surface by introducing two corrective steps (Tzabiras, 2004). First, following the local flow lines, points a on transverse line (K) lead to points b on (K+1) as shown in Figure 2.4 and a new transverse cut is generated downstream.

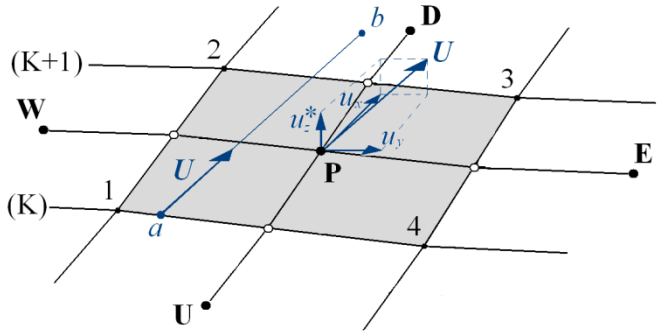

Figure 2.4 First step for correcting the free surface.

Next, this new cut is corrected by δz so that the flow rate through the corresponding surface panel becomes equal to zero (Fig.2.5). To accelerate convergence, the method may be applied over a number on surface panels in the longitudinal direction (Tzabiras, 1997). Anyhow, to avoid convergence problems the surface renewal is restricted by an external parameter which stabilizes the whole procedure but decelerates convergence.

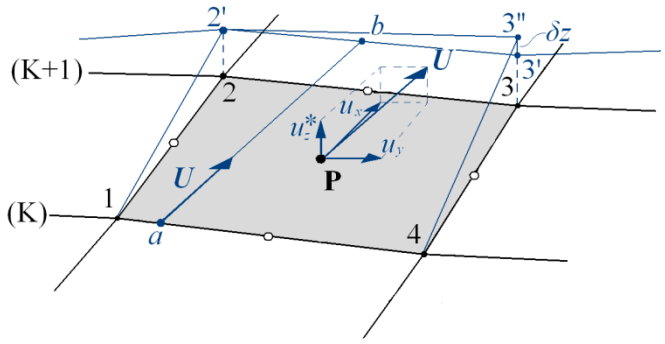

Figure 2.5 Second step for correcting the free surface.

After the water surface is updated, the potential problem is solved and the whole procedure is repeated until the dynamic boundary condition converges. The satisfaction of the dynamic boundary condition is tested through $\overline{|\delta z|}$ which is the mean value of the absolute difference between the calculated and the ideal hydrostatic pressure at the control points of all surface panels, transformed in [m]. Owing to the free-surface approximation with quadrilateral panels, this value decreases as the problem converges but exhibits a limiting behavior. Therefore, convergence with respect to $\overline{|\delta z|}$ is satisfied, when it becomes lower than a suitable value depending on both the Froude number and the scale. By definition, the smaller the limiting value of $\overline{|\delta z|}$, the more accurate the solution. An example of the convergence history is presented in Figure 2.6. The surface grid starts with 10,000 surface panels and changes every 50 steps up to the final of 22,000.

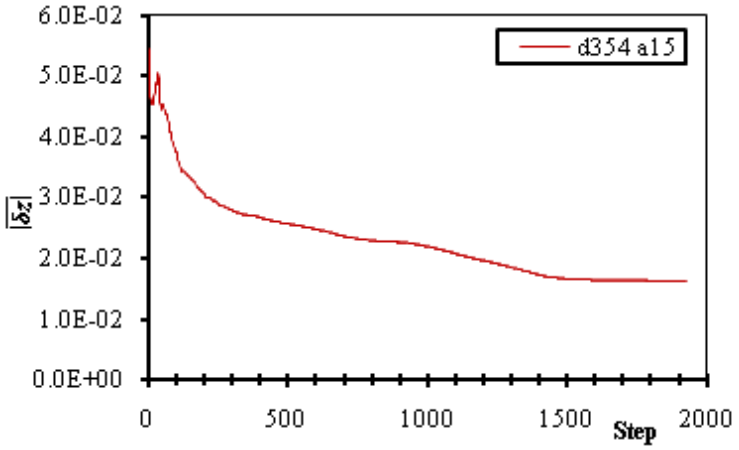

Figure 2.6 Convergence of the dynamic boundary condition, Test case *D354*, V_S=15 kn, *Fn*=0.279, design displacement condition (run d354a15a).

Since the free-surface is updated at each iteration, the wave resistance and the value of the respective coefficient C_W also change. An example of the convergence history of C_W, for the above case is presented in Figure 2.7.

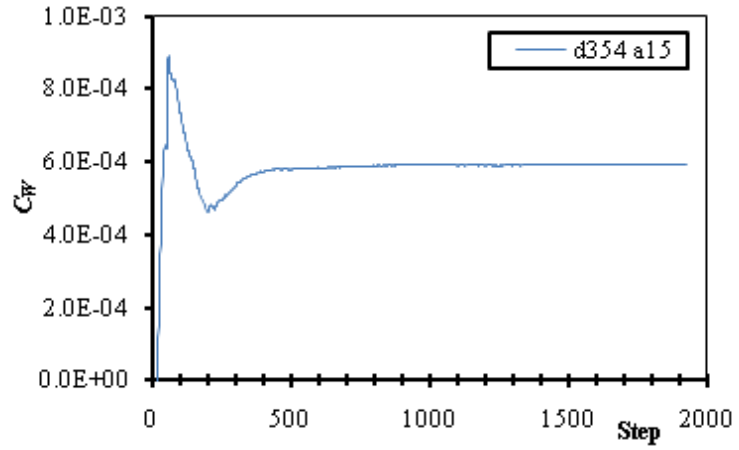

Figure 2.7 Convergence of the wave resistance coefficient. Test case *D354*, V_S=15 kn, *Fn*=0.279, design displacement condition (run d354a15a).

Finally, the method can also be applied to ships with both “dry” and “wetted” transom sterns. In the above cases a further domain of panels is introduced on the water surface, astern the transom (Fig.2.15). The method is applied without any special difficulty, by simply overlapping one line at the boundary of the two domains in order to compute the new free surface. The condition of the transom (wetted or dry) is prescribed by the user (see 2.4.5). When the transom is declares “dry” then the first row panels of the stern domain are bound to the transom edge. In the case were the transom is declared “dry”, extra panels are added on the transom surface and the height of the first row panels of the stern domain is calculated using the method of this paragraph.

2.3 Calculation of C_W, Dynamic *Sinkage* and *Trim*

The wave resistance as well as the vertical forces and moments are calculated by integrating the pressure on the hull panels. As wave resistance R_W in this work, we define the pressure resistance, since the potential theory is unable to predict any other resistance component (viscous pressure and frictional). Hence the wave resistance is defined as the integral on the surface of the hull of the projection of the dynamic pressure (the total pressure minus the hydrostatic pressure) on *x*-axis (longitudinal):

$$R_W = \iint_{WS}(p^* - \rho g h) \cdot (\boldsymbol{n} \cdot \boldsymbol{i})\, \mathrm{d}s \tag{2.3.1}$$

where $\boldsymbol{n}$ is the unit vector normal to the body surface and $\boldsymbol{i}$ the one parallel to the *x*-axis. The wave resistance coefficient C_W is then defined as:

$$C_W = -\frac{R_W}{\frac{1}{2}\cdot\rho\cdot WS\cdot V_S{}^2} \tag{2.3.2}$$

where ρ is the water density, *WS* is the actual wetted surface, as calculated by the present method and V_S is the ship's speed.

The integration on the surface of the hull, of the projection of the total pressure on *z*-axis (vertical), gives the vertical force and moment that cause the ship to change its attitude.

$$R_Z = \iint_{WS} p^* \cdot (\boldsymbol{n} \cdot \boldsymbol{k})\, \mathrm{d}s \tag{2.3.3}$$

where $\boldsymbol{k}$ is the unit vector, parallel to the *z*-axis.

This force is used to calculate the dynamic *sinkage* (eq. 2.3.4) and *trim* (eq. 2.3.5), whenever this is required and the longitudinal position of the centre of gravity (c.g.), x_g is known. *Trim* is the total (hydrostatic + hydrodynamic) trim and is defined as positive by stern while *sinkage* is defined as the increase of draft at x=0 with respect to the ship's reference system (Figure 2.1).

$$sinkage = \frac{\Delta - R_Z}{\rho g A_{WL}} \tag{2.3.4}$$

$$\tan(trim) = \frac{\Delta\cdot x_g - R_Z\cdot x_p}{\rho g I_{yy}} \tag{2.3.5}$$

where g is the gravitational acceleration, A_{WL} is the water plane area, x_p is the longitudinal position of the center of pressure, Δ is the displacement and I_{yy} is the second moment of the water plane area, about *y*-axis.

The procedure of changing the ship attitude starts after a user defined number of iterations. In between two consecutive calculations of *sinkage* and *trim*, a number of iterations, defined by the user, are performed, to allow for a degree of convergence for the free-surface. This procedure is followed until convergence for free-surface, wave resistance, sinkage and trim is achieved.

The convergence rates for sinkage and trim at *Fn*=0.279 for the Test Case *D354*, are presented in Figures2.8a & 2.8b respectively. The calculations for the sinkage and trim start after 200 steps and then are carried out every 50 steps. Ultimately it is the convergence of the dynamic boundary condition on the free surface after 1800 iterations (Fig. 2.6) that dictates the overall convergence in this case, since all other values converge after about 800 iterations.

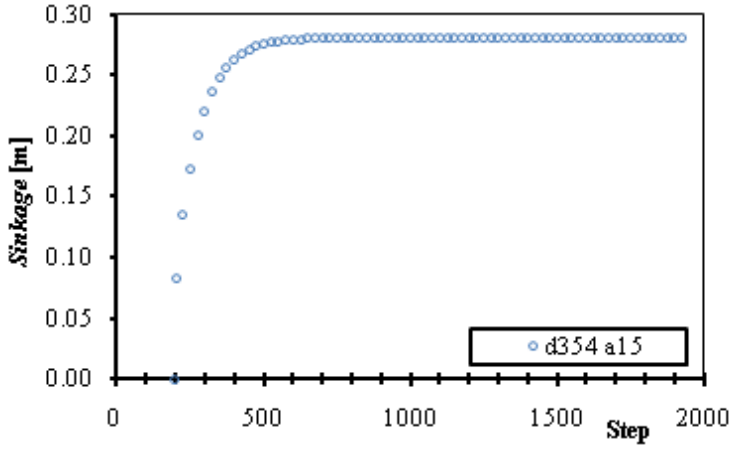

Figure 2.8a Convergence of *dynamic sinkage*. Test case *D354*, V_S=15 kn, *Fn*=0.279, design displacement condition (run d354a15a).

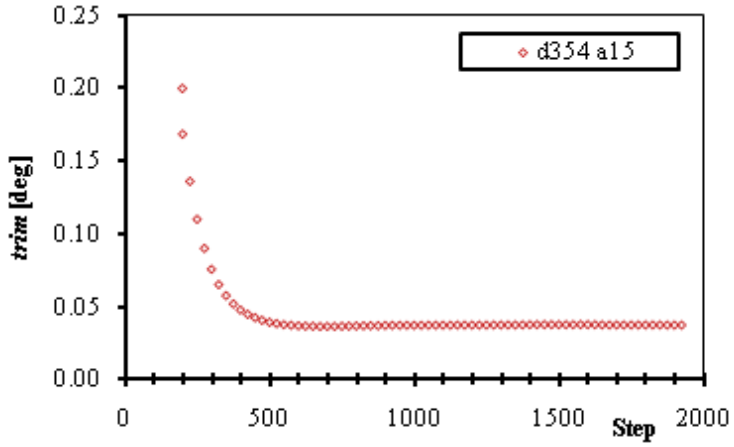

Figure 2.8b Convergence of *trim*. Test case *D354*, V_S=15 kn, *Fn*=0.279, design displacement condition (run d354a15a).

2.4 Geometrical Representation of the Hull

In order to obtain the required input data for the generation of the panels, the common practice of describing the hull surface by means of transverse 2D sections is adopted. Specifically the conformal mapping method has been employed to represent analytically each section. The latest version (Tzabiras, 2009) of this method is adopted and its fundamental features are described in the sequel.

It is common that the number of input sections is relatively small, while the required number of sections for the generation of the panels is significantly larger. Several methods for interpolating input sections are incorporated in the program, an overview of which is given later.

In order to model a variety of hull shapes, the hull surface is divided into regions. The existence of each region as well as other options concerning the generation of the panels are also discussed in later paragraphs.

2.4.1 *Conformal Transformation of a 2D Section*

The general conformal transformation that maps a ship-like section reads (Kerczek, 1969):

$$z = c_0 + c_{-1}\zeta + \sum_{n=1}^{N} c_n \zeta^{-n} \tag{2.4.1}$$

where ζ is the complex plane of the unit circle and z the section plane. If the curve is symmetric with respect to the y-axis, Figure 2.9, coefficients c_n reduce to the real α_n and the real and imaginary parts of z in Equation (2.4.1) are expanded as:

$$x = \alpha_{-1}\cos\varphi + \sum_{n=1}^{N} \alpha_n \cos(-n\varphi)$$

$$y = \alpha_0 + \alpha_{-1}\sin\varphi + \sum_{n=1}^{N} \alpha_n \sin(-n\varphi) \tag{2.4.2}$$

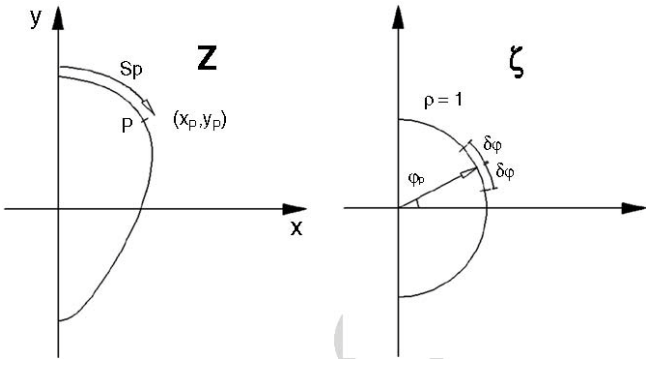

Figure 2.9 The transformation of a ship section on the unit circle.

In Equation (2.4.2), φ stands for the argument of point (x,y) on the circle plane, while the coefficients α_n can be calculated after (Tzabiras, 1986), either through the integrals:

$$a_0^{(1)} = \frac{1}{2\pi}\int_0^{2\pi} x(\varphi)d\varphi$$

$$a_{-1}^{(1)} + a_1^{(1)} = \frac{1}{\pi}\int_0^{2\pi} x(\varphi)\cos(\varphi)d\varphi \qquad (2.4.3a)$$

$$a_n^{(1)} = \frac{1}{\pi}\int_0^{2\pi} x(\varphi)\cos(\varphi)d\varphi, n > 2$$

or the integrals:

$$a_0^{(2)} = \frac{1}{2\pi}\int_0^{2\pi} y(\varphi)d\varphi$$

$$a_{-1}^{(2)} + a_1^{(2)} = \frac{1}{\pi}\int_0^{2\pi} y(\varphi)\sin(\varphi)d\varphi \qquad (2.4.3b)$$

$$a_n^{(2)} = \frac{1}{\pi}\int_0^{2\pi} y(\varphi)\sin(\varphi)d\varphi, n > 2$$

Expressions (2.4.3a) and (2.4.3b) show that coefficients α_{-1}, α_0, …, α_n can be calculated analytically in two ways, which for $N\to\infty$ result in equal values. However, since a finite number N is used in real applications, the evaluation of integrals (2.4.3a) and (2.4.3b) finds different values for $\alpha_n^{(1)}$ and $\alpha_n^{(2)}$ and their effectiveness depends on the section shape. In order to find an optimum representation of an arbitrary 2D section, a linear relation is assumed to hold between the two approximations:

$$a_n = ra_n^{(1)} + (1-r)a_n^{(2)}, n = -1, \dots, N \qquad (2.4.4)$$

The weight factor r is defined by minimizing the total error:

$$E_t = \sum_P [(x_P - x_{aP})^2 + (y_P - y_{aP})^2] \qquad (2.4.5)$$

Where P is the number of data points (x_P,y_P) that describe the section contour and (x_{aP},y_{aP}) the corresponding analytical expressions through Eq. (2.4.2). Introducing r, these expressions are analyzed as:

$$x_{aP} = \left[ra_{-1}^{(1)} + (1-r)a_{-1}^{(2)}\right]\cos\varphi_P$$

$$+ \sum_{n=1}^{N}[ra_n^{(1)} + (1-r)a_n^{(2)}]\cos(-n\varphi_P) \qquad (2.4.6a)$$

$$y_{aP} = \left[ra_0^{(1)} + (1-r)a_0^{(2)}\right] + \left[ra_{-1}^{(1)} + (1-r)a_{-1}^{(2)}\right]\sin\varphi_P$$

$$+ \sum_{n=1}^{N}[ra_n^{(1)} + (1-r)a_n^{(2)}]\sin(-n\varphi_P) \qquad (2.4.6b)$$

Then r is defined by solving the linear Equation:

$$\frac{\partial E_t}{\partial r} = 0 \tag{2.4.7}$$

It should be noted that the coefficients α_1 and α_{-1} are uniquely defined from the linear system which is derived by evaluating the second of integrals (2.4.3a) and (2.4.3b). As the number of coefficients increases, the weight factor r changes. The general trend is that for $H \gg B$ $r \rightarrow 0$ while for $B \gg H$ $r \rightarrow 1$, where B is the beam and H the draft of the section.

For a particular section, the iterative procedure of (Kerczek, 1969) is followed, i.e. calculations start with four coefficients and proceed by increasing their number up to an initially defined N or until the total error becomes smaller than a certain limit. Anyhow, the evaluation of integrals (2.4.3a) and (2.4.3b) requires the calculation of angles φ_P, i.e. the arguments of points P on the circle plane. In the original work of Von Kerczek and Tuck (1969) the angle φ_P was defined by finding the minimum distance between the particular point and the analytical representation, by increasing φ monotonically. However, this procedure fails when applied in complex sections and results to irregular representations, e.g. (Kerczek, 1969, Tzabiras 1995). To overcome the problem, an improvement has been introduced that calculates angles φ_P in a two-step procedure. In the first step, it is assumed that φ_P is a function of S_P where S is the contour integral of the section calculated by:

$$S_p = S_{p-1} + \sqrt{(x_p - x_{p-1})^2 + (y_p - y_{p-1})^2} \tag{2.4.8}$$

Next, introducing a set of known angles φ_i, the values of S_i are computed analytically through the conformal representation. Then, the angles φ_P are defined by linear or cubic-spline interpolation of the corresponding length (Eq. 2.4.8) with respect to S_i, (Tzabiras, 1996). The distribution of φ_i depends on the variation of curvature around the section contour, i.e. points are concentrated in concave regions. This method proved to be stable and quite fast but, since it is based on the approximation of S_P through the data points, it may produce inaccurate representations in regions of high curvature. Therefore, it is applied only in the intermediate steps, while in the last iteration (maximum N) a second procedure is followed that calculates φ_P by finding the minimum distance of P from the analytic representation of the section in the range $[\varphi_P-\delta\varphi, \varphi_P+\delta\varphi]$ i.e. not monotonically, where $\delta\varphi \approx 0.1\pi$ (Figure 2.9).

The above procedure is followed for both bulbous bow sections and general sections which may be symmetrical only in y-axis (including asymmetric sterns, (Tzabiras, 1996)). For normal ship sections that are also symmetrical in x, the general transformation (Eq. (2.4.3)) becomes:

$$z = \sum_{n=1}^{N} a_n \zeta^{3-2n} \tag{2.4.9}$$

However, in normal ship sections the section contour cuts usually the x-axis at non-orthogonal angles. This problem has been raised in (Kerczek, 1983) by applying first a Karman-Trefftz transformation. Consequently a two-step transformation has to be applied. Although this method has been used successfully (Tzabiras, 1997b) it may produce irregularities when sections are interpolated because it is very sensitive on the calculation of the intersection angle. This is why the original approximation is employed, taking also into account that any probable deviations are restricted locally at the upper part of the ship, located above the free surface. Besides, substantial

improvement can be achieved by using an adequate number of data points in this region.

2.4.2 *Interpolation of Sections*

While the conformal mapping is initially applied to a set of data stations, the effective generation of intermediate transverse sections is indispensable for generating fine grids that are required to perform accurate potential flow calculations. In all relevant methods, the general approach is to calculate the coefficients of any desired section by interpolating among those obtained for the original data. The first attempt (Kerczek, 1969) was based on a polynomial interpolation. However, the developed procedure was unsuccessful and the use of cubic splines was found to be very accurate (Kerczek, 1983). For complex ship hulls exhibiting rapid longitudinal variation of geometry, an effective alternative is to apply a simple cubic interpolation on subsequent stations (Tzabiras, 1997).

However, the aforementioned methods have been unsuccessful at bulbous bows or sterns, where any interpolation among the data sections produces quite irregular representations. To face the problem, a different procedure is employed (Tzabiras, 2009). At first, the program generates data points on the required transverse plane by using cubic interpolation among those at four neighboring stations. The latter are calculated by the transformation of points defined introducing an equal angle spacing on the unit cycle. Then, the resulting contour is transformed according to the prescribed conformal mapping technique and the coefficients are stored as new data. The whole procedure is automatic, i.e. a set of longitudinal positions is defined in sensitive regions and the corresponding coefficients are calculated and stored just after the calculations are completed for the original sections.

2.4.3 *Subdivision of the Hull Surface*

Modern hull shapes are rather complicated. The bow may be flared or vertical and feature a bulb, while the stern may be of the traditional cruiser-type or it may feature a “dry” or “wetted” transom. Finally in many modern designs a stern bulb is adopted. In order for the program to be able to handle the different hull shapes, the hull surface is subdivided in five regions (Figure 2.10).

The first region is the portion of the hull, in front of the fore perpendicular (*FP*) and above the bulb. The fore perpendicular is defined here as the vertical line tangential to the hull’s centerline at the bow of the ship, near the intersection of the centerline with the water line. The second region is the bow bulb, defined as the portion of the hull, in front of the fore perpendicular and below the first region.

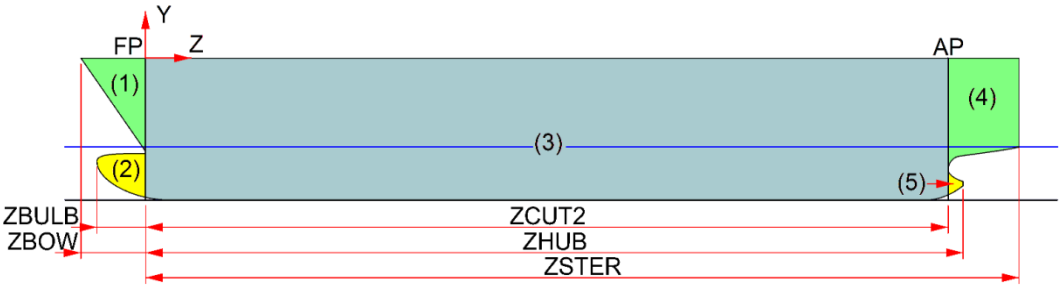

Figure 2.10 Definition of the hull regions, the data input coordinates' system and the main dimensions.

The fourth region contains the stern and is the portion of the hull, astern the aft perpendicular (*AP*) and above the stern bulb (when there is one). When the stern of the ship features a stern bulb, the aft perpendicular is defined as the vertical line tangential to the centerline, near the stern of the ship and the intersection of the centerline with the water line. In all other cases the location of the aft perpendicular is arbitrary. The fifth region is the stern bulb, defined as the portion of the hull, astern the aft perpendicular and below the fourth region. Finally the third region is the portion of the hull, astern the fore perpendicular and in front of the aft perpendicular. Regions (1) and (2) form the longitudinal section (A), region (3) forms the longitudinal section (B) and finally regions (4) and (5) form the longitudinal section (C). The third region is the only requisite region in order for the program to be executed, although some of the stern options are only applicable to the fourth region, hence in order to use them, the fourth region must be defined.

Although the existence of a region is prescribed by the user, the program generates panels only on the submerged portions of each of them. When a region is not at all submerged, the program ignores it altogether. If during the solution a portion of a region becomes submerged, the program will automatically generate panels on it. Figures 2.11a-c, depict the panels generated on the bow of the Test Case *D354* in different conditions. In Figure 2.11a the ship is at rest and at partial displacement condition, hence the bow bulb is only partially submerged. In Figure 2.11b the ship is at speed (V_S=15 kn), at partial displacement condition, hence the bow bulb is fully submerged but the bow region (1) is not submerged. Finally in Figure 2.11c the ship is at speed (V_S=15 kn), at design displacement condition, hence the bow bulb is fully submerged while the bow region is partially submerged. The panels of each region form a separate computational domain.

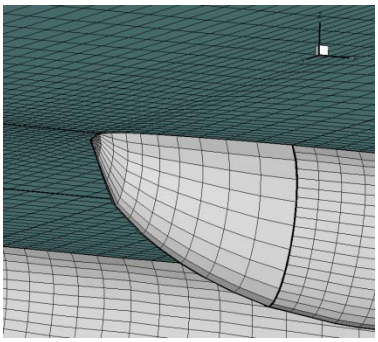

Figure 2.11a Panels at the bow of the Test case *D354*, partial displacement condition, V_S=0 kn.

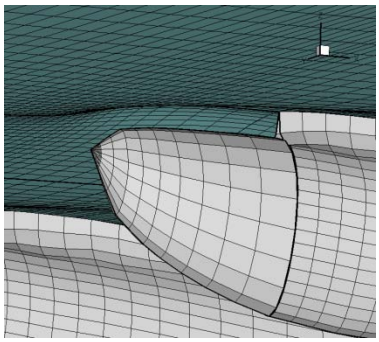

Figure 2.11b Panels at the bow of the Test case *D354*, partial displacement condition, V_S=15 kn, *Fn*=0.279. (run d354b15a).

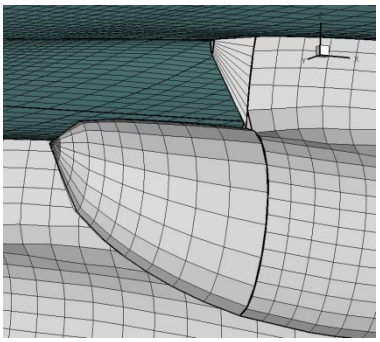

Figure 2.11c Panels at the bow of the Test case *D354*, design displacement condition, V_S=15 kn, *Fn*=0.279. (run d354a15a).

2.4.4 *Data Input Method*

The input data required for the execution of the program are grouped into two sets, the geometry of the hull and variables concerning the generation of the panels and the numerical solution. The program can handle asymmetric hulls, that is, the inner and outer half may differ although the two hulls ought to be symmetric with respect to the ship's center plane.

As mentioned in the previous paragraph, each half of the hull is divided in up to five regions. Each hull region is described by a set number of 2D transverse sections. These 2D sections are input to the program as coefficients of their respective conformal mapping (see 2.4.1). The transformation is done separately using another in-house developed program, by *Professor Tzabiras*, *conformal.f*, (see Appendix C), which applies the conformal mapping and returns the coefficients in a binary file named *file1*. By that name the potential program expects to read the coefficients for the outer half of the hull, while the data for the inner half are read from another binary file named *file2*. In the case were the hull is asymmetric, the conformal mapping program is used twice and the output file for the inner half is renamed by the user as *file2*.

The conformal mapping program reads the 2D sections as groups of properly sorted and oriented points from two text files, *data2* and *data3* (see Appendix C). The points are given in these files as coordinates of the input coordinate system. The origin point of the above system is located at the fore perpendicular (Fig. 2.10), at the height of the main deck. The *z*-axis coincides with the longitudinal direction and the *z*-values increase towards the stern. The *y*-axis coincides with the vertical direction and the *y*-values increase with height. Finally the *x*-axis completes a left-handed coordinates system.

In order to reduce the effort required to prepare the data for the conformal mapping program, a new software was developed by the author of the present work. The software name *sorting.f90*, is a program written in *Fortran* 90, that reads unsorted coordinates from text files and prepares the input files for the execution of *conformal.f*. The new software proved very useful since a large number of hulls were tested during this investigation. The software may also be used for preparing data for the *RANS* codes developed in-house, since the too demand the use of the same conformal mapping program. For more details on *sorting.f90* see Appendix D.

2.4.5 *Panel Generation Options*

As mentioned in the previous paragraph, the input data required for the execution of the program are grouped into two categories, the geometry of the hull and the variables concerning the generation of the panels and the numerical solution. The later are read from the input data text file *dinp*. A list of the most important variables of *dinp*, are presented in Appendix A. In this paragraph we will focus on those variables concerning the definition of the hull features and the generation of the panels.

In paragraph 2.1.3 it was mentioned that only a portion of the theoretically infinite water surface is modeled. The shape of the computational domain is an orthogonal trapezoid around one of the hulls, where it's longitudinal edge lies on the ship's center plane. The extend and shape of the computational domain is defined by the user and input to the program by means of four variables given in Table 2.1 and Figure 2.12.

Table 2.1. Variables defining the computational domain.

Name	Value	Meaning
ZG1	<0.	Longitudinal position of the first row of points [m].
ZG4	>0.	Longitudinal position of the last row of points [m].
DEXFIR	>0.	The half-beam of the domain at the first row of points [m].
DEXLAS	>0.	The half-beam of the domain at the last row of points [m].
	=0.	DEXLAS = DEXFIR + tan(39.5°) x (ZG1+ZG4)

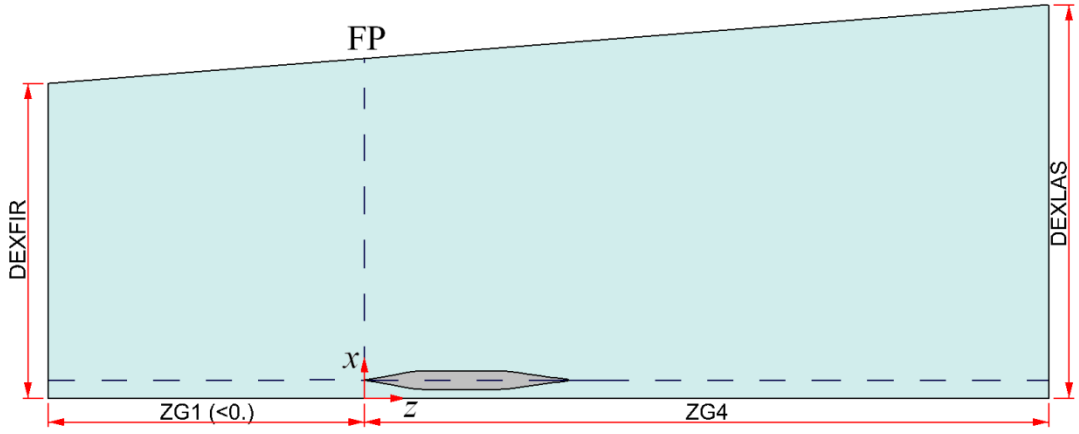

Figure 2.12 Definition of the computational domain and its main dimensions.

The program has the ability to model various features of modern hulls, such as bulbous bows, stern bulbs and transoms. The definition and dimensions of the different features are input through the values of variables of *dinp*. A list of those variables are given in Table 2.2.

Figures 2.13 a & b depict the panels on the bow of two test cases. The first, hull *C*, features a vertical bow (ITRB=2, IBULB=0) while the second, hull *B428*, features a traditional flared bow with bulb (ITRB=1, IBULB=2). Both test cases are at design displacement condition, V_S=15 kn and *Fn*= 0.263 and 0.260 respectively.

Figures 2.14 a & b depict the panels on the stern of two test cases. The first, hull *E*, features a vertical stern (LTRA=-1, IHUB=0) while the second, hull *D354*, features a traditional cruiser stern with bulb (LTRA=0, IHUB=2) and a blended with the ship lines seat for a podded propulsor. Both test cases are at design displacement condition, V_S=15 kn and *Fn*= 0.276 and 0.279 respectively.

Figures 2.15a & b depict the panels on the stern of a catamaran ship with deep transom. In Fig.2.15a, the transom is "dry" (LTRA=+2, IHUB=0), *Fn*= 0.667, while in Fig.2.15b the transom is "wet" (LTRA=+1, IHUB=0), V_S=0.0 kn. The

configuration of the "dry" transom should be used with care because due to the nature of the potential flow, may lead to considerable decrease in the value of C_W.

The longitudinal position of the transom may be prescribed by the user (ZTRANS, Table 2.2) alternatively, at every iteration the program finds the rearmost partially submerged section and sets the transom position equal to the longitudinal position of that section.

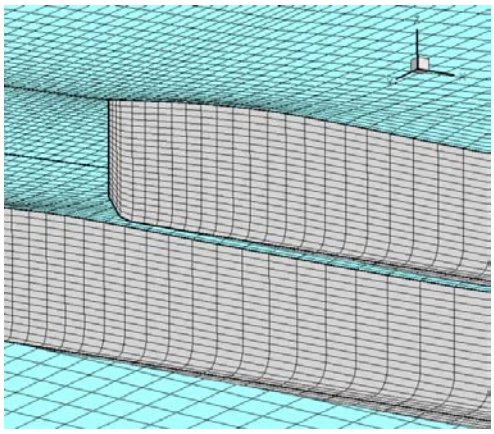

Figure 2.13a Panels at the bow of the Test case *C*, full load condition, V_S=15 kn, *Fn*=0.263. (run cca15).

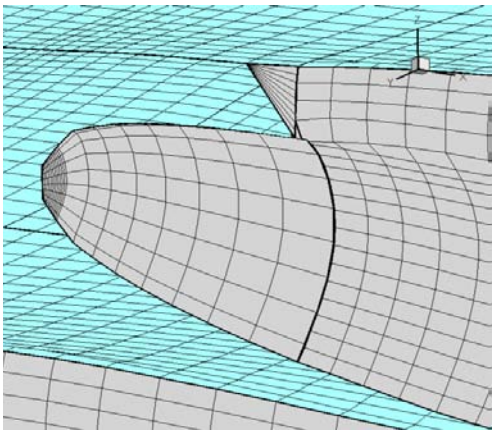

Figure 2.13b Panels at the bow of the Test case *B428*, full load condition, V_S=15 kn, *Fn*=0.260. (run b428a15).

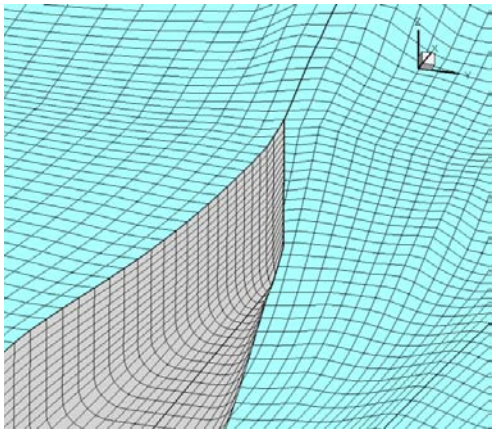

Figure 2.14a Panels at the stern of the Test case *E*, full load condition, V_S=15 kn, *Fn*=0.276. (run cea15).

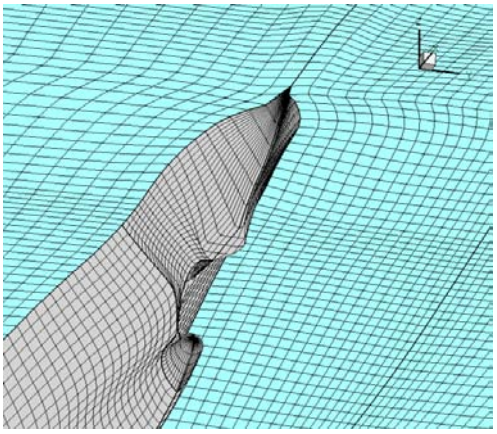

Figure 2.14b Panels at the stern of the Test case *D354*, full load condition, V_S=15 kn, *Fn*=0.279. (run d354a15a).

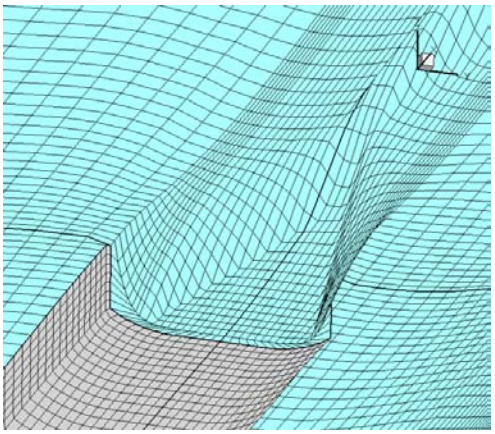

Figure 2.15a Panels at the stern of a

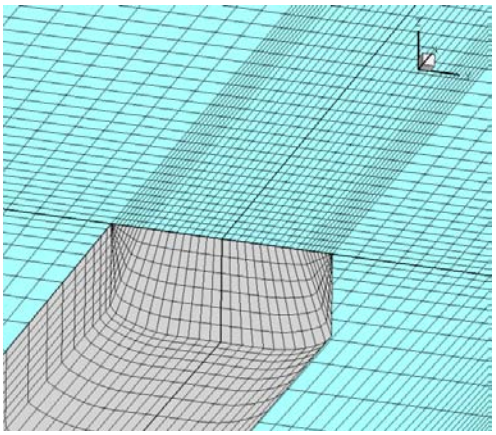

Figure 2.15b Panels at the stern of a

catamaran with "dry" transom, *Fn*=0.667. catamaran with "wet" transom, V_S=0.0 kn.

Table 2.2. Variables concerning the dimensions and features of the hull.

Name	Value	Meaning
XGRAV	>0.	Longitudinal position of the center of gravity [m].
YGRAV	<0.	Transverse position of the centerline of a demi-hull [m].
ZGRAV	<0.	Vertical position of the center of gravity [m].
NCAT	1	The ship is considered a monohull.
	>1	The ship is considered a catamaran.
ITRB	1	The bow ends at a single point.
	2	The bow ends at a vertical line.
IBUL	0	Ship without bow bulb.
	2	Ship with bow bulb.
IHUB	0	Ship without stern bulb.
	2	Ship with stern bulb.
LTRA	0 or -2	Cruiser type stern leading to a single point.
	-1	Cruiser type stern leading to a vertical line.
	+1	"Dry" transom stern.
	+2	"Wetted" transom stern.
ZBULB	<0.	Longitudinal position of the bow bulb tip [m].
ZBOW	<0.	Longitudinal position of the bow [m].
ZCUT1		Longitudinal position of fore perpendicular [m].
ZCUT2	>0.	Longitudinal position of the 2nd cutting point[m].
ZCUT3	>0.	Longitudinal position of aft perpendicular [m].
ZSTER	>0.	Longitudinal position of the stern [m].
ZMID	>0.	Longitudinal position of interchange between NK3B and NK3S [m].
ZG34	≥0.	Height of skeg [m].
ZTRANS	≥0.	Longitudinal position of the transom [m] (If ZTRANS = 0 and LTRA>0, the program finds at every step the rearmost partially submerged section K and sets ZTRANS = Z(K+1)).
ZHUB	>0.	Longitudinal position of the stern bulb tip [m].

The panels on the hull and water surface are grouped in transverse rows. That is a number of transverse sections is defined by the user and then the program generates rows of panels in between the two consecutive sections. The sections used for the generation of the panels differ from those input to the program and are generated from the later by means of interpolation (see 2.4.2). The number of sections used is defined by the user and refer to the entire hull, not just the submerged portion of it and may alter during the execution of the program. So the solution may start with a small number of panels and as the solution advances, the number of panels, increases up to a user defined maximum. The distribution of the rows is also controlled by the user. The variables controlling the number and distribution of the rows, are given in Table 2.3 and Figure 2.16.

It must be pointed out that the meaning of the variables NKBL and NK2 depend on the shape of the bow profile. If the length of region (1) is greater than the length of the bulb (region (2)) (abs(ZBOW)>abs(ZBULB)), then NK2 sections are created on the bulb and NK2+NKBL sections are created on region (1) as well as on the water surface, in front of the fore perpendicular. If the length of the bulb is greater (abs(ZBOW)<abs(ZBULB)), then NK2 sections are created on region (1) and NK2+NKBL sections are created on the bulb as well as on the water surface (see Fig.2.16). The actual number of sections on the water surface may differ from the one prescribed by the user since variables DZWMIN and DZWMAX determine the minimum length for the water surface panels. Hence some of the sections may be ignored.

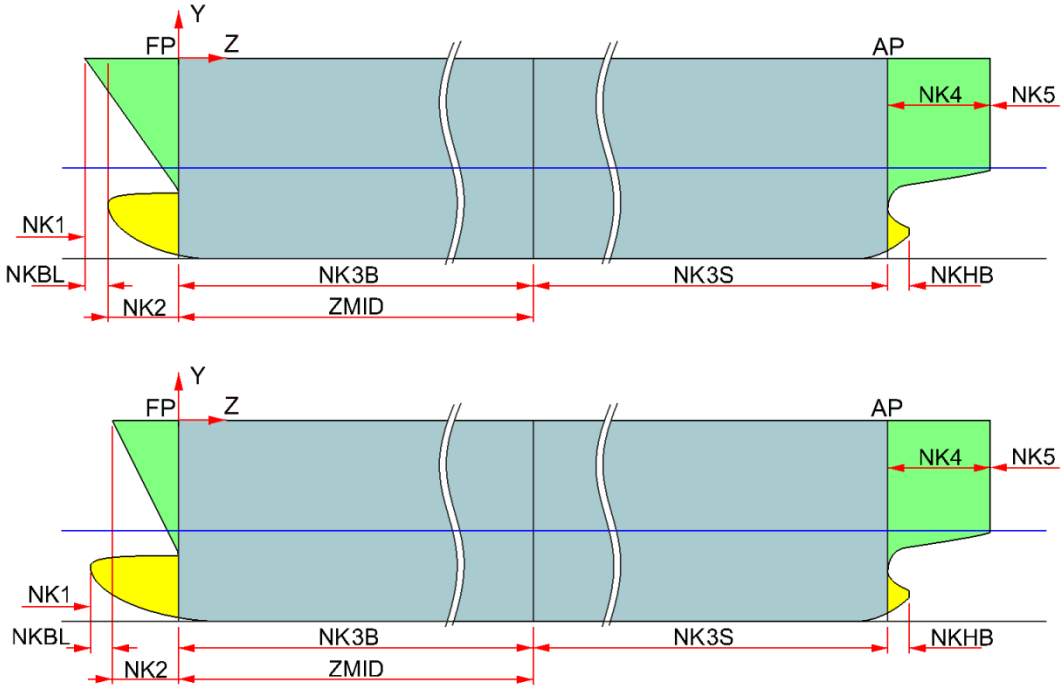

Figure 2.16 Number of sections in the longitudinal direction.

In the transverse direction, the number of panels is also defined by the user and may vary as the solution advances. The variables controlling the number and distribution of the panels in the transverse direction, are given in Table 2.4 and Figure 2.17.

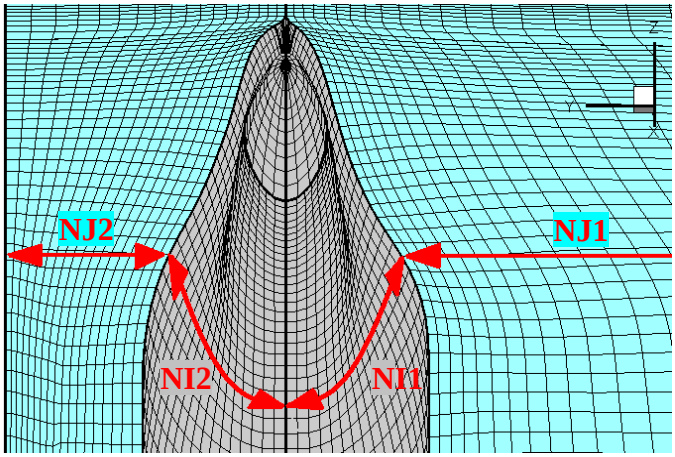

Figure 2.17 Number of points in the transverse direction.

Variables NI1M, NI1S, NI1F, NI2M, NI2S, NI2F give the relative increase of the panels for the outer and inner halves of the hall respectively. The actual maximum number of panels for each section of the hull are given by the variables NI1, NI2, NI3, NI4 and NI5. For example if NI1M=20, NI1S=5 and NI1F=0, while NI3=60 and NI4=40, then for iterations IT=1,…,MASG-1, NI3=60/20*5=15 and NI4=40/20*5=10, for IT=MASG,…,2*MASG-1, NI3=2*60/20*5=30 and NI4=2*40/20*5=20 and so forth, until NI3 and NI4 are given their respective maxim values NI3=60 and NI4=40.

Table 2.3. Variables defining the number and distribution of the rows of panels.

Name	Values	Meaning
MASG	>0	Step at which the number of panels is increased.
NKBL	>0	Number of longitudinal sections on the bow bulb.
NIBU	≥0	Number of sections linearly interpolated between the first and second section on the bow bulb.
NKHB	>0	Number of longitudinal sections on the stern bulb.
NK1	>0	Number of panels, in front of min(ZBOW,ZBULB).
NK2	>0	Number of panels, between max(ZBOW,ZBULB) and ZCUT1.
N3B	>0	Number of panels, between ZCUT1 and ZMID.
N3S	>0	Number of panels, between ZMID and ZCUT3.
NK4	>0	Number of panels, between ZCUT3 and ZSTER.
NK5	>0	Number of panels, astern ZSTER .
N*M	>0	Maximum value of N* (N* = NK1, NK2, NK3B, NK3S, NK4, NK5).
N*S	≥0	Increment of N* (if =0 then N*S=N*M).
N*F	≥0	Initial value of N* (if =0 then N*F=N*S).
DZBULB	>0.	Length of the first panel of the bow bulb (z>ZBULB) [m].
DZBOWM1	>0.	Length of the first panel of in front of the bow (z<min(ZBOW,ZBULB)) [m].
DZBOWP1	>0.	Length of the first panel of aft the bow (z>min(ZBOW,ZBULB)) [m].
DZKB1M1	>0.	Length of the last panel before ZCUT2 [m].
DZSTERM1	>0.	Length of the first panel of in front of the stern [m].
DZSTERP1	>0.	Length of the first panel of aft the stern [m].
DZKF1	>0.	Length of the first panel of aft ZCUT1 [m].
DZHUB	>0.	Length of the first panel of the stern bulb (z<ZHUB) [m].
DZWMIN	>0.	Minimum value of the minimum allowable length of the free surface panels [m].
DZUMAX	>0.	Maximum value of the minimum allowable length of the free surface panels [m].

Table 2.4. Variables defining the number and distribution of panels in the transverse direction.

Name	Values	Meaning
MASG	>0	Step at which the number of panels is increased.
NI1M	>0	Maximum value of NI1, the number of panels in the circumferential direction, on the outer half of the hull.
NI1S	≥0	Increment of NI1 (if =0 then NI1S=NI1M).
NI1F	≥0	Initial value of NI1 (if =0 then NI1F=NI1S).
NI2M	>0	Maximum value of NI2, the number of panels in the circumferential direction, on the inner half of the hull.
NI2S	≥0	Increment of NI2 (if =0 then NI2S=NI2M).
NI2F	≥0	Initial value of NI2 (if =0 then NI2F=NI2S).
NJ1M	>0	Maximum value of NJ1, the number of panels in the transverse direction, on the outer half of the water surface.
NJ1S	≥0	Increment of NJ1 (if =0 then NJ1S=NJ1M).
NJ1F	≥0	Initial value of NJ1 (if =0 then NJ1F=NJ1S).
NJ2M	>0	Maximum value of NJ2, the number of panels in the transverse direction, on the inner half of the water surface.
NJ2S	≥0	Increment of NJ2 (if =0 then NJ2S=NJ2M).
NJ2F	≥0	Initial value of NJ2 (if =0 then NJ2F=NJ2S).
NI1	>0	Maximum overall number of point in the circumferential direction, on the hull section (1)
NI2	>0	Maximum overall number of point in the circumferential direction, on the hull section 2)
NI3	>0	Maximum overall number of point in the circumferential direction, on the hull section (3)
NI4	>0	Maximum overall number of point in the circumferential direction, on the hull section (4)
NI5	>0	Maximum overall number of point in the circumferential direction, on the hull section (5)
INTR	≥0	Number of panels on the radial direction, on the transom for LTRA=+2.
APLUS	>0.	Beam of the first panel at the bow [m].
BPLUS	>0.	Beam of the first panel at ZMID [m].
BPLUSS	>0.	Beam of the first panel at the stern [m].

3. TEST CASES & DISCUSSION

The program described in Section 2 of the present, was used to calculate the wave resistance coefficient C_W, the dynamic *sinkage* and *trim* as well as the free water surface for a number of test cases. In all thirteen (13) different hull shapes were tested in a speed range of 10 to 20 knots and for two load conditions, condition *A*: design displacement, $\Delta \approx 2600$ tn and condition *B*: partial displacement, $\Delta \approx 2200$ tn. In total during this investigation 258 executions (runs) of the program were realized, of which 148 were used for the calculation of C_W and the rest were test runs used to check the grid size independence (see 3.2) or to test various program features.

The hull shapes were provided by *Ass. Professor George Zarafonitis* of the *Ship Design Laboratory* of *N.T.U.A.* and were produced automatically during an optimization process aiming at minimizing the resistance of a catamaran vessel under geometrical, displacement and trim constrains.

In this process the *Computer Aided Engineering* (*CAE*) software *NAPA* (Naval Architectural PAckage), is deployed for the generation of the hulls, the Potential flow panel method of *Shipflow* is used to evaluate the wave resistance (the objective function) of the hulls and the multi objective optimization software *modeFRONTIER* is used for optimizing the hull shape (Zarafonitis, 2003).

The procedure started with hulls *A, B, C, D* and *E*. Hulls *B377, B401, B422* and *B428* were found to be most efficient of the first optimization. Hulls *C377, C423* and *C427* were found to be most efficient of the second optimization while hull *D354* was the optimal hull of the third optimization. In the following the results obtained with the present method, are compared to the results of another potential solver, *Shipflow*. The *Shipflow* results were kindly provided by *Ass. Prof. Zarafonitis* and *Mr. Mourkogiannis* of the *Ship Design Laboratory* of *N.T.U.A.*

It should be pointed out that the numerical method of *Shipflow* is different from that of Section 2 also the wave resistance is calculated differently. Namely wave resistance is calculated from the wave energy passing through a transverse section astern the ship. As mentioned in 2.3, in this work wave resistance is considered equal to the pressure resistance, since the potential theory is unable to predict any other resistance component.

3.1 *Main Particulars of the Test Cases*

The test cases may be grouped into three bunches, initial designs, first optimization and third and fourth optimization. The main particulars as well as the total number of panels used for each hull are given in Tables 3.1 (initial designs), 3.2 (first optimization) and 3.3 (second and third optimization). The total number of panels may vary from that of Tables 3.1-3.3 depending on the wave pattern and the according submergence of the hull (see 2.4.3, Fig. 2.10). Figures 3.1-3.3 depict the hull shapes of the test cases. The multiformity of the test cases allowed us to verify the ability of the program to solve the flow problem around greatly varying hull shapes. In Figures 3.1-3.3 the center line and the flat of side are displayed in black, the stations (transverse sections) in blue, waterlines in red while bowlines and buttock

lines are displayed in green. Finally the condition A and B waterlines are displayed in blue.

The transom of hulls *A* and *C* is substantially above the water line so in effect both ships' stern are treated as cruiser type. The stern of hulls *B* and *D* is of a rather peculiar shape since the waterlines are normal to the centerline at their intersections. This type of stern had to be treated as a transom stern of unknown longitudinal position (see 2.4.5). Finally hulls *C247, C423, C427* and *D354* feature at their stern a blended with the ship lines seat for a podded propulsor. In later paragraphs results are also presented for modified hulls *C247, C423, C427* and *D354* without the pod seat arrangement.

Table 3.1. Main Particulars of hulls *A, B, C, D* & *E* (initial hulls).

Hull			***A***		***B***		***C***		***D***		***E***	
Total Number of Panels			**18,708**		**21,062**		**18,632**		**21,176**		**17,756**	
Condition			**A**	**B**	**A**	**B**	**A**	**B**	**A**	**B**	**A**	**B**
Overall Length	L_{OA}	**m**	80.000		80.000		92.000		92.000		80.000	
Calm Waterline Length	L_{WL}	**m**	76.694	75.801	72.026	68.063	87.925	87.530	83.832	80.419	80.000	80.000
Total Beam	B_{OA}	**m**	21.000		21.000		18.500		18.500		21.000	
Demihull Beam	B_{HULL}	**m**	5.500		5.500		5.300		5.300		5.000	
Bulb Length	L_{BULB}	**m**	-		-		-		-		-	
Depth	D	**m**	9.000		9.000		9.000		9.000		9.000	
Distance of demihulls from Center Plane	$S/2$	**m**	7.750		7.750		6.600		6.600		8.000	
Draft at Fore Perpendicullar	T_F	**m**	4.275	3.648	4.600	3.980	3.770	3.200	4.310	3.720	3.720	3.125
Freeboard at Fore Perpendicullar	FB_F	**m**	4.725	5.352	4.400	5.020	5.230	5.800	4.690	5.280	5.280	5.875
Trim at zero speed (positive by bow)	t	**deg**	0.000	0.000	0.000	0.000	0.000	0.000	0.000	0.000	0.000	0.000
Total Wetted Surface (at zero speed)	WSA	$\mathbf{m^2}$	2122	1901	1700	1492	1876	1668	1858	1631	1775	1583
Total Displacement	Δ	**tn**	2560	2145	2560	2145	2560	2145	2560	2145	2560	2145
Total Volume of Displacement	V	$\mathbf{m^3}$	2498	2093	2498	2093	2498	2093	2498	2093	2498	2093
Longitudinal position of Center of Buoyancy	LCB	**m**	35.928	34.556	35.712	34.869	48.453	48.098	44.396	43.543	40.000	40.000
Longitudinal position of Center of Flotation	LCF	**m**	43.767	42.762	40.933	39.216	50.692	49.821	49.682	47.951	40.000	40.000

Table 3.2. Main Particulars of hulls *B377*, *B401*, *B422* & *B428* (first optimization).

Hull			***B377***		***B401***		***B422***		***B428***	
Total Number of Panels			**21,167**		**21,129**		**21,185**		**21,111**	
Condition			**A**	**B**	**A**	**B**	**A**	**B**	**A**	**B**
Overall Length	L_{OA}	**m**	89.870		99.870		89.938		100.160	
Calm Waterline Length	L_{WL}	**m**	80.003	78.844	90.003	89.054	80.003	78.844	90.003	89.054
Total Beam	B_{OA}	**m**	21.000		18.665		21.000		18.665	
Demihull Beam	B_{HULL}	**m**	6.624		6.835		6.520		6.548	
Depth	D	**m**	10.200		10.200		10.200		10.500	
Bulb Length	L_{BULB}	**m**	2.720		3.060		2.210		3.325	
Distance of demihulls from Center Plane	$S/2$	**m**	7.190		5.915		7.245		6.060	
Draft at Fore Perpendicullar	T_F	**m**	3.400	2.940	3.400	2.960	3.400	2.940	3.400	2.960
Freeboard at Fore Perpendicullar	FB_F	**m**	6.800	7.260	6.800	7.240	6.800	7.260	6.800	7.240
Trim at zero speed (positive by bow)	t	**deg**	0.000	0.000	0.000	0.000	0.000	0.000	0.000	0.000
Total Wetted Surface (at zero speed)	WSA	m^2	1637	1459	1726	1540	1638	1459	1738	1550
Total Displacement	Δ	**tn**	2530	2114	2525	2117	2529	2371	2525	2120
Total Volume of Displacement	V	m^3	2468	2062	2464	2066	2467	2313	2464	2068
Longitudinal position of Center of Buoyancy	LCB	**m**	37.743	37.154	41.665	41.110	37.635	37.341	42.169	41.589
Longitudinal position of Center of Flotation	LCF	**m**	41.616	39.811	45.516	43.533	41.403	39.572	46.162	44.184

Table 3.3. Main Particulars of hulls *C247, C423, C427* & *D354* (second & third optimizations).

Hull			***C247***		***C423***		***C427***		***D354***	
Total Number of Panels			**22,024**		**22,024**		**22,024**		**22,062**	
Condition			**A**	**B**	**A**	**B**	**A**	**B**	**A**	**B**
Overall Length	L_{OA}	**m**	89.786		83.618		89.588		88.650	
Calm Waterline Length	L_{WL}	**m**	78.563	81.466	78.283	81.446	78.563	81.466	78.283	81.446
Total Beam	B_{OA}	**m**	21.000		21.000		21.000		21.000	
Demihull Beam	B_{HULL}	**m**	6.080		6.270		6.260		7.090	
Depth	D	**m**	13.500		13.200		13.200		12.180	
Bulb Length	L_{BULB}	**m**	3.150		3.520		3.300		3.532	
Distance of demihulls from Center Plane	$S/2$	**m**	7.460		7.365		7.370		6.955	
Draft at Fore Perpendicullar	T_F	**m**	4.140	3.120	4.130	3.080	4.140	3.120	4.130	3.080
Freeboard at Fore Perpendicullar	FB_F	**m**	9.360	10.380	9.070	10.120	9.360	10.380	9.070	10.120
Trim at zero speed (positive by bow)	t	**deg**	0.517	1.173	0.396	1.093	0.240	0.936	0.200	0.860
Total Wetted Surface (at zero speed)	WSA	m^2	1759	1559	1747	1558	1734	1542	1683	1501
Total Displacement	Δ	**tn**	2647	2228	2638	2223	2631	2213	2633	2208
Total Volume of Displacement	V	m^3	2582	2173	2574	2169	2567	2159	2569	2154
Longitudinal position of Center of Buoyancy	LCB	**m**	36.002	36.802	35.797	36.659	35.950	36.765	35.752	36.550
Longitudinal position of Center of Flotation	LCF	**m**	38.753	37.603	38.174	37.686	38.521	37.820	38.286	37.603

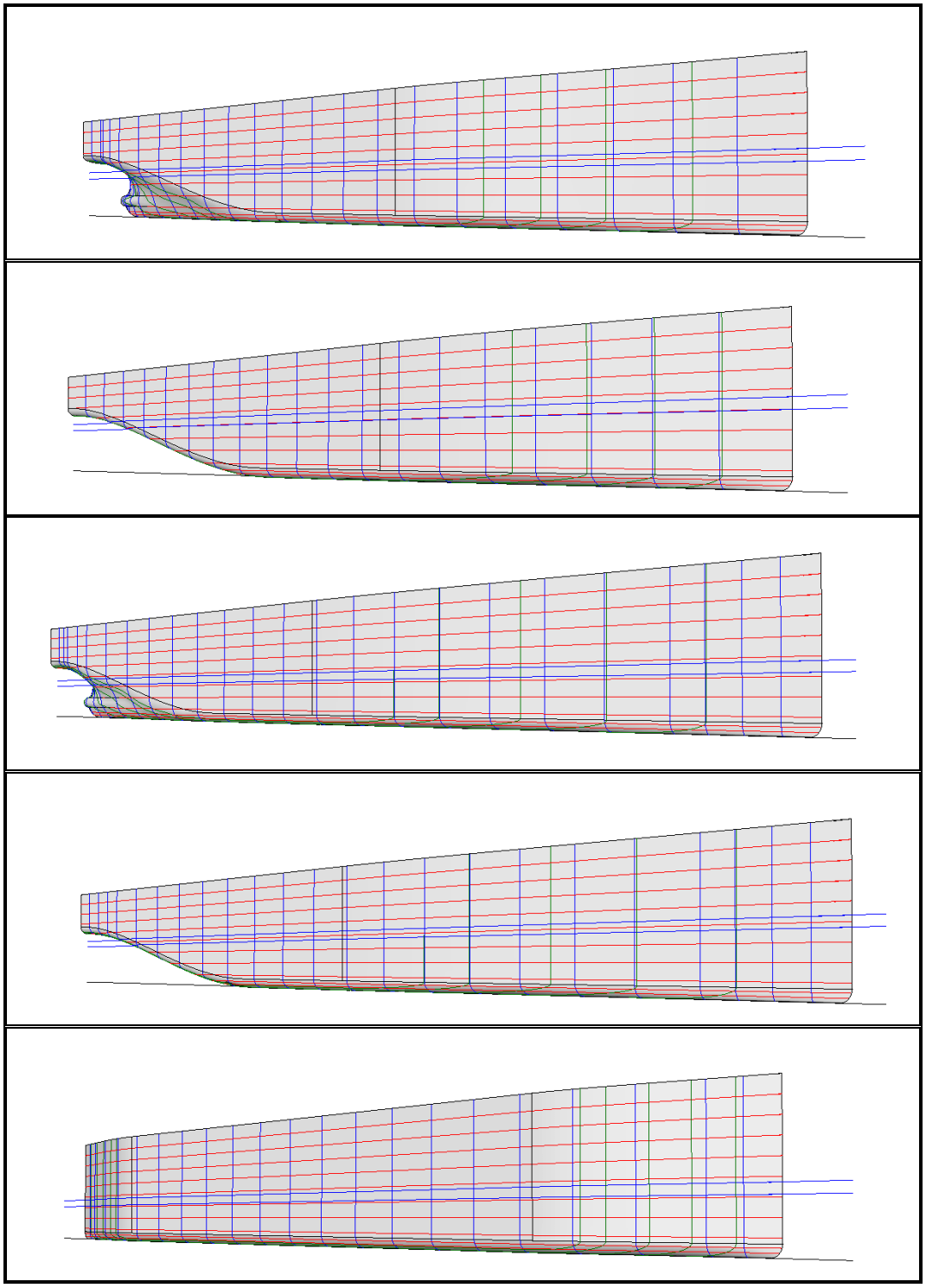

Figure 3.1a. Hull shapes (bow) *A*, *B*, *C*, *D* & *E* (initial hulls).

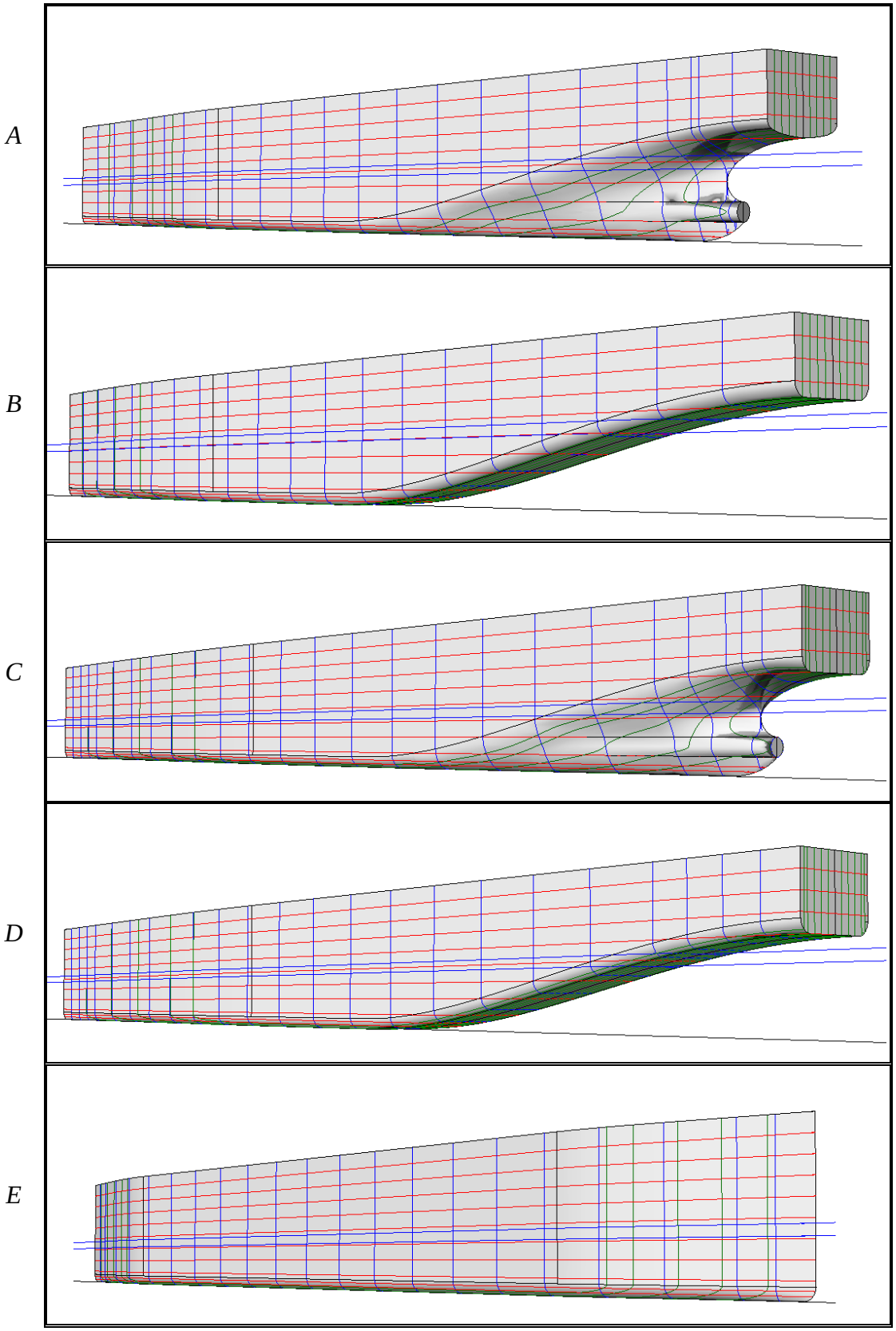

Figure 3.1b. Hull shapes (stern) *A*, *B*, *C*, *D* & *E* (initial hulls).

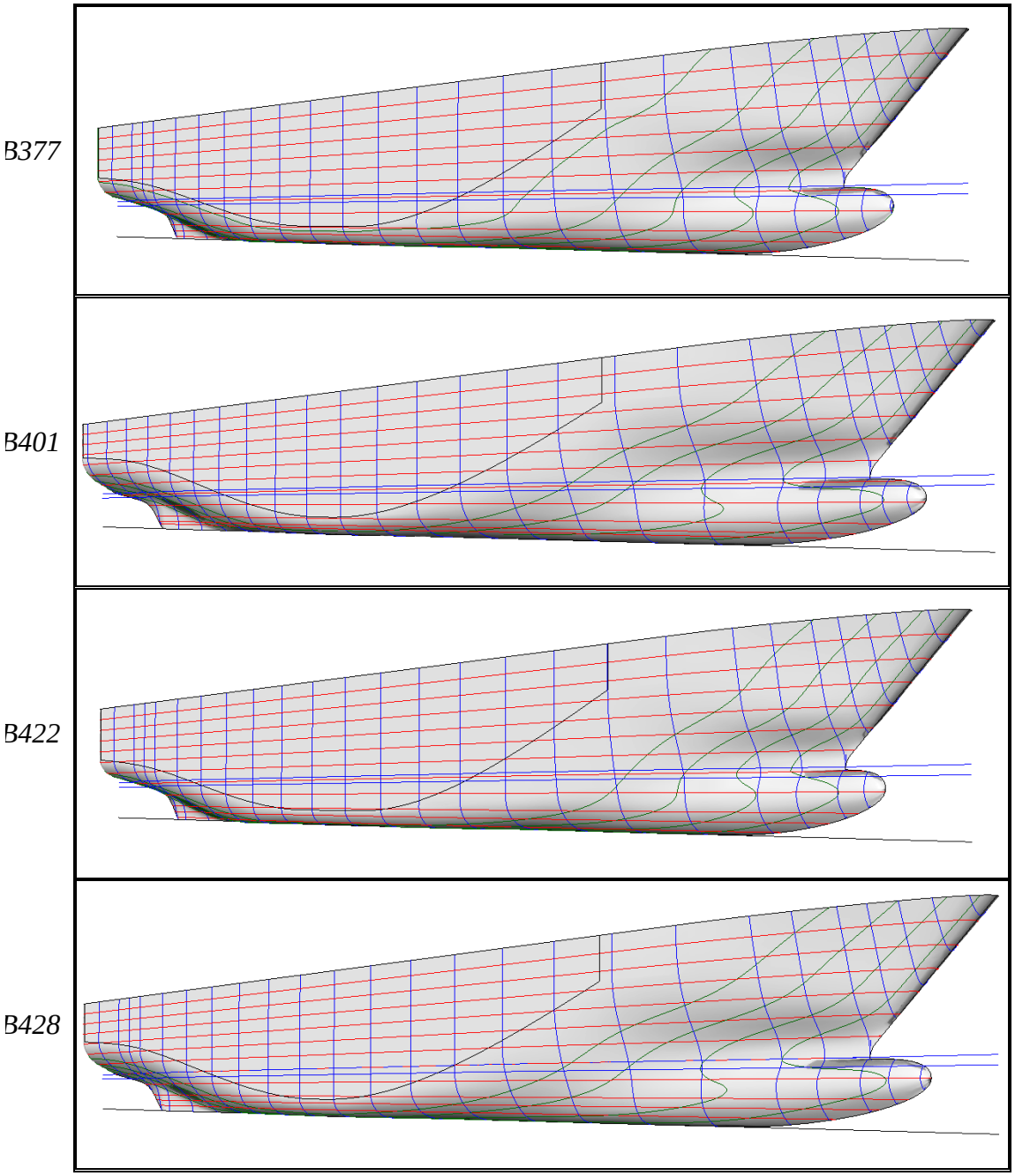

Figure 3.2a. Hull shapes (bow) *B377*, *B401*, *B422* & *B428* (first optimization).

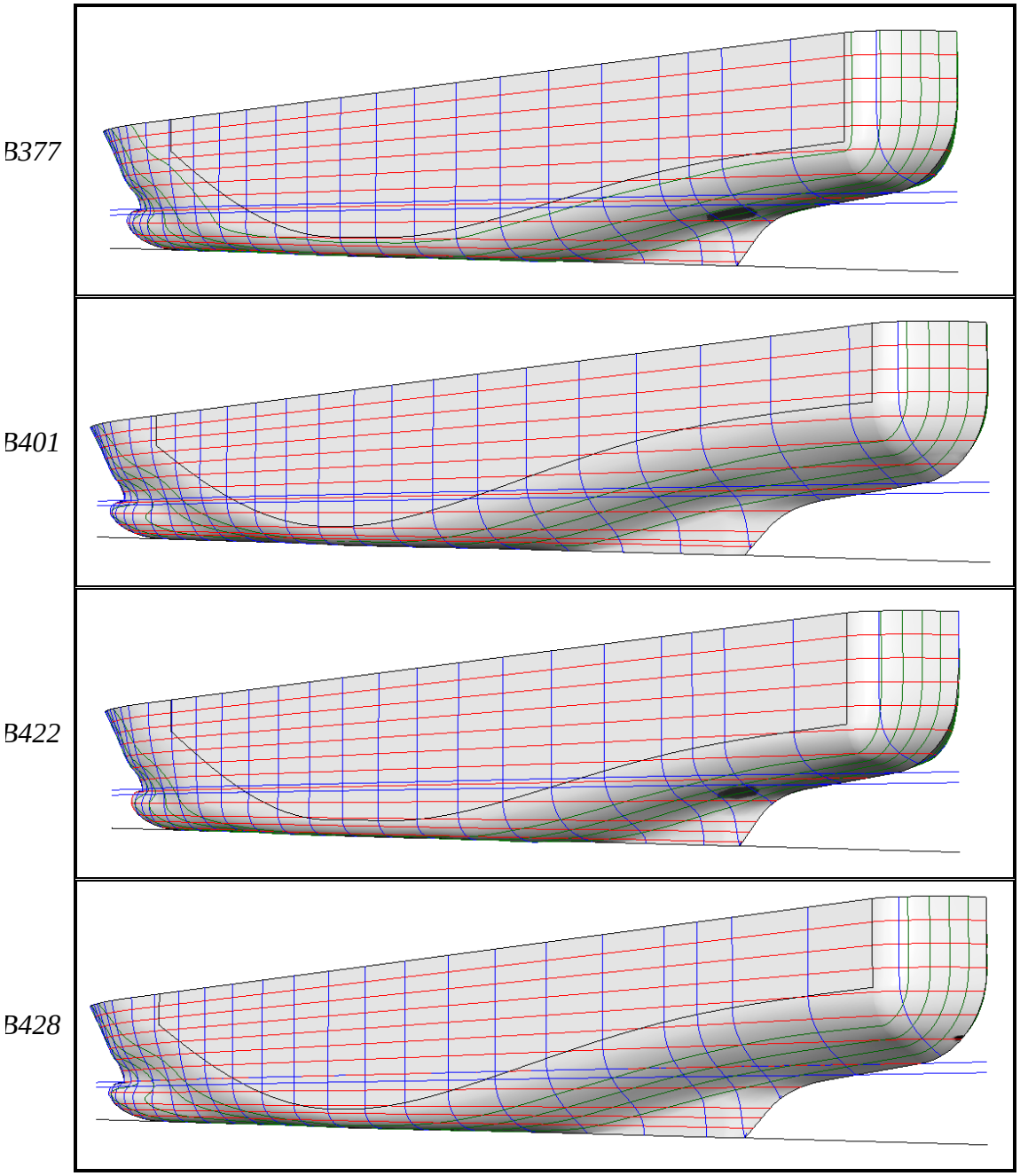

Figure 3.2b. Hull shapes (stern) *B377*, *B401*, *B422* & *B428* (first optimization).

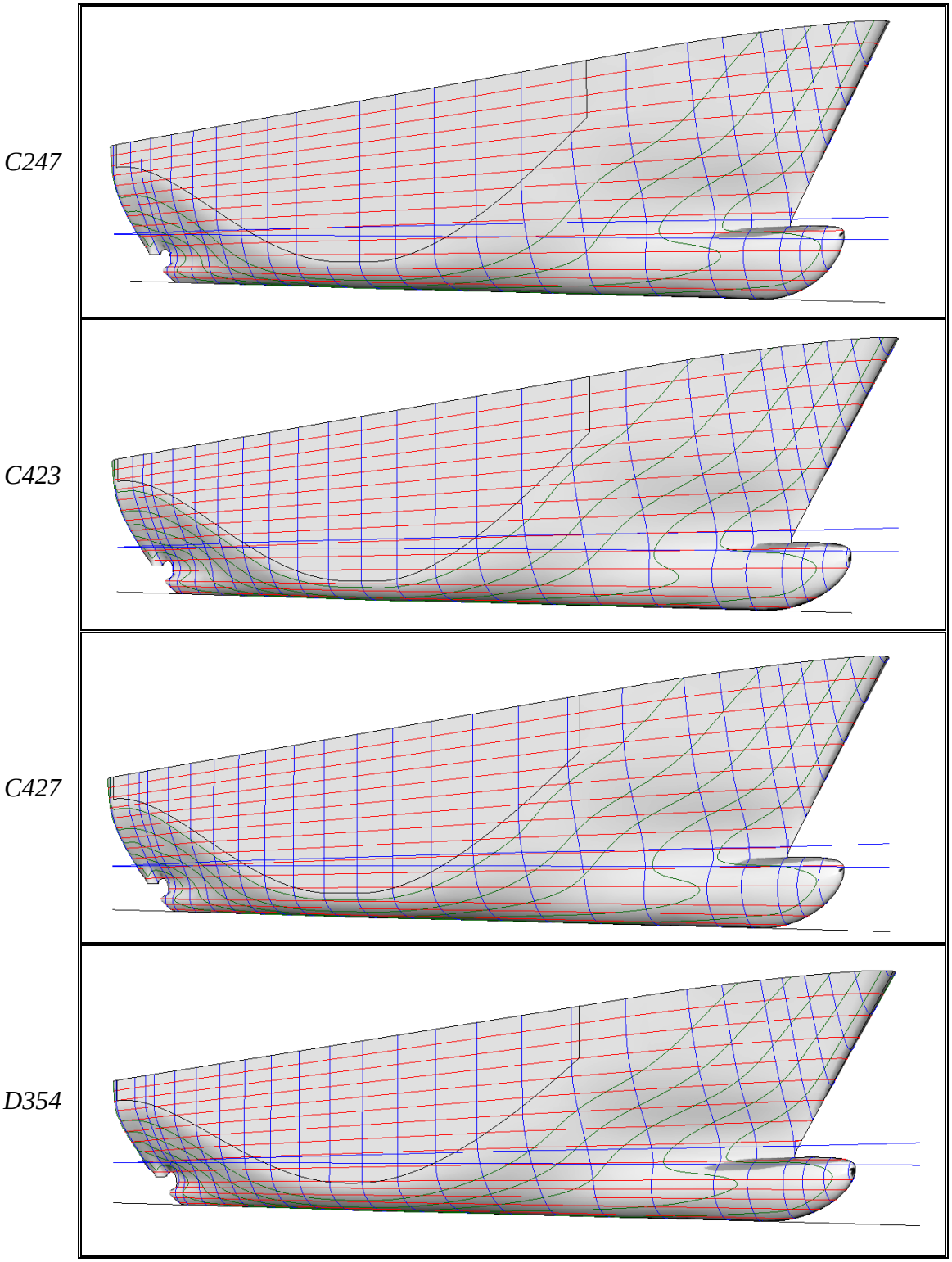

Figure 3.3a. Hull shapes (bow) *C247, C423, C427* & *D354* (second & third optimizations).

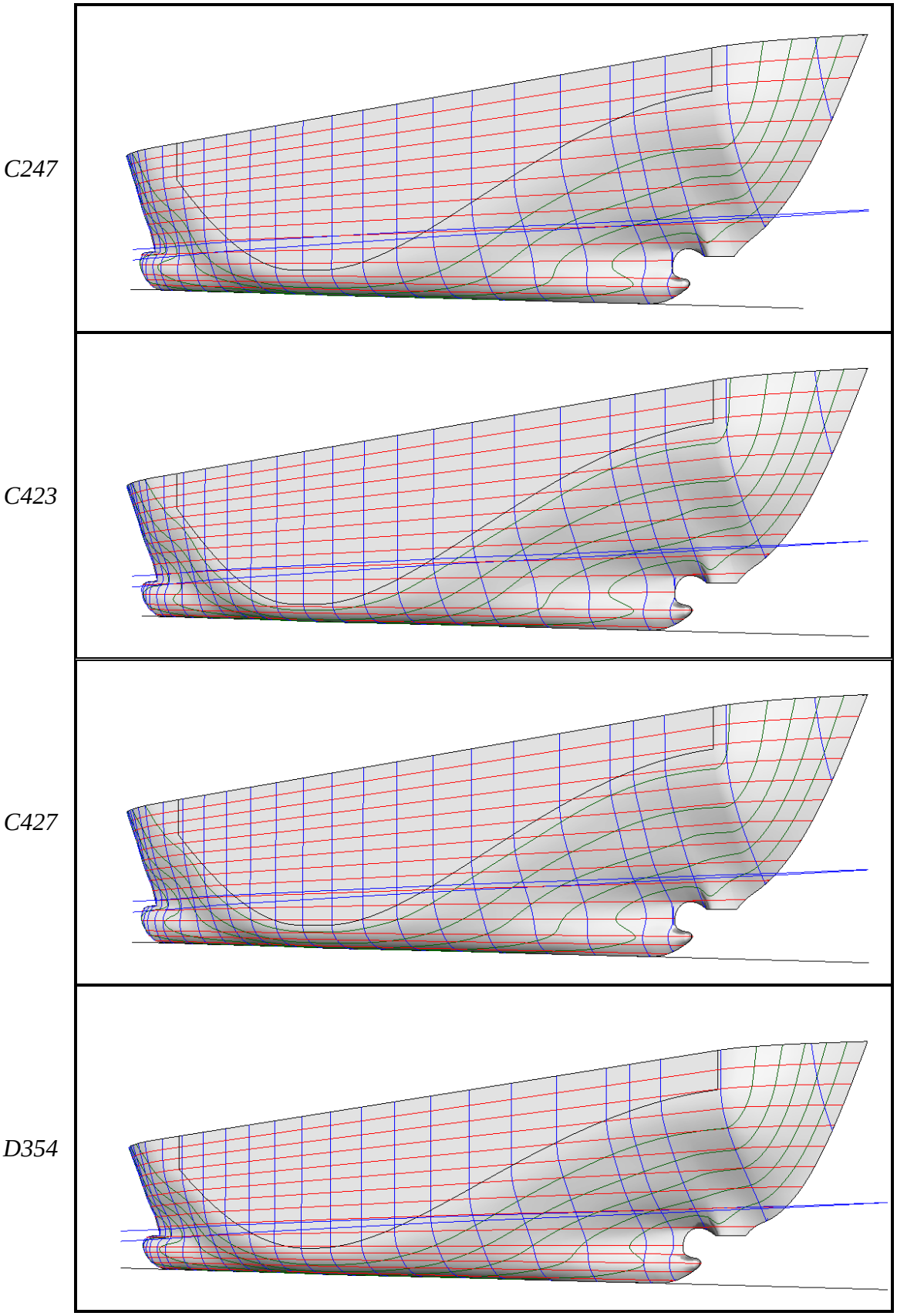

Figure 3.3b. Hull shapes (stern) *C247, C423, C427* & *D354* (second & third optimizations).

3.2 Sensitivity Analysis on the Number of Panels

As with all numerical methods, the accuracy of the solution is directly connected the fineness of the discretization. An infinitively fine discretization should in theory provide the exact solution. In practice errors introduced by the numerical method as well as round of errors reduce the accuracy of the method hence after a certain level of fineness the solution remains unchanged. At that point we say that we obtain a solution indifferent of the grid size. For numerical calculations it is of great importance to determine the required level of discretization since an increased number of panels leads to increased CPU time and RAM requirement. The latter was very important in this investigation since as mentioned in 2.2, the method for calculating the free surface necessitates fine discretizations to obtain satisfactory results.

To determine the necessary number of panels a systematic series of computations were conducted. Using as a reference the number of panels used in previous investigations we determined that a total of 22,000 panels was needed. Following that, 9 cases were examined, were the number of panels in each direction differed 10% between them, from 50% up to 130% of the reference case (run d354a15a). The CPU time as well as the amount of RAM required to store the problem variables is proportional to the square of the number of panels, hence a 10% increase in the number of panels in each direction leads to a 21% increase of panels and 46% increase in RAM and CPU time.

The hull used in this investigation was *D354* at design displacement condition and V_S=15 kn, *Fn*=0.289. In all cases the computational domain (one-half of the domain since the problem is symmetric, see Fig. 2.12) extended 120 m (≈1.5 L_{WL}) fore and 260 m (≈3.0 L_{WL}) aft the fore perpendicular. At its foremost it extended 120 m in transverse direction while at its rear most 150.0m (L_{WL}). The above dimensions were a result of previous investigations (Tzabiras, 2009) and no further test was done on them. The same dimensions were used in all calculations. The trapezoid shape of the domain is the direct result of a ship generated wave pattern. Finally all variables concerning the distribution of the panels (see Tables 2.3 & 2.4) were kept the same, in effect favoring, relatively speaking, the cases with coarser discretization, since the number panels is that way increased in areas of importance. Finally all cases were left to complete 2000 iterations.

Figures 3.4a-c depict the panels on the hull and the water surface, in the immediate vicinity of the hull, for the smallest number of panels case (d354a15b), the reference case (d354a15a) and the case with the highest number of panels (d354a15h).

The total number of panels, RAM requirement as well as the calculated values for the wave resistance coefficient, $|\delta z|$, dynamic sinkage, trim and actual wetted surface for the above mentioned cases are presented in Table 3.4, while the differences in the results between each computation and the one with the fineness discretization (run d354a15h) are given in Table 3.5. Figures 3.5-3.8 depict the results of Table 3.4. Figures 3.9 and 3.10 depict the water elevation contours for cases d354a15b (5,448) (top) and d354a15h (37,648) (bottom) and d354a15a (22,062) (top) and d354a15h (37,648) (bottom) respectively. Figure 3.11 depicts the wave cuts at a distance of 10 [cm] from the side of the hull for the cases of Figs 3.9 & 3.10. Figures 3.12-3.15 depict the convergence histories for C_W, $|\delta z|$, *sinkage* and *trim* for all case.

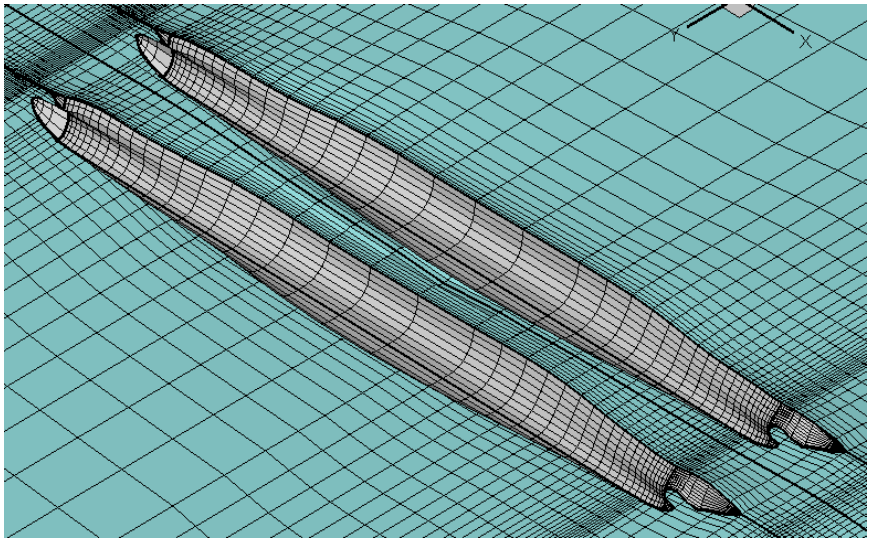

Figure 3.4a. Panels on the hull and water surface, run d354a15b, total number of panels: 5,448.

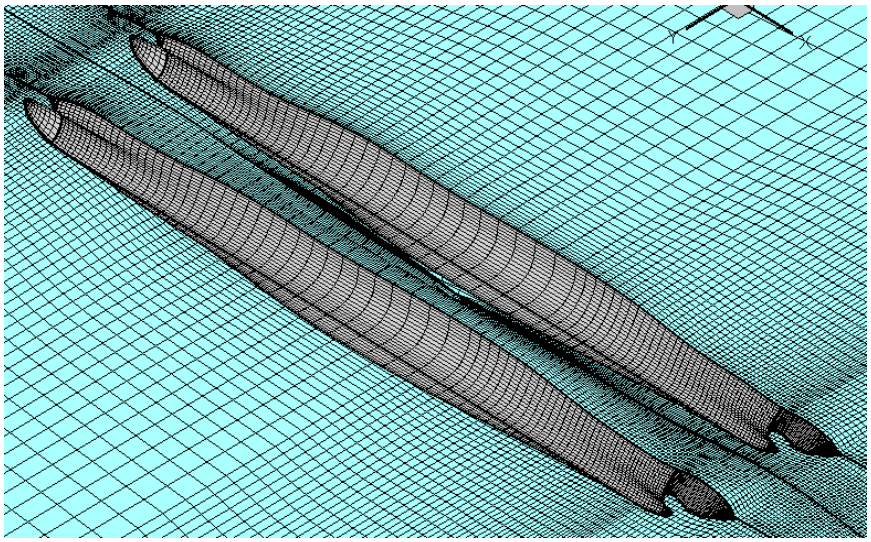

Figure 3.4b. Panels on the hull and water surface, run d354a15a, total number of panels: 22,062.

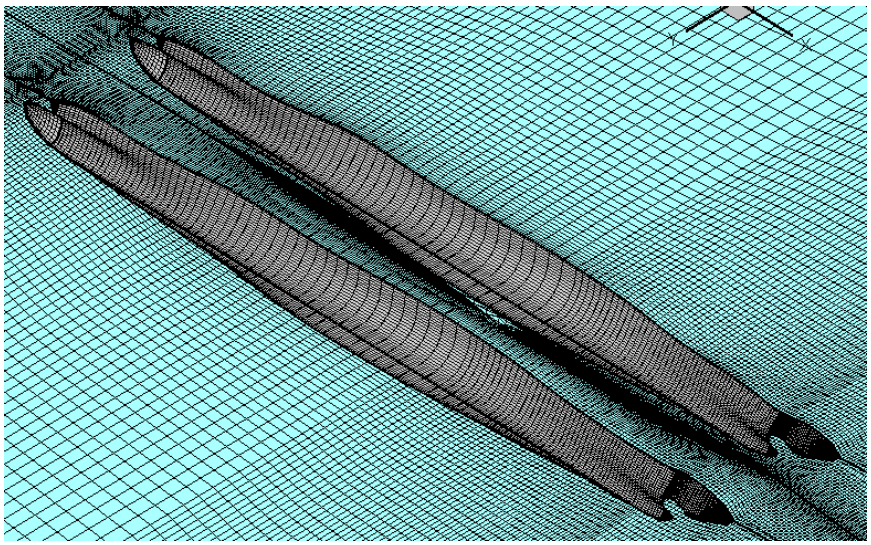

Figure 3.4c. Panels on the hull and water surface, run d354a15h, total number of panels: 37,648.

Table 3.4. Results of the sensitivity analysis.

Run Name	Number of Panels	RAM Usage GB	C_W	$\overline{\lvert\delta z\rvert}$ m	*Sinkage* m	*Trim* deg	*WS* m^2
d354a15b	**5,448**	0.35	1.104E-04	2.220E-02	0.297	0.030	1725.00
d354a15k	**7,836**	0.69	3.724E-04	1.988E-02	0.288	0.035	1726.90
d354a15j	**10,853**	1.32	4.447E-04	1.908E-02	0.284	0.037	1728.00
d354a15c	**14,039**	2.20	5.509E-04	2.018E-02	0.280	0.041	1728.50
d354a15f	**17,685**	3.49	5.676E-04	1.704E-02	0.279	0.041	1727.70
d354a15a	**22,062**	5.41	5.905E-04	1.641E-02	0.280	0.037	1729.40
d354a15g	**26,695**	8.09	6.058E-04	1.621E-02	0.280	0.038	1730.20
d354a15d	**31,909**	11.33	5.919E-04	1.628E-02	0.280	0.037	1730.80
d354a15h	**37,648**	15.77	5.970E-04	1.574E-02	0.279	0.038	1731.10

Table 3.5. Error of the Results.

Run Name	Number of Panels	C_W	$\overline{\lvert\delta z\rvert}$	*Sinkage*	*Trim*	*WS*
d354a15b	**5,448**	-81.50%	41.05%	6.50%	-20.53%	-0.35%
d354a15k	**7,836**	-37.63%	26.31%	3.27%	-7.73%	-0.24%
d354a15j	**10,853**	-25.51%	21.24%	1.80%	-1.60%	-0.18%
d354a15c	**14,039**	-7.72%	28.23%	0.65%	9.87%	-0.15%
d354a15f	**17,685**	-4.93%	8.29%	0.04%	8.80%	-0.20%
d354a15a	**22,062**	-1.10%	4.27%	0.54%	-0.80%	-0.10%
d354a15g	**26,695**	1.48%	2.99%	0.36%	0.27%	-0.05%
d354a15d	**31,909**	-0.86%	3.44%	0.50%	-2.67%	-0.02%

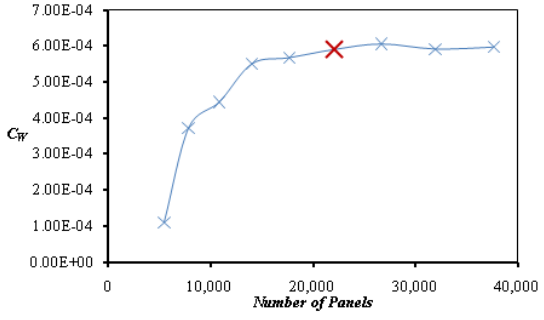

Figure 3.5. Calculated values for C_W.

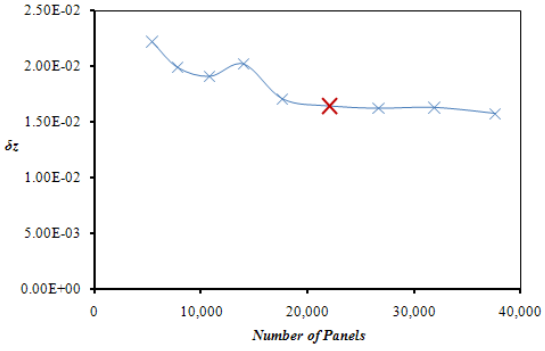

Figure 3.6. Calculated values for $\overline{\lvert\delta z\rvert}$.

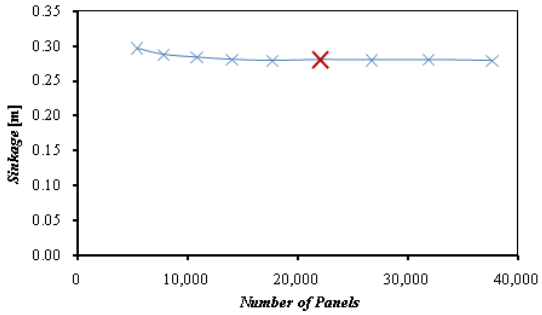

Figure 3.7. Calculated values for sinkage.

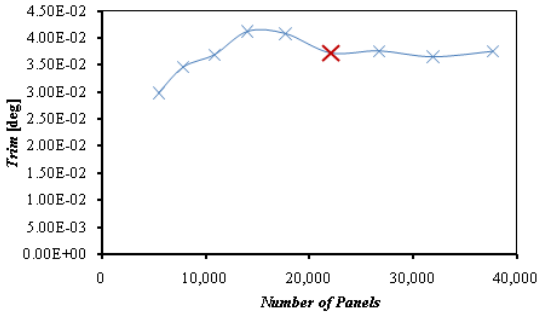

Figure 3.8. Calculated values for trim.

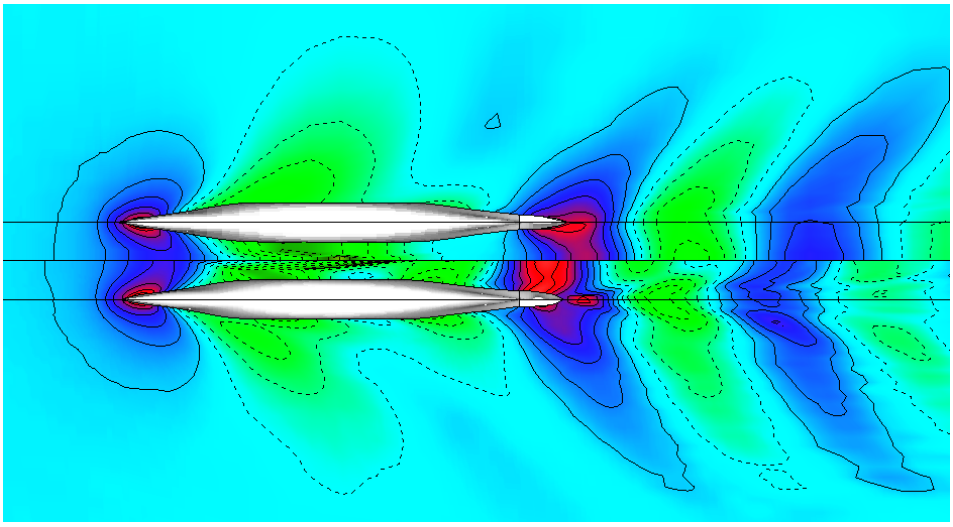

Figure 3.9. Water surface elevation contour, d354a15b (5,448 panels - top) and d354a15h (37,648 panels - bottom).

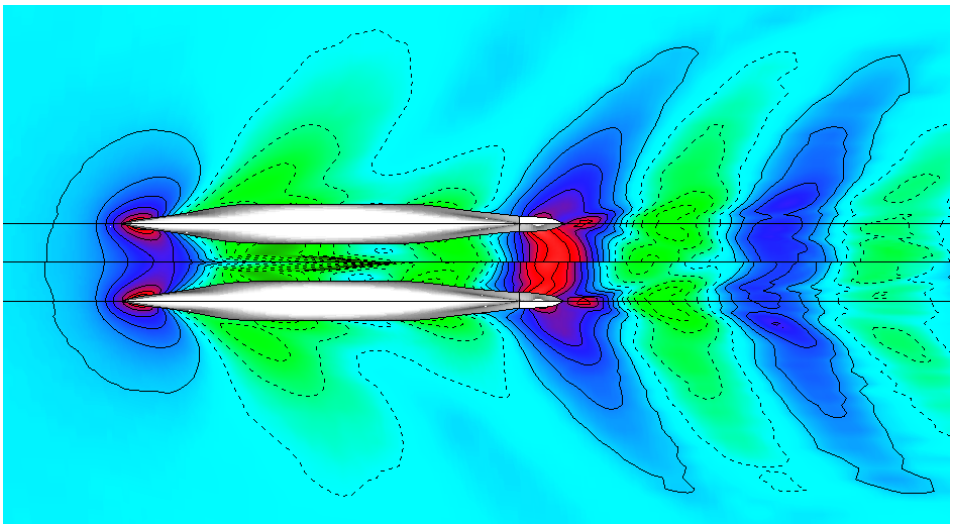

Figure 3.10. Water surface elevation contour, d354a15a (22,062 panels - top) and d354a15h (37,648 panels - bottom).

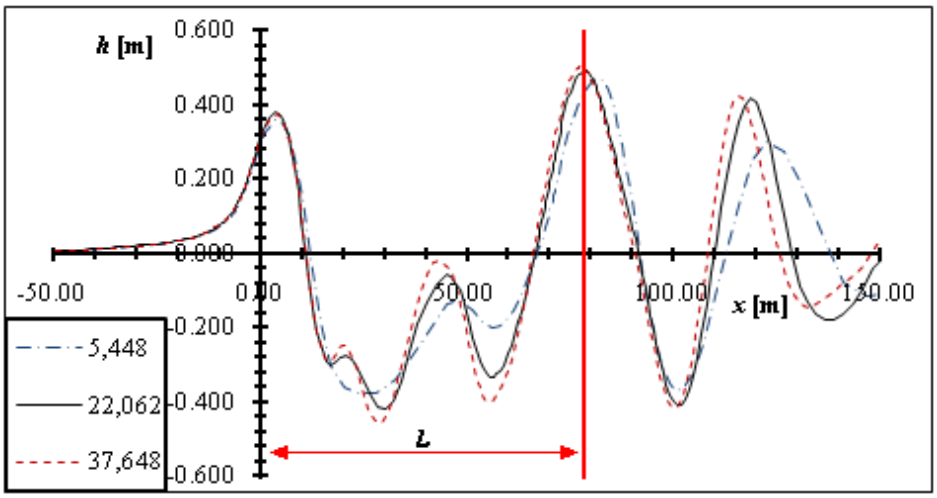

Figure 3.11. Wave cuts, 10 cm from the side of the hull.

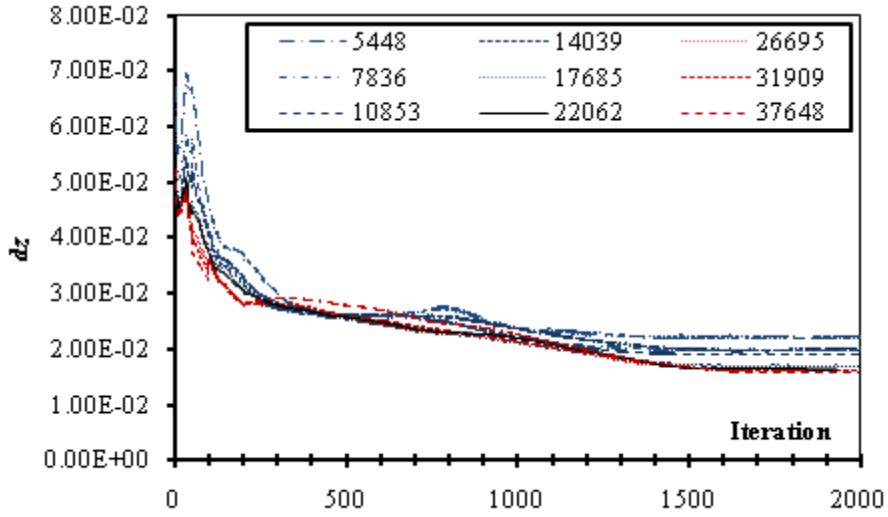

Figure 3.12. Convergence history of the pressure residual $\overline{|\delta z|}$.

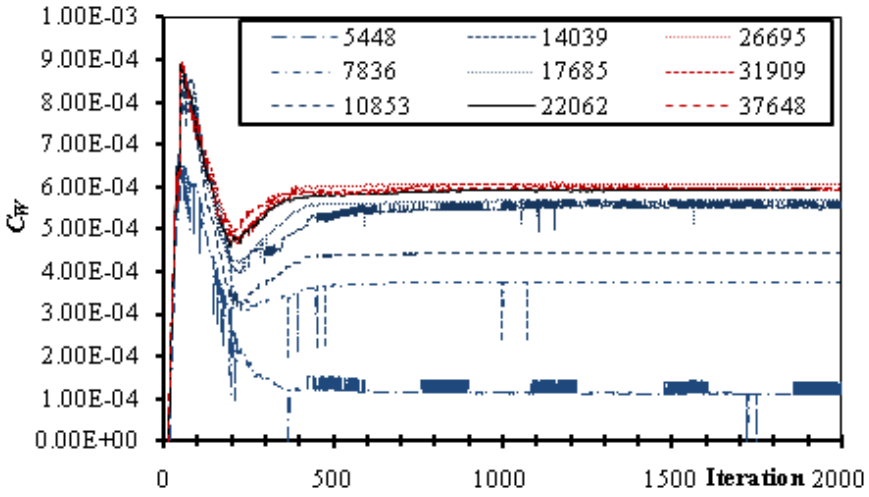

Figure 3.13. Wave resistance coefficient C_W, convergence history.

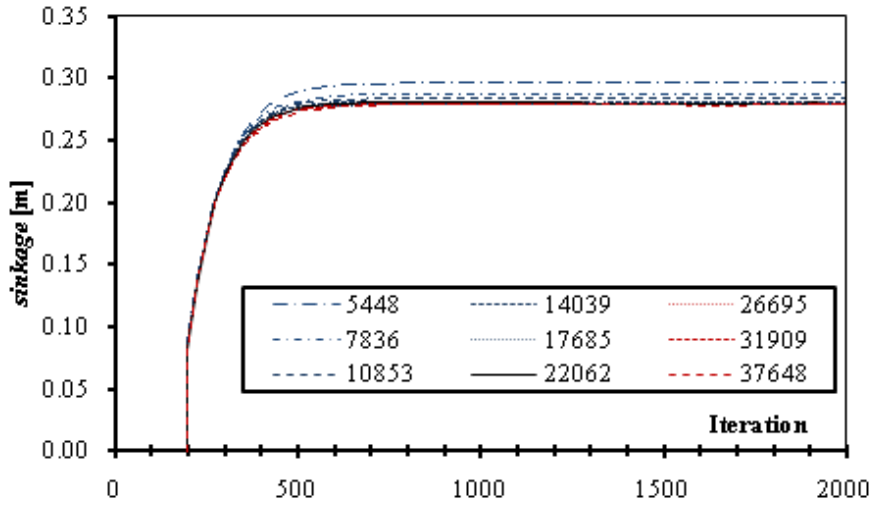

Figure 3.14. *Sinkage* convergence history.

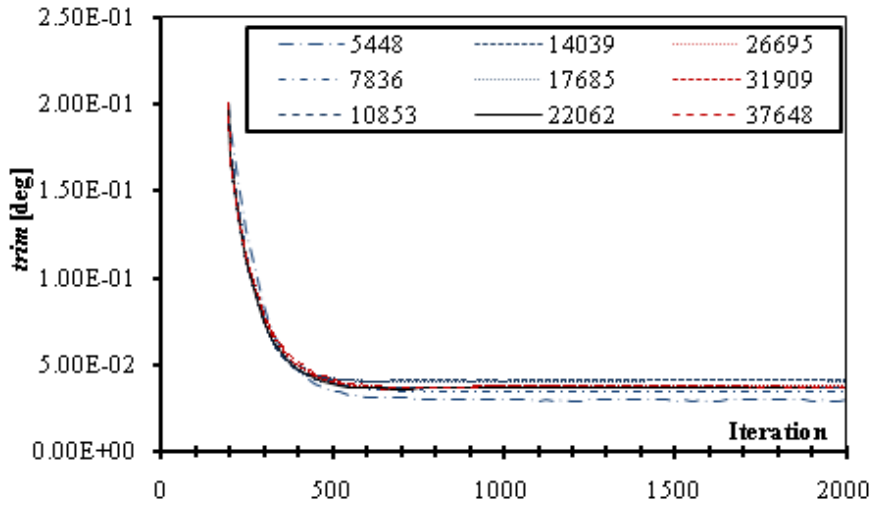

Figure 3.15. *Trim* convergence history.

From Tables 3.4 and 3.5 as well as from figures 3.5-3.8 we were able to confirm that the original estimation that 22,000 panels are adequate stands. In terms of the wave resistance coefficient, the difference between the reference case and the one with the maximum number of panels is about 1% hence an increase in the number of panels is hard to justify keeping in mind the consequences in terms of computing time and RAM requirements. Another interesting find is that even with a substantially smaller number of panels, sinkage and wetted surface can be accurately predicted mainly because they are both affected by the flow field very near the hull, were the dimensions of the panels are smaller in any case. On the other hand trim seems harder to predict although this is probably due to its very small values, since both sinkage and trim are the consequence of the same force. The above findings are quite important since we establish that small numbers of panels can be used when one is only interested in sinkage, trim and wetted surface calculations. An example of the above is in the analysis of experimental results were the actual wetted surface can be used in the calculation of the resistance coefficients (Tzabiras, 2009).

An examination of figures 3.9-3.11 suggests that coarser grids tents to "smooth-out" the wave pattern, while very coarse grids fail completely to calculate some of the smallest features of the waves, for example the small local crest immediately in front of the first trough. Furthermore the wave length seems also to be affected; coarser grids produce waves with greater wave length. The reference case seems to be able to predict all of the wave features but still the wave pattern differs from the one of cases with finer discretization. Although this seems to have a small effect on the wave resistance, it might be of great importance when one is interesting in the shape of the free surface, say to use it as a rigid boundary for viscous calculations (Tzabiras, 2008, 2009).

With regard to convergence rates, data on figures 3.12-3.15 sagest that it is indifferent to the number of panels except for C_W, where the coarser discretizations lead to very different results and the convergence history is very different as well, although convergence is yet achieved after the same amount of iterations. Figures 3.6 and 3.12 suggests that the limiting value for $\overline{|\delta z|}$ is decreased as the number of panels increases although only slightly for more than 17,000 panels. Hence it is confirmed that finer discretization produces more accurate results.

Finally we should point out that the required number of panels is a function of the *Froude* number; in low *Fn* the waves are shorter in length as well as height. The former creates the need for smaller panels in order to maintain an acceptable amount of panels on every wave. Furthermore thin hulls with small entrance angles and minimum flare of the bow bodyplan, tend to create a particularly thin and elongated bow wave hence require many panels in the transverse direction adjacent to the hull. An example is given in Figure 3.16 where the panels at the bow of a racing flat-water kayak are depicted at V_S= 5.153 m/s and *Fn*=0.73.

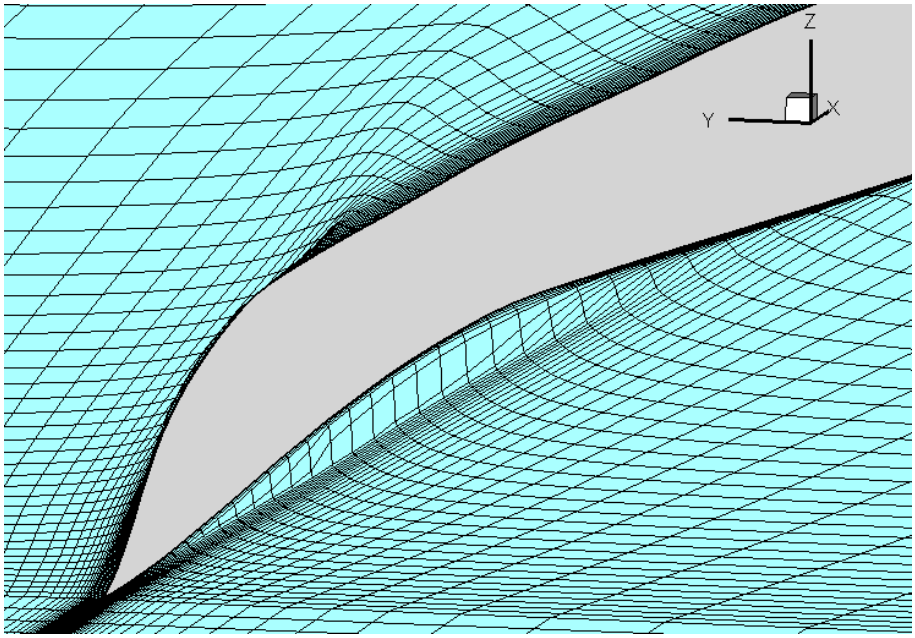

Figure 3.16. Panels near the bow of a racing flat-water kayak, V_S= 5.153 [m/s] and *Fn*=0.73.

3.3 Results of the Test Cases

Using the program described in Section 2 of the present, the wave resistance coefficient C_W, dynamic *sinkage* and *trim* as well as the free water surface were calculated for the test cases of 3.1. The speed range in knots, of the calculations for each test case is presented in Table 3.6. In the following paragraphs indicative results are presented in the form of charts, while all acquired results are numerically presented in the Tables of Appendix F. In the following the calculation of C_W is done using the actual *WS* as numerically calculated by each program, trim is the total (hydrostatic + hydrodynamic) trim, in [deg] and is positive by stern. Furthermore as condition A we refer to the design displacement, while as B we refer to the partial displacement condition.

Table 3.6. Speed range [kn] of the numerical calculations for every test case.

Initial Designs

Hull	Condition	
	A	**B**
A	10.00 ÷ 20.00	15.00
B	10.00 ÷ 20.00	15.00
C	10.00 ÷ 20.00	15.00
D	10.00 ÷ 20.00	15.00
E	10.00 ÷ 20.00	15.00

First Optimization

Hull	Condition	
	A	**B**
B377	14.00, 15.00	14.00, 15.00
B401	10.00 ÷ 20.00	10.00 ÷ 20.00
B422	14.00, 15.00	14.00, 15.00
B428	15.00	15.00

Second Optimization

Hull	Condition	
	A	**B**
C247	10.00 ÷ 16.00	10.00 ÷ 16.00
C423	10.00 ÷ 16.00	10.00 ÷ 16.00
C427	10.00 ÷ 16.00	10.00 ÷ 16.00

Third Optimization

Hull	Condition	
	A	**B**
D354	10.00 ÷ 16.00	10.00 ÷ 16.00

3.3.1 *Results for the Initial Designs*

Figures 3.17-3.21 depict the values of C_W as calculated by means of both the program presented herein and *Shipflow*, for hulls *A, B, C, D* & *E* respectively, at the condition A. Figures 3.22 & 3.23 depict the results of C_W, for hulls *A* to *E* at the condition A, obtained with *Catamaran* and *Shipflow* respectively. Figures 3.24 & 3.25 depict the results of *sinkage* and *trim*, calculated with *Catamaran*.

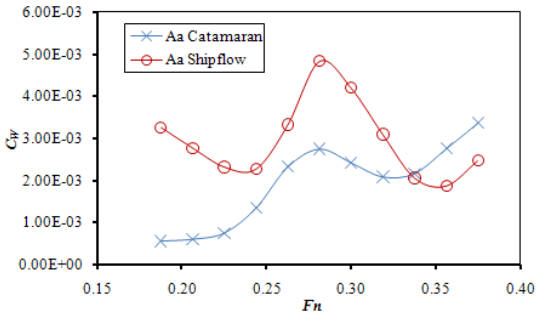

Figure 3.17. Hull *A*, Condition A, C_W.

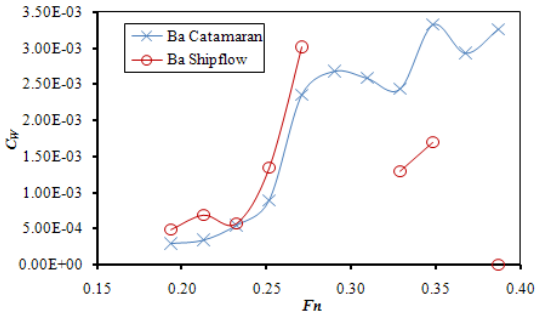

Figure 3.18. Hull *B*, Condition A, C_W.

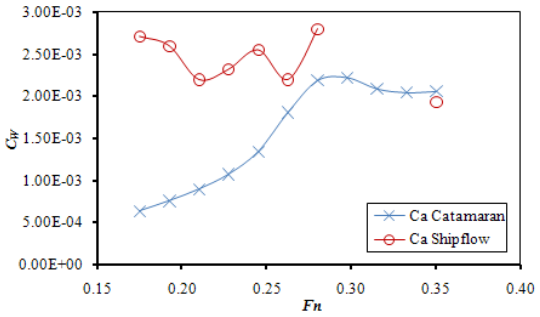

Figure 3.19. Hull *C*, Condition A, C_W.

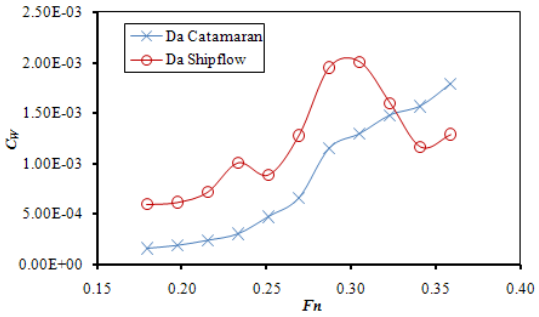

Figure 3.20. Hull *D*, Condition A, C_W.

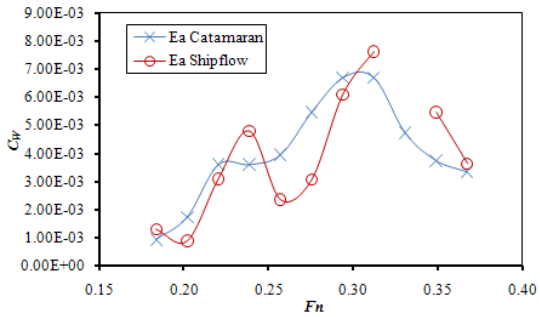

Figure 3.21. Hull *E*, Condition A, C_W.

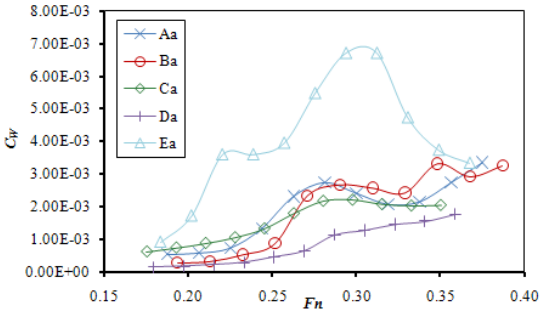

Figure 3.22. Hulls *A, B, C, D* & *E*, Condition A, C_W (*Catamaran*).

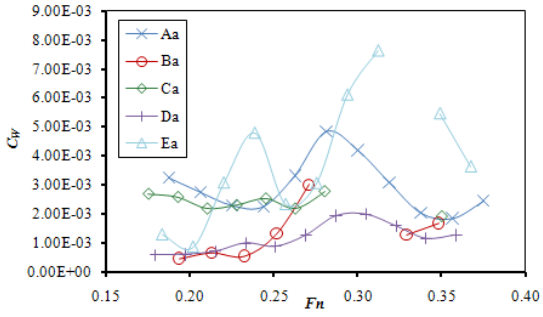

Figure 3.23. Hulls *A, B, C, D* & *E*, Condition A, C_W (*Shipflow*).

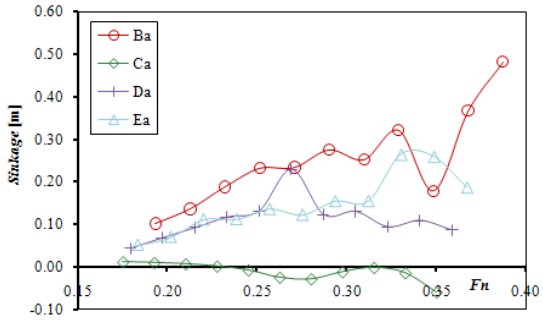

Figure 3.24. Hulls *A, B, C, D* & *E*, Condition A, *Sinkage*.

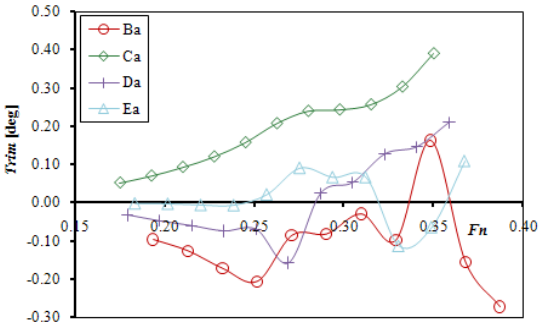

Figure 3.25. Hulls *A, B, C, D* & *E*, Condition A, *Trim*.

3.3.2 *Results for the Designs of the First Optimization*

Figures 3.26 & 3.27 depict the values of C_W, for hull *B401* calculated by means of both programs, at the conditions A & B respectively. Figures 3.28 & 3.29 depict the values of C_W for hull *B401* at both conditions, calculated with *Catamaran* & *Shipflow* respectively. Figures 3.30 & 3.31 depict the values of *sinkage* for hull *B401* at the conditions A & B respectively. Figures 3.32 & 3.33 depict the values of *trim* for hull *B401* at the conditions A & B respectively. Figure 3.34 depicts the results for C_W, for hulls *B377, B401, B422* & *B428* at the condition A, calculated with *Catamaran*, while Figure 3.35 presents the respective data calculated with *Shipflow*. In the later two figures, the most efficient of the initial hulls, hull *D*, is included for comparative reasons.

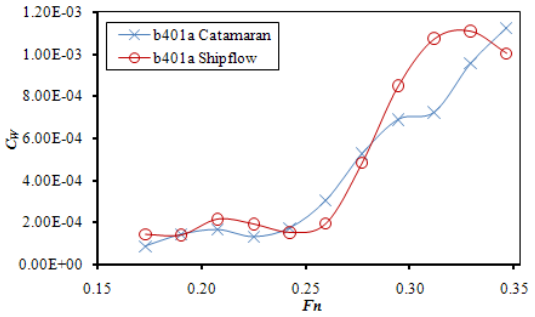

Figure 3.26. Hull *B401*, Condition A, C_W.

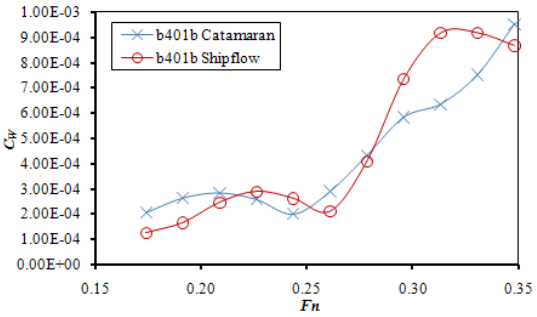

Figure 3.27. Hull *B401*, Condition B, C_W.

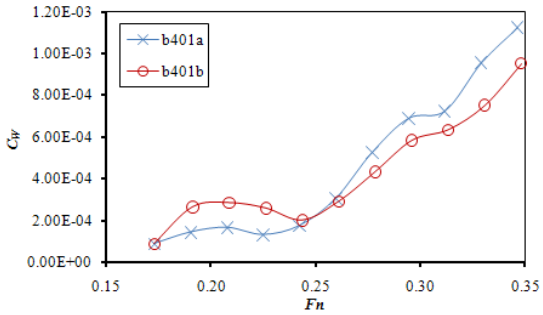

Figure 3.28. Hull *B401*, Conditions A & B, C_W (*Catamaran*).

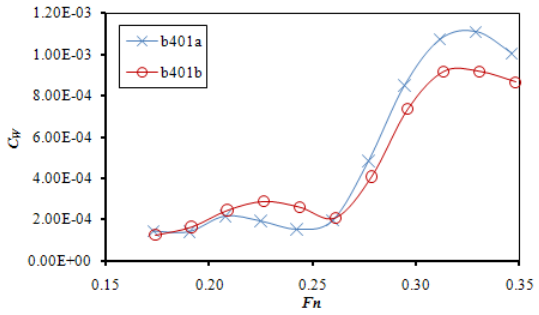

Figure 3.29. Hull *B401*, Conditions A & B, C_W (*Shipflow*).

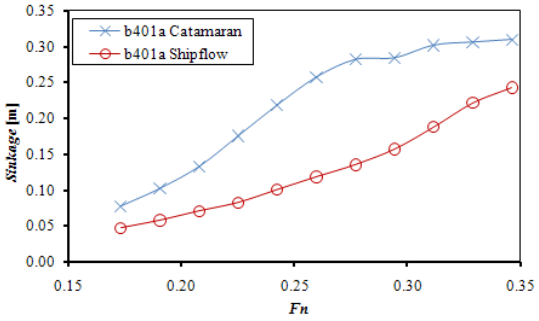

Figure 3.30. Hull *B401*, Condition A, *Sinkage*.

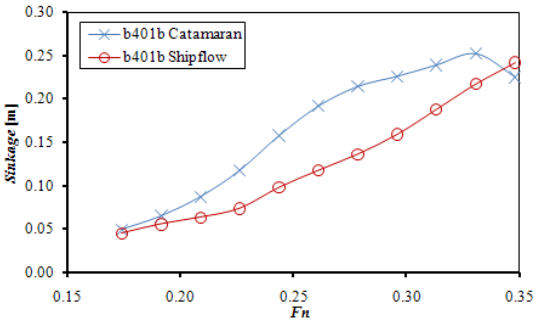

Figure 3.31. Hull *B401*, Condition B, *Sinkage*

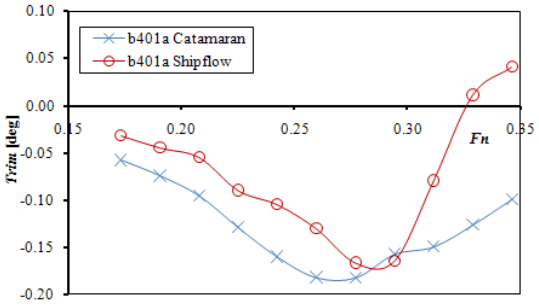

Figure 3.32. Hull *B401*, Condition A, *Trim*.

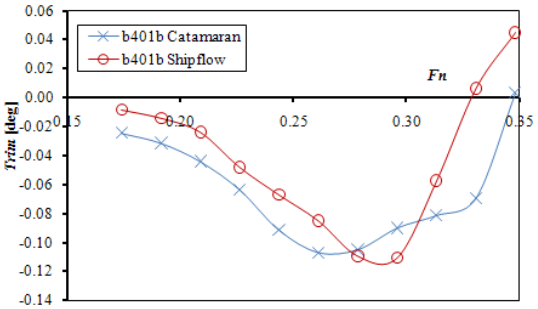

Figure 3.33. Hull *B401*, Condition B, *Trim*.

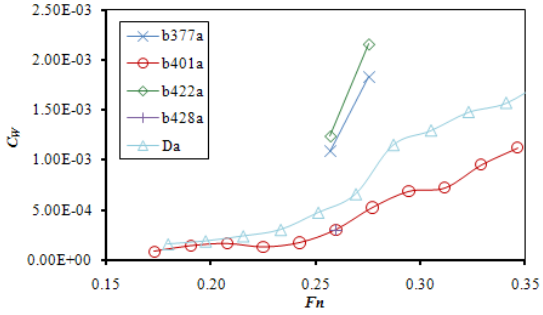

Figure 3.34. Hulls *B377*, *B401*, *B422*, *B428* & *D*, Condition A, C_W (*Catamaran*).

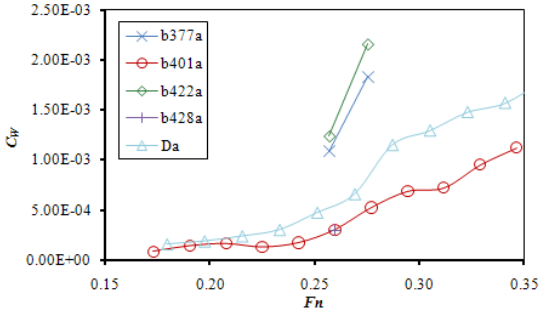

Figure 3.35. Hulls *B377*, *B401*, *B422*, *B428* & *D*, Condition A, C_W (*Shipflow*).

3.3.3 *Results for the Designs of the Second & Third Optimization*

Figures 3.36 & 3.37 depict the values of C_W for hull *C247* calculated by means of both programs, at the conditions A & B respectively. Figures 3.38 & 3.39 depict the values of C_W for hull *C423*, at the conditions A & B respectively. Figures 3.40 & 3.41 depict the values of C_W for hull *C427*, at the conditions A & B respectively. Figures 3.42 & 3.43 depict the values of C_W for hull *D354*, at the conditions A & B respectively. Figures 3.44 & 3.45 depict the results for C_W, for hulls *C247*, *C423*, *C427*& *D354*, at the condition A, calculated with *Catamaran* & *Shipflow* respectively. Figures 3.46 & 3.47 present the respective data for the Condition B. In the later four figures, the most efficient hull of the first optimization, hull *B401*, is included for comparative reasons. Figures 3.48 & 3.49 depict the results for *sinkage*, for hulls *C247*, *C423*, *C427*& *D354*, calculated with *Catamaran*, at the condition A & B respectively. Figures 3.50 & 3.51 present the respective data for *trim*.

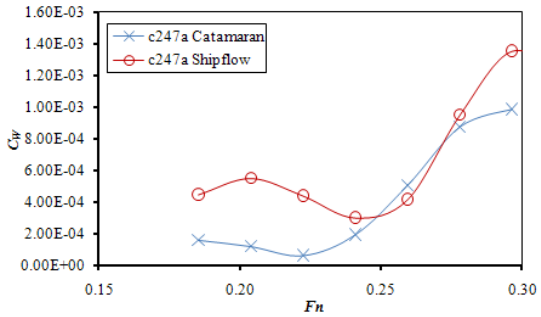

Figure 3.36. Hull *C247*, Condition A, C_W.

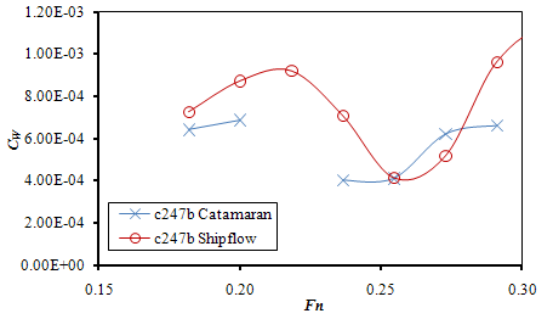

Figure 3.37. Hull *C247*, Condition B, C_W.

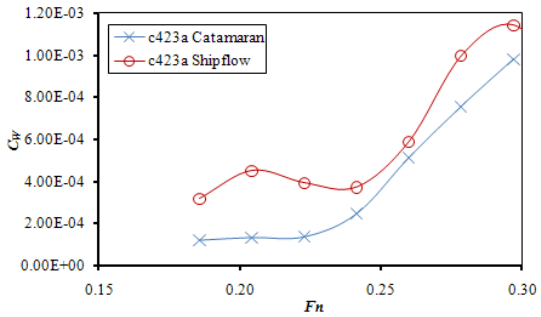

Figure 3.38. Hull *C423*, Condition A, C_W.

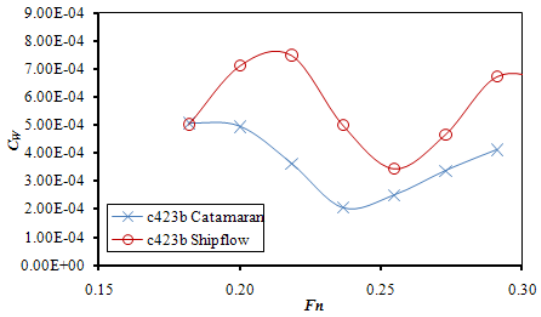

Figure 3.39. Hull *C423*, Condition B, C_W.

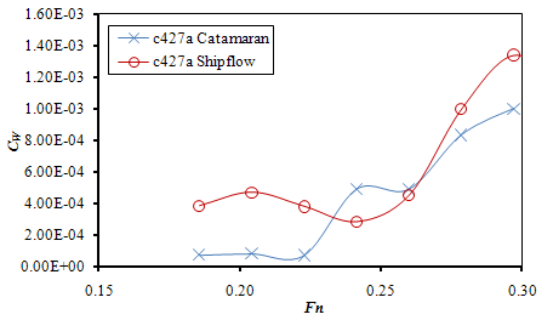

Figure 3.40. Hull *C427*, Condition A, C_W.

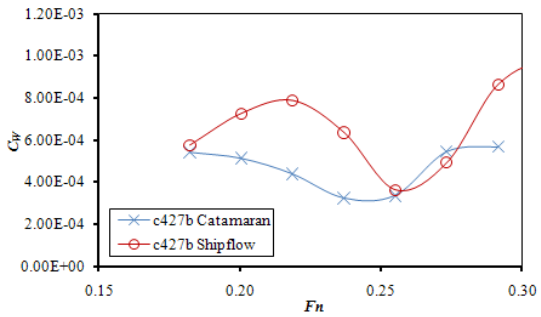

Figure 3.41. Hull *C427*, Condition B, C_W.

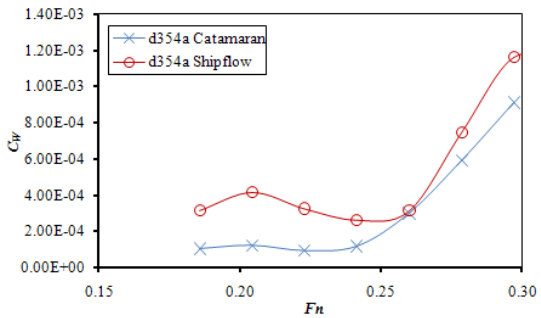

Figure 3.42. Hull *D354*, Condition A, C_W.

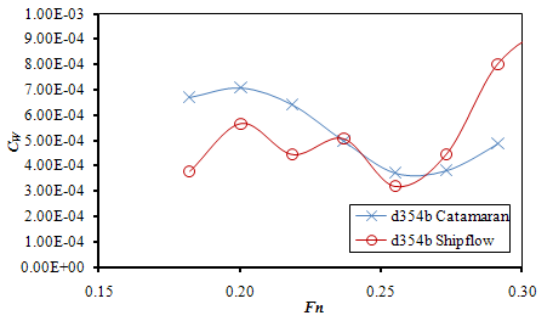

Figure 3.43. Hull *D354*, Condition B, C_W.

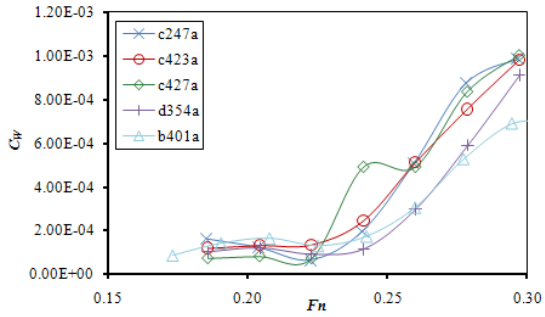

Figure 3.44. Hulls *C247*, *C423*, *C427*, *D354* & *B401*, Condition A, C_W (*Catamaran*).

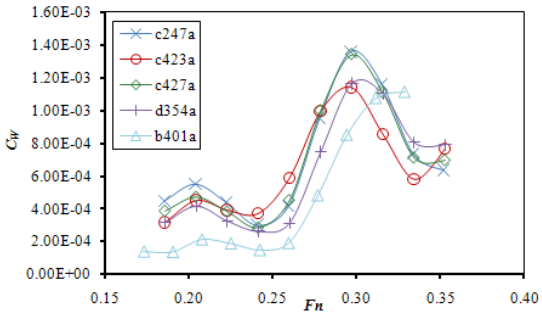

Figure 3.45. Hulls *C247*, *C423*, *C427*, *D354* & *B401*, Condition A, C_W (*Shipflow*).

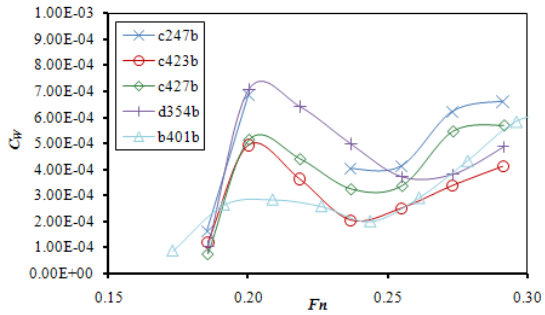

Figure 3.46. Hulls *C247*, *C423*, *C427*, *D354* & *B401*, Condition B, C_W (*Catamaran*).

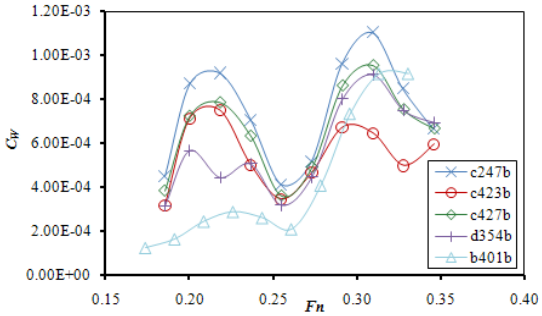

Figure 3.47. Hulls *C247*, *C423*, *C427*, *D354* & *B401*, Condition B, C_W (*Shipflow*).

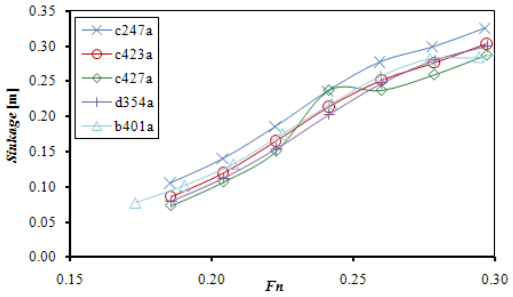

Figure 3.48. Hulls *C247*, *C423*, *C427* & *D354*, Condition A, *Sinkage*.

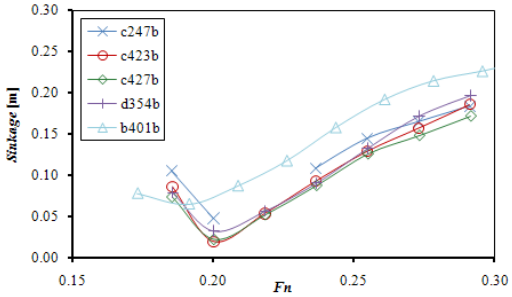

Figure 3.49. Hulls *C247*, *C423*, *C427* & *D354*, Condition B, *Sinkage*.

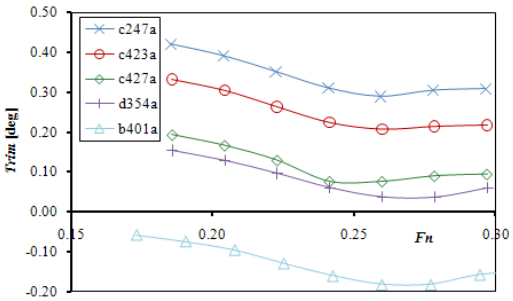

Figure 3.50. Hulls *C247*, *C423*, *C427* & *D354*, Condition A, *Trim*.

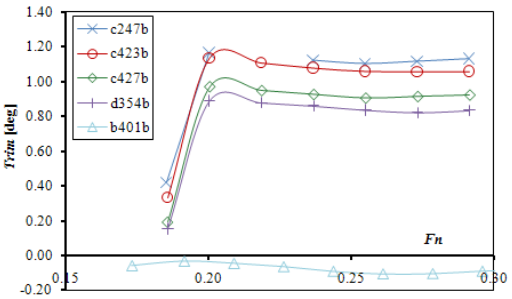

Figure 3.51. Hulls *C247*, *C423*, *C427* & *D354*, Condition B, *Trim*.

A further series of numerical experiments was conducted in order to validate the effect of the seat configuration for the podded propulsor, on the wave resistance, sinkage and trim. The experiments were done on all four hulls of the third and fourth optimization and the hull shapes were modified at the stern area (Section (5)). The results are presented in table form in Appendix F. The results for hull *D354* are presented in the following figures. Figures 3.52 & 3.53 depict the values of C_W for hull *D354*, with and without the pod seat arrangement, at the conditions A & B respectively. Figures 3.54 & 3.55 depict the values of *sinkage* for hull *D354*, with and without the pod seat arrangement, at the conditions A & B respectively. Finally Figures 3.56 & 3.57 depict the values of *trim* for hull *D354*, with and without the pod seat arrangement, at the conditions A & B respectively.

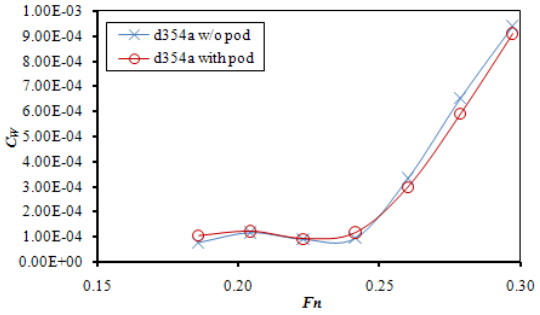

Figure 3.52. Hull *D354* with and without the pod seating configuration, Condition A, C_W.

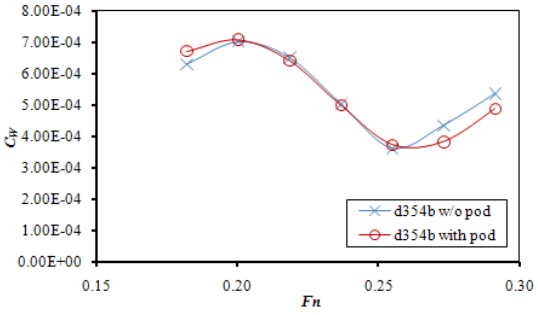

Figure 3.53. Hulls Hull *D354* with and without the pod seating configuration, Condition B, C_W.

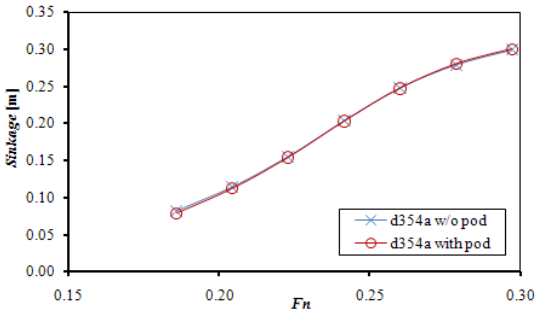

Figure 3.54. Hull *D354* with and without the pod seating configuration, Condition A, *Sinkage*.

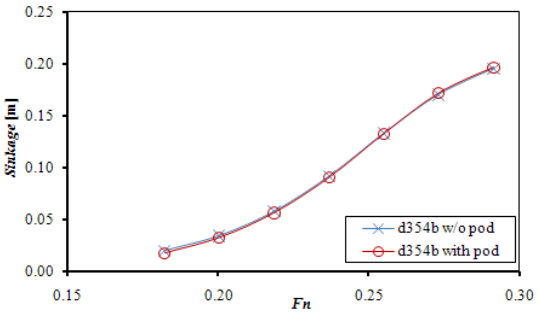

Figure 3.55. Hull *D354* with and without the pod seating configuration, Condition B, *Sinkage*.

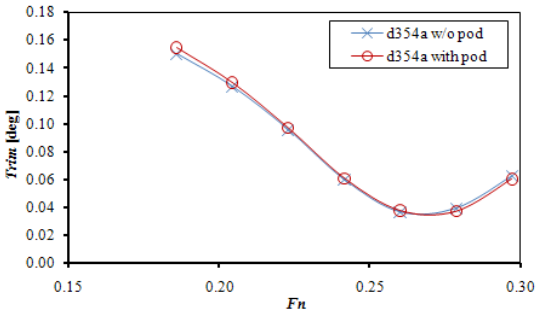

Figure 3.56. Hull *D354* with and without the pod seating configuration, Condition A, *Trim*.

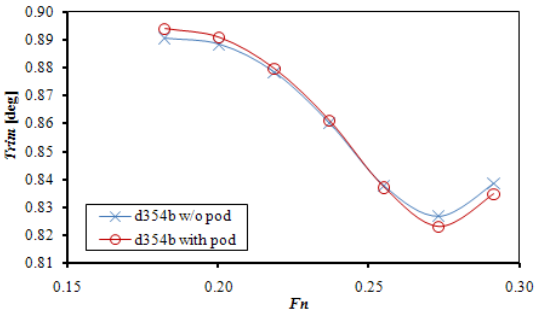

Figure 3.57. Hull *D354* with and without the pod seating configuration, Condition B, *Trim*.

3.3.4 *Fee-surface Elevation Contours & Wave-cuts*

Using the shape of free-surface calculated by solving the potential problem we can present the surface elevation contour as well as wave-cuts. In the following figures, the contours have the same range of ± 0.80 m and the levels of the contour are set apart by 0.08 m. The wave-cuts were acquired as the intersection of the water surface with a vertical, longitudinal plane, parallel to the ship's center line. The cutting plane is located in all cases 0.10 m of the maximum waterline beam, which coincides with the overall beam.

In Figures 3.58-.360, the contours for the most and least efficient of the initial designs (*D* and *E*), the first optimization (*B401* and *B422*) and the third and fourth oprimizations (*D354* and *C247*) respectively are presented. In all cases the condition is A and the speed is 15 kn. The most efficient hull is presented on the top half, while the least efficient hull is presented on the lower half of each figure. In Figure 3.61 the contours referring to the condition A (top) and the condition B (bottom) are presented for hull *D354*, at V_S=15 kn, *Fn*=0.279. Finally Figure 3.62 depicts the contours for hull *D354*, condition A, at V_S=13 kn, *Fn*=0.242 (top) and V_S=15 kn, *Fn*=0.279.

Figure 3.63 depicts the wave-cuts for the initial hulls at V_S=15 kn, condition A while Figure 3.64 depicts the wave-cuts for the most efficient (*D*) and the least efficient (*E*) of the initial hulls. Figure 3.65 depicts the wave-cuts for the initial hulls at V_S=15 kn, condition B. Figure 3.66 depicts the wave-cuts hull *D* at V_S=15 kn and conditions A and B.

Figure 3.67 depicts the wave-cuts for the hulls of the first optimization as well as the most efficient of the initial hulls, *D*, at V_S=15 kn, condition A, while Figure 3.68 depicts the wave-cuts for the most efficient (*B401*) and the least efficient (*B422*) hulls of first the optimization. Figure 3.69 depicts the wave-cuts for the hulls of the first optimization as well as the most efficient of the initial hulls, *D*, at V_S=15 kn, condition B. Figure 3.70 depicts the wave-cuts for hull *B401* at V_S=15 kn and conditions A and B.

Figure 3.71 depicts the wave-cuts for the hulls of the second and third optimizations as well as the most efficient hull of the first optimization, *B401*, at V_S=15 kn, condition A while Figure 3.72 depicts the wave-cuts for the most efficient (*D354*) and the least efficient (*C247*) hulls. Figure 3.73 depicts the wave-cuts for the hulls of the second and third optimizations as well as the most efficient hull of the first optimization, *B401*, at V_S=15 kn, condition B. Figure 3.74 depicts the wave-cuts for hull *D354* at V_S=15 kn, *Fn*=0.279 and conditions A and B. Figure 3.75 depicts the wave-cuts for hull *D354* at V_S=11, 13, 15 kn, *Fn*=0.204, 0.242, 0.279 and condition A. Finally in Figure 3.76 the wave-cuts at V_S=15 kn, *Fn*=0.279 and condition A for the hull *D354* with and without the pod seat configuration are presented.

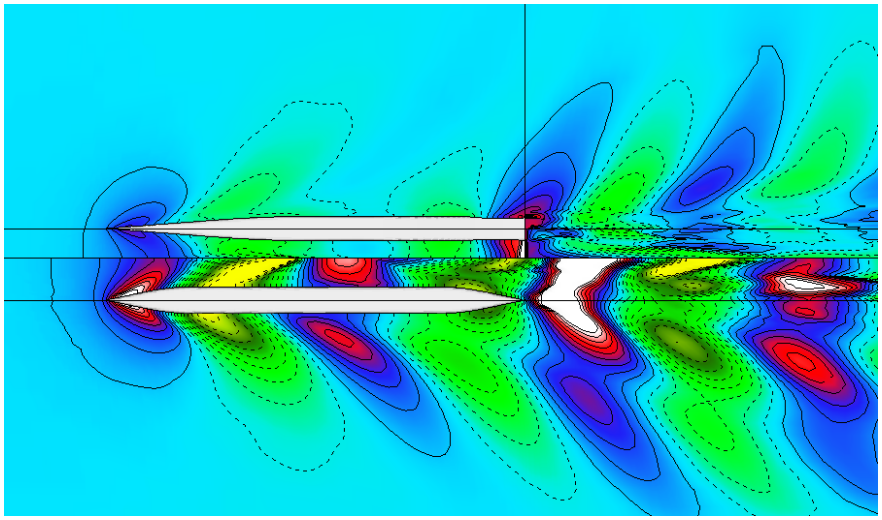

Figure 3.58. Free-surface elevation contours. Top half: hull *D*, V_S=15 kn, *Fn*=0.269, Condition A. Lower half: hull *E*, V_S=15 kn, *Fn*=0.276, Condition A.

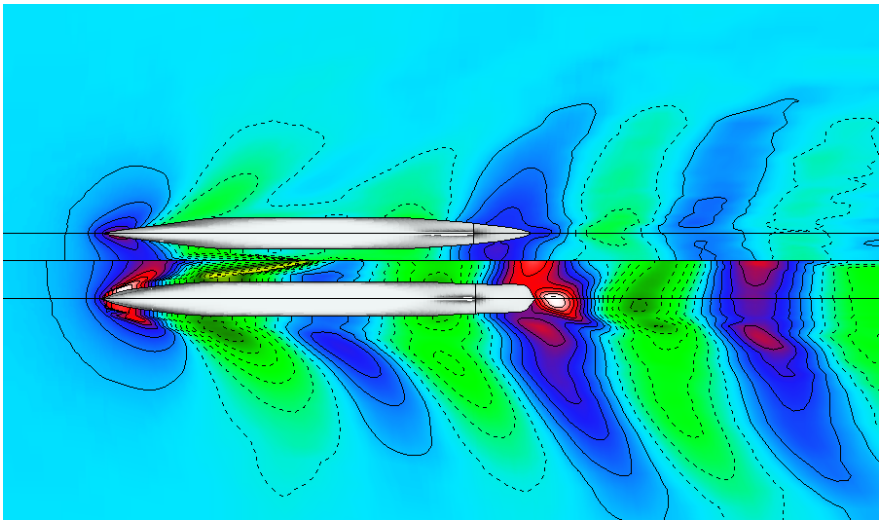

Figure 3.59. Free-surface elevation contours. Top half: hull *B401*, V_S=15 kn, *Fn*=0.260, Condition A. Lower half: hull *B422*, V_S=15 kn, *Fn*=0.275, Condition A.

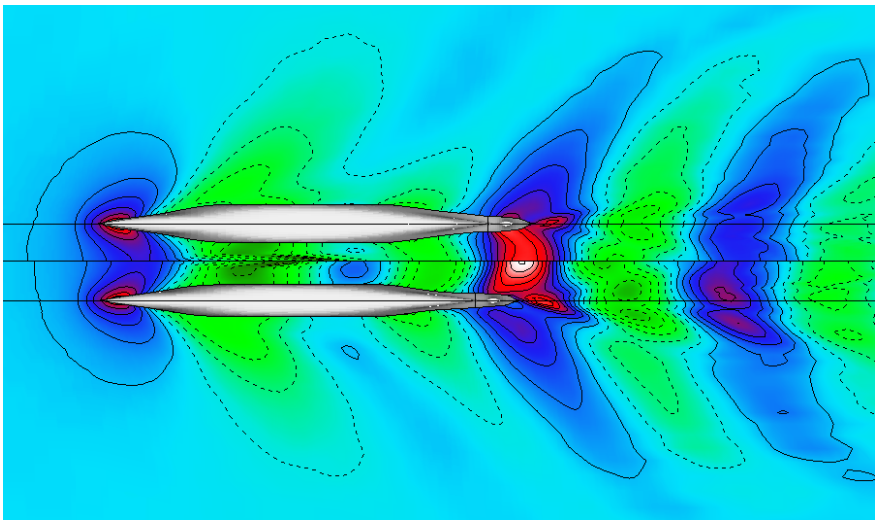

Figure 3.60. Free-surface elevation contours. Top half: hull *D354*, V_S=15 kn, *Fn*=0.279, Condition A. Lower half: hull *C247*, V_S=15 kn, *Fn*=0.278, Condition A.

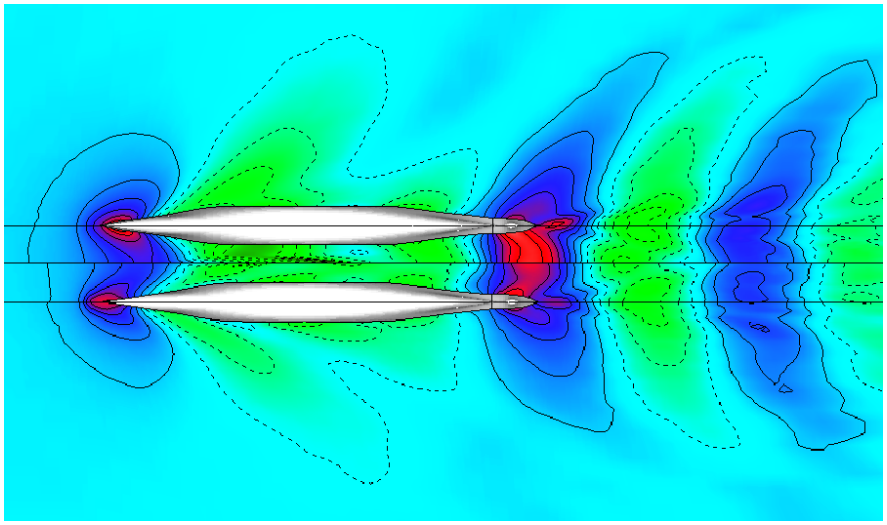

Figure 3.61. Free-surface elevation contours. Top half: hull *D354*, V_S=15 kn, *Fn*=0.279, Condition A. Lower half: hull *D354*, V_S=15 kn, *Fn*=0.279, Condition B.

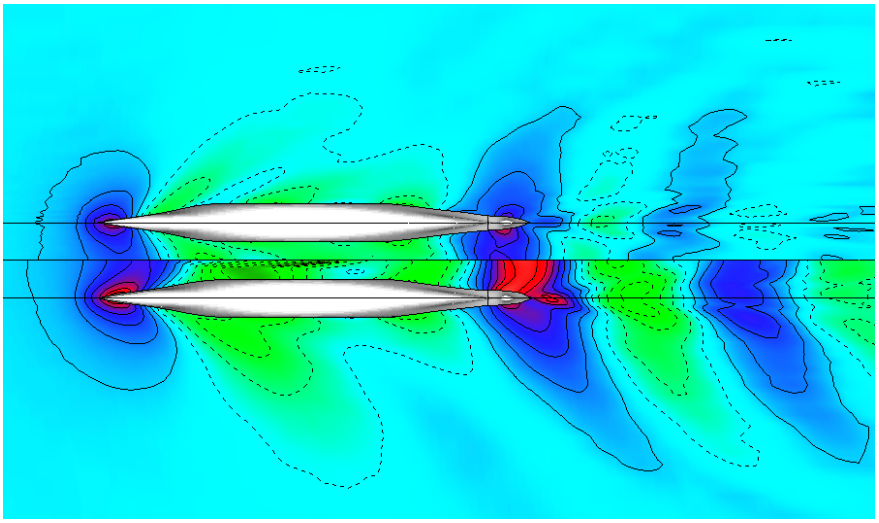

Figure 3.62. Free-surface elevation contours. Top half: hull *D354*, V_S=13 kn, *Fn*=0.242, Condition A. Lower half: hull *D354*, V_S=15 kn, *Fn*=0.279, Condition A.

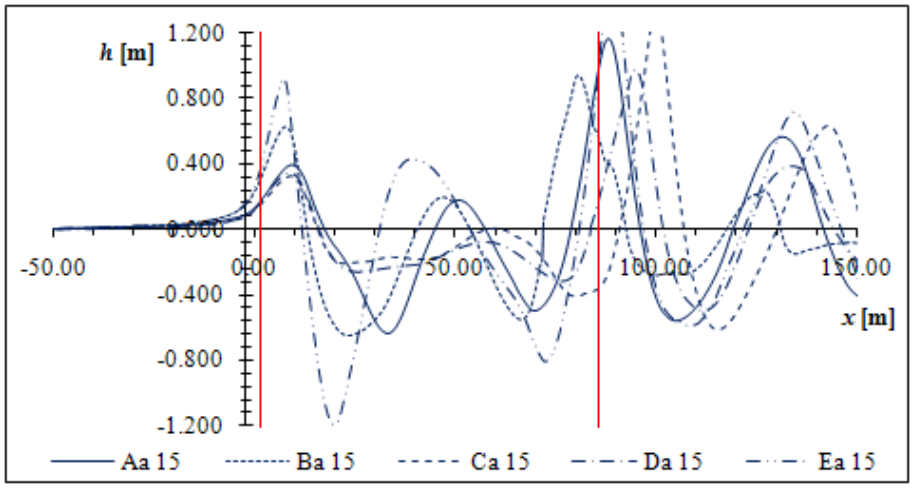

Figure 3.63. Wave-cuts. V_S= 15 kn, Condition A, hulls *A* (*Fn*=0.281), *B* (*Fn*=0.290), *C* (*Fn*=0.263), *D* (*Fn*=0.269) & *E* (*Fn*=0.276).

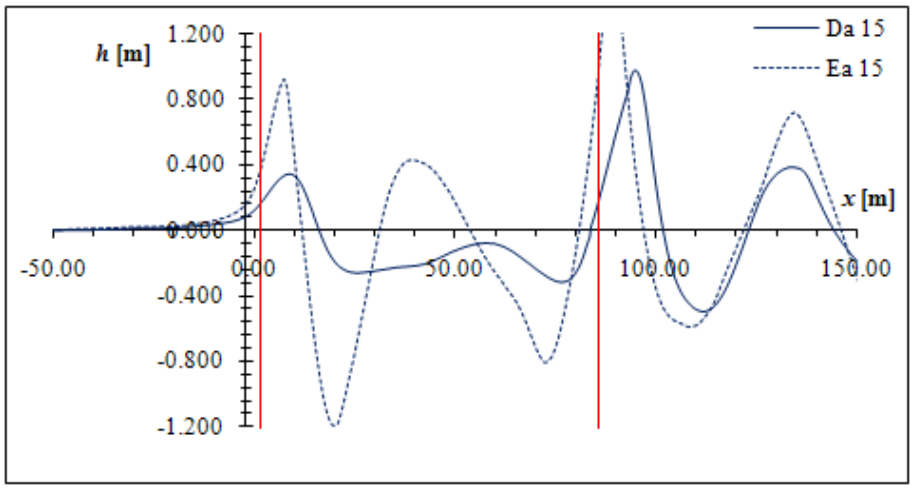

Figure 3.64. Wave-cuts. V_S= 15 kn, Condition A, hulls *D* (*Fn*=0.269) & *E* (*Fn*=0.276).

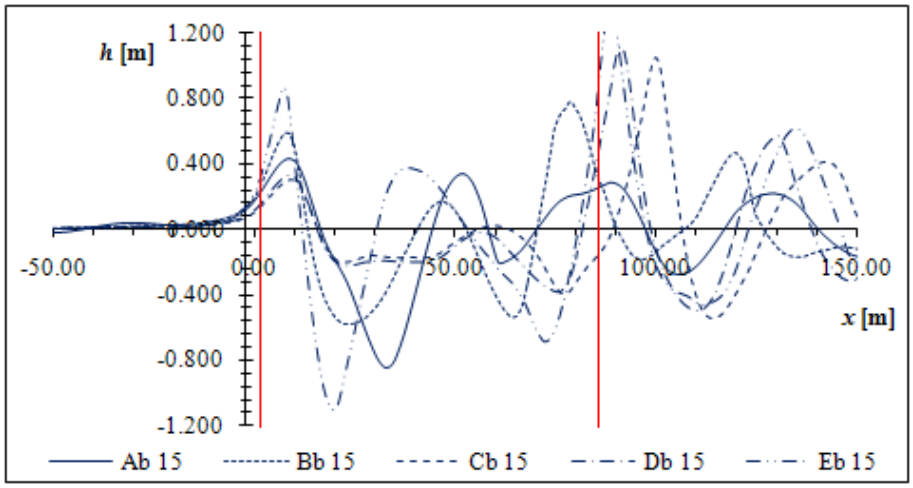

Figure 3.65. Wave-cuts. V_S= 15 kn, Condition B, hulls *A* (*Fn*=0.281), *B* (*Fn*=0.290), *C* (*Fn*=0.263), *D* (*Fn*=0.269) & *E* (*Fn*=0.276).

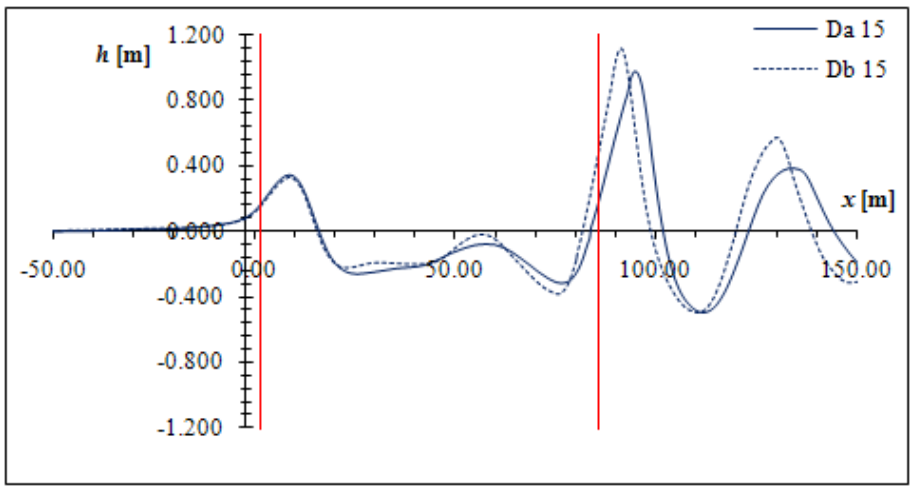

Figure 3.66. Wave-cuts. Hull *D*, V_S= 15 kn, *Fn*=0.269, Conditions A & B.

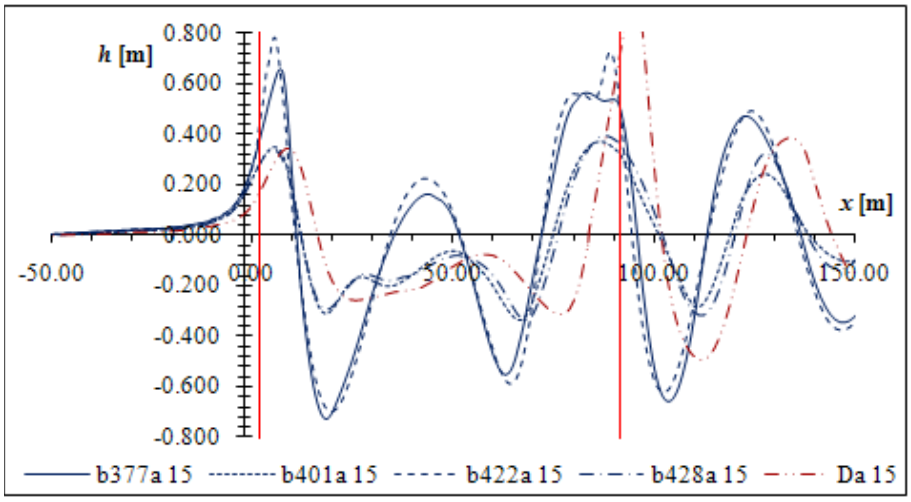

Figure 3.67. Wave-cuts. V_S= 15 kn, Condition A, hulls *B377* (*Fn*=0.276), *B401* (*Fn*=0.260), *B422* (*Fn*=0.275), *B428* (*Fn*=0.260) & *D* (*Fn*=0.269).

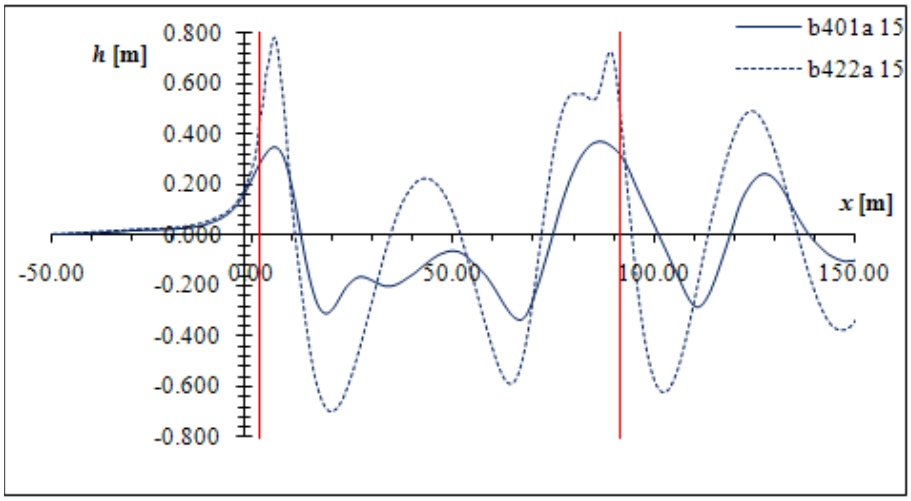

Figure 3.68. Wave-cuts. V_S= 15 kn, Condition A, hulls *B401* (*Fn*=0.260) & *B422* (*Fn*=0.275).

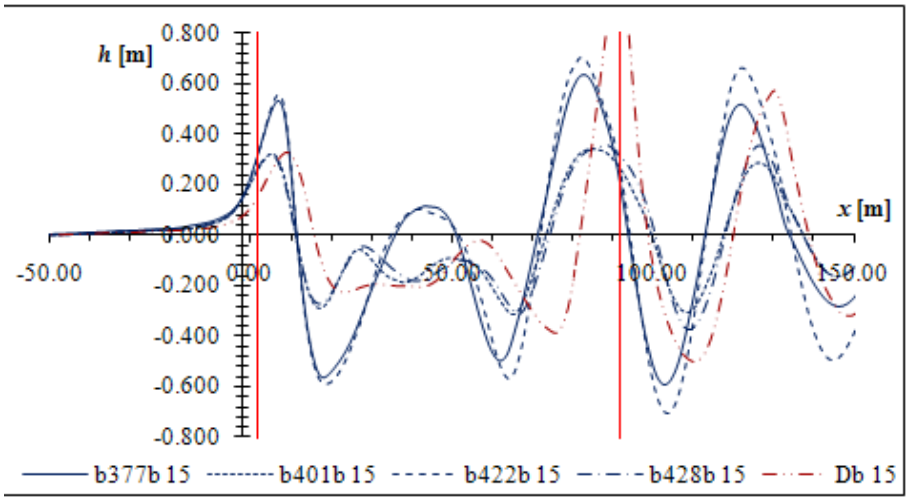

Figure 3.69. Wave-cuts. V_S= 15 kn, Condition B, hulls *B377* (*Fn*=0.276), *B401* (*Fn*=0.260), *B422* (*Fn*=0.275), *B428* (*Fn*=0.260) & *D* (*Fn*=0.269).

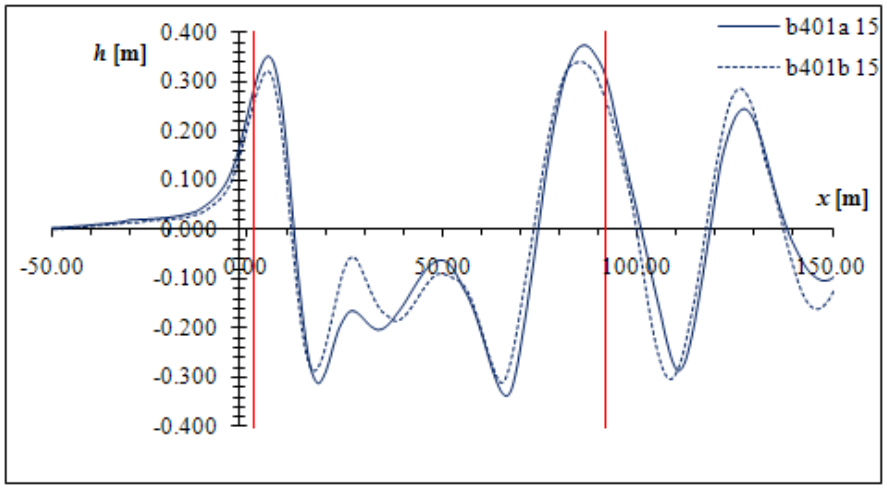

Figure 3.70. Wave-cuts. Hull *B401*, V_S= 15 kn, *Fn*=0.260, Conditions A & B.

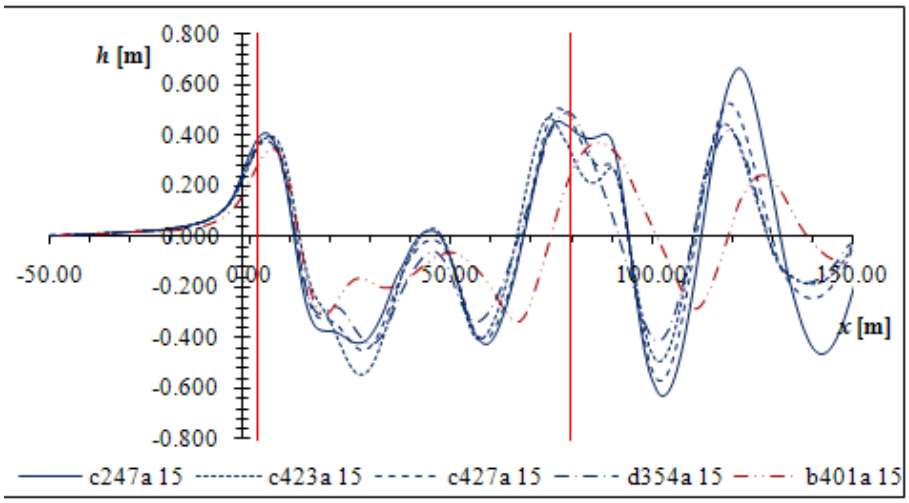

Figure 3.71. Wave-cuts. V_S= 15 kn, Condition A, hulls *C247* (*Fn*=0.278), *C423* (*Fn*=0.279), *C427* (*Fn*=0.278), *D354* (*Fn*=0.279) & *B401* (*Fn*=0.260).

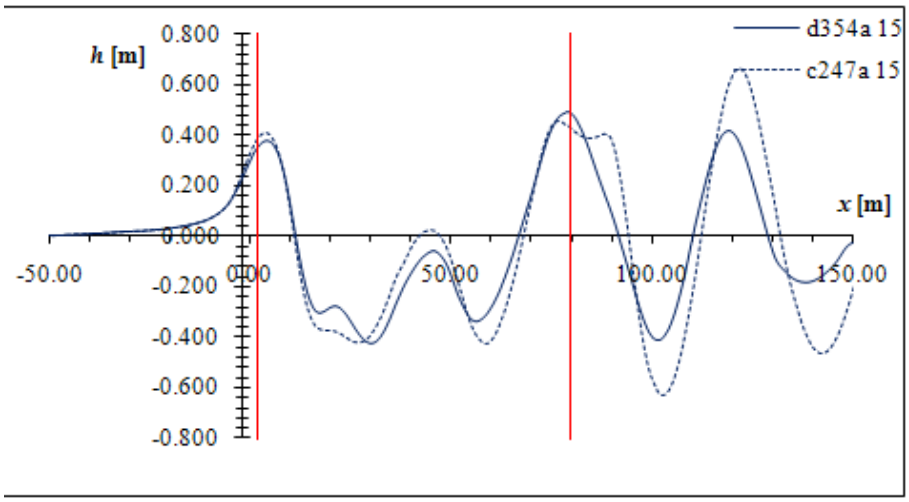

Figure 3.72. Wave-cuts. V_S= 15 kn, Condition A, hulls *D354* (*Fn*=0.279) & *C247* (*Fn*=0.278).

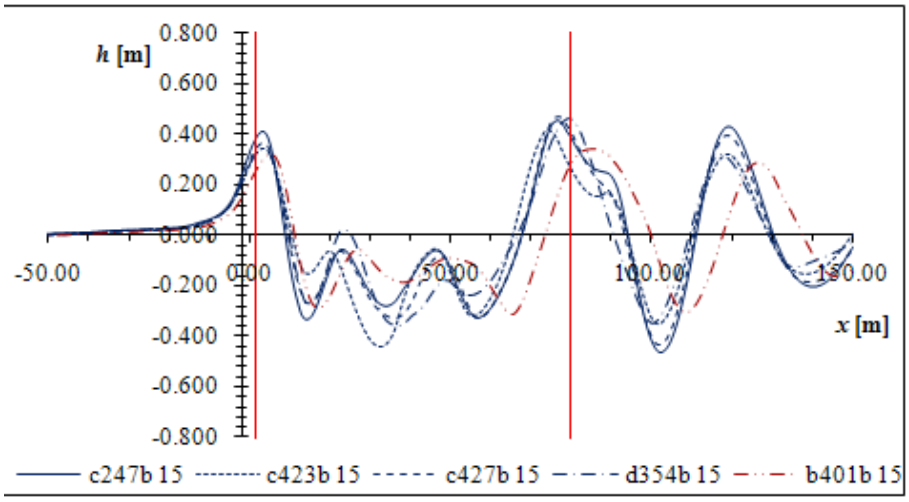

Figure 3.73. Wave-cuts. V_S= 15 kn, Condition A, hulls *C247* (*Fn*=0.278), *C423* (*Fn*=0.279), *C427* (*Fn*=0.278), *D354* (*Fn*=0.279) & *B401* (*Fn*=0.260).

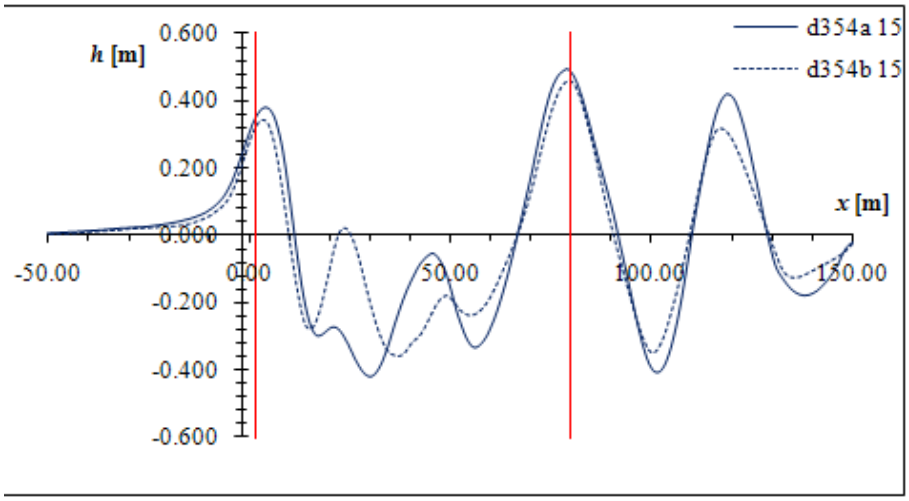

Figure 3.74. Wave-cuts. Hull *D354*, V_S= 15 kn, *Fn*=0.279, Conditions A & B.

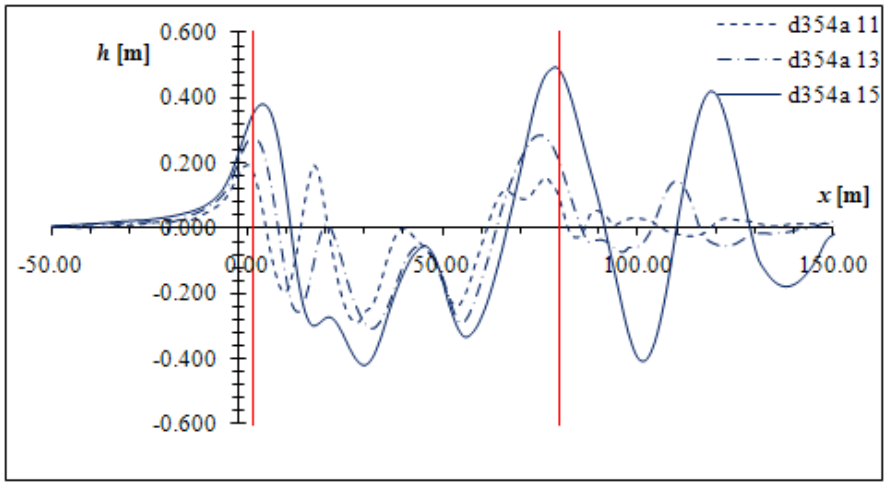

Figure 3.75. Wave-cuts. Hull *D354*, Condition A, V_S= 11,13,15 kn, *Fn*=0.204,0.242,0.279.

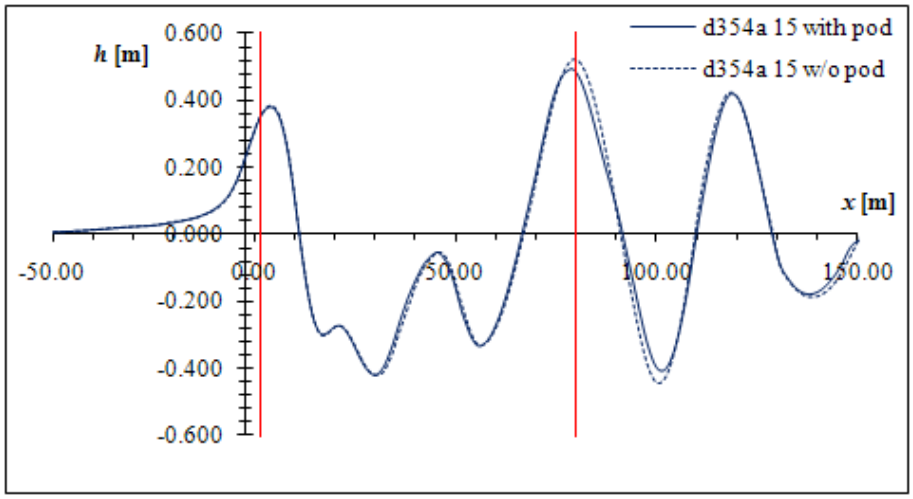

Figure 3.76. Wave-cuts. V_S= 15 kn, *Fn*=0.279, Condition A, Hull *D354* with and without the pod seat configuration.

3.4 Discussion on the Test Cases

One aim of this work was to compare the results generated with the presented method, with those generated with *Shipflow*. In Tables 3.7 and 3.8 the values for the wave resistance coefficient C_W calculated with *catamaran* and *shipflow* respectively, for all test cases at V_S=15 kn and both condition A and B are presented. In the last column, the rank of each hull is given, based on the average value of C_W. From Tables 3.7 and 3.8 it is immediately obvious there is a considerable difference in the values of C_W. That in some extend can be attributed to the difference in the method of calculation of C_W. On the other hand both programs are in good agreement when it comes to determining the most efficient hull form. Both programs find hulls *D, B401, D354* to be the most efficient among those of the initial designs, the first optimization and the second & third optimizations respectively. Furthermore the ranking of the four most efficient hulls overall is the same, *B401, B428, D354* and *C423*, starting from the most efficient. It should be pointed out that the fact that the second and third optimizations produced inferior hulls compared to the first, is due to differences in the constrains.

Upon examination of the figures concerning the wave resistance coefficient, one notices the fact that the curves produced with both programs, have similar characteristics, although differ considerably in their values. For example in Figure 3.38 (*C423*, Condition A) both programs predict the first hump of the wave resistance at $Fn\approx0.20$. The first hump is followed by a trough at $Fn\approx0.23$ according to *catamaran*. *Shipflow* seems to give relatively higher values at the hump and also shift the trough to $Fn\approx0.25$. After that both programs predict a rapid increase of C_W with a second hump at $Fn\approx0.30$. In the case of *catamaran*, this second hump is very slight, almost step like, while *Shipflow* predicts a very high second hump. At the partial displacement condition, both programs predict that the first hump is considerably higher. In general *Shipflow* seems to shift the features of the curves at higher *Fn* and also seems to produce curves with considerably higher local extremes. Since no experimental data are available for the test cases, one cannot be sure which program better reflects the reality. When comparing the C_W curves of the two conditions (Figs. 3.28, 3.29) it is obvious that the partial displacement condition is characterized by higher first hump, up to Fn=0.25, after which it presents lower values of C_W .

Concerning sinkage and trim, both programs are in better agreement (Figs. 3.30-3.33) although the absolute values are considerably different. With regard to sinkage, both programs predict an almost linear increase with *Fn*. Trim on the other hand exhibits a quite different behavior. In the range $Fn\approx0.15$-0.25, trim decreases almost linearly and after a local minimum at $Fn\approx0.25$-0.27 it is increased but more gradually than it decreased, After $Fn\approx0.30$trim seams to stabilize. Although most hull exhibit the abovementioned behavior, trim may have positive or negative values depending on the hull shape. The reader should be reminded that in this work trim is considered positive by stern. Both programs seem to agree that both sinkage and trim exhibit similar behavior in both loading conditions, and that sinkage has greater values in the case of condition A, while Trim has smaller values in the case of condition A agreement (Figs. 3.30-3.33).

Table 3.7. Calculated values of C_W with *Catamaran*, at V_S=15 kn.

Hull		*Fn*	Wave Resistance Coefficient C_W			
			Condition		Average	Rank
			A	B		
Initial Designs	***A***	0.281	2.758E-03	1.178E-03	1.968E-03	10
	B	0.290	2.684E-03	2.656E-03	2.670E-03	12
	C	0.263	1.809E-03	-	1.809E-03	9
	D	0.269	6.592E-04	1.619E-03	1.139E-03	7
	E	0.276	5.475E-03	4.522E-03	4.998E-03	13
First optimization	***B377***	0.276	1.831E-03	1.667E-03	1.749E-03	8
	B401	0.260	3.056E-04	2.908E-04	2.982E-04	1
	B422	0.275	2.160E-03	1.951E-03	2.055E-03	11
	B428	0.260	3.008E-04	3.064E-04	3.036E-04	2
Second & Third optimization	***C247***	0.278	8.761E-04	6.206E-04	7.484E-04	6
	C423	0.279	7.568E-04	3.370E-04	5.469E-04	4
	C427	0.278	8.354E-04	5.458E-04	6.906E-04	5
	D354	0.279	5.905E-04	3.815E-04	4.860E-04	3

Table 3.8. Calculated values of C_W with *Shipflow*, at V_S=15 kn.

Hull		*Fn*	Wave Resistance Coefficient C_W			
			Condition		Average	Rank
			A	B		
Initial Designs	***A***	0.281	4.842E-03	3.824E-03	4.333E-03	12
	B	0.290	-	-	-	-
	C	0.263	2.200E-03	1.880E-03	2.040E-03	10
	D	0.269	1.278E-03	1.673E-03	1.476E-03	9
	E	0.276	3.070E-03	-	3.070E-03	11
First optimization	***B377***	0.276	1.930E-04	1.589E-03	8.910E-04	7
	B401	0.260	1.960E-04	2.100E-04	2.030E-04	1
	B422	0.275	2.264E-04	1.937E-03	1.082E-03	8
	B428	0.260	1.787E-04	2.317E-04	2.052E-04	2
Second & Third optimization	***C247***	0.278	9.516E-04	5.163E-04	7.340E-04	5
	C423	0.279	9.981E-04	4.668E-04	7.325E-04	4
	C427	0.278	9.986E-04	4.922E-04	7.454E-04	6
	D354	0.279	7.483E-04	4.467E-04	5.975E-04	3

The presence of the pod seat configuration does not seem to have any considerable effect on C_W, sinkage or trim (Figs, 3.52-3.57). Especially sinkage exhibits only minor differences in both conditions. With regard to C_W the hull with the pod seat exhibits higher values for Fn<0.25 and lower values thereafter in both conditions. Trim also has higher values for the hull with the pod seat, for Fn<0.25 and lower values thereafter in both conditions. The wave pattern is also very similar. The wave-cuts of Figure 3.76 are identical for about 90% of the waterline length, after which the hull without the pod seat exhibits slightly higher waves. It should be pointed out though that the difference in geometry between the hulls with and without the pod seat, is located at the very aft of the hull, in a region where viscous phenomena are known to play predominant role in both the formation of the waves and the total resistance, hence the potential solvers are rather inadequate for evaluating the effect of such a configuration as a pod seat.

Regarding the wave patterns it is immediately obvious that the hulls with the higher value of C_W are characterized by taller waves, which of course is to be expected. Characteristic case of the above are Figures 3.59 and 3.68 in which the wave contours and wave-cuts for hulls B401 and B422 are presented, for the condition A and V_S=15 kn. Furthermore hull of similar shape such as hulls C247, C423 & C427 present similar wave patterns (Figs. 3.71, 3.73). Of particular interest is Figure 3.75 were wave-cuts for hull *D354*, condition A are presented for V_S=11,13,15 kn, Fn=0.204,0.242,0.279. The gradual increase in height and length is obvious, exactly as predicted by the wave resistance theory.

In conclusion the program proved to be very stable and capable of dealing with very different hull shapes. With regard to wave resistance, the predictions are not accurate enough due mainly to the viscous effects at the stern of the ship. The prediction of the wave patterns is accurate except near and abaft the stern, were visous effects are dominant. On the other hand sinkage, trim and wetted surface can be accurately predicted even when using relatively coarse discretization. Finally potential solvers may be used with confidence in optimizing the hull shape with respect to the wave resistance since both programs rank the hulls in the same order.

4. CONCLUDING REMARKS

4.1 Numerical Method

- The potential free-surface flow solver *catamaran.f*, was used to calculate the wave resistance coefficient C_W, the dynamic *sinkage* and *trim* as well as the free water surface for a number of test cases. The numerical results were compared with those acquired with *Shiplow*.

- Input variables DSURMA and DSURMI restrict the surface renewal in order to avoid convergence problems, hence decelerating convergence.

- Underelaxation factors URFVS and URFPS stabilize the process.

- Convergence with respect to $\overline{|\delta z|}$ is satisfied, when it becomes lower than a suitable value depending on both the *Froude* number and the scale.

- The smaller the limiting value of $\overline{|\delta z|}$, the more accurate the solution.

- $\overline{|\delta z|}$ is sensitive to changes of URFPS. There are two values of URFPS, one positive and one negative, that minimize $\overline{|\delta z|}$.

- $\overline{|\delta z|}$ is sensitive to changes of DSURMI and becomes smaller as DSURMI decreases.

- Smaller values of DSURMI slow convergence substantially.

- The wave resistance coefficient is sensitive to changes of URFPS and less in changes of DSURMI. With regard to URFPS, C_W seems to converge to two different values as the absolute value of URFPS becomes bigger.

- The computational domain is an orthogonal trapezoid surrounding one of the hulls where it's longitudinal edge lies on the ship's center plane.

- An adequate extend for the computational domain is 1.5 L_{WL} fore and 3.0 L_{WL} aft the fore perpendicular in the longitudinal direction while in the transverse direction 1.5·L_{WL} at its foremost and 2.0·L_{WL} at its rear most.

- The CPU time as well as the amount of RAM required to store the problem variables is proportional to the square of the number of panels.

- A total of 22,000 panels is needed to accurately predict the wave resistance coefficient.

- Substantially smaller number of panels is required for predicting sinkage, trim and wetted surface.

- Convergence rates are indifferent to the number of panels.

- The required number of panels is a function of the *Froude* number; in low *Fn* the waves are shorter in length, requiring smaller panels in order to maintain an acceptable level of discretization.

- The shape of the free-surface is very sensitive to the number of panels used, even when wave resistance seems to be predicted accurately.

- The limiting value for $\overline{|\delta z|}$ is decreased as the number of panels increases. Hence finer discretization produces more accurate results with respect to the free-surface.

- Coarser grids tent to "smooth-out" the wave pattern, while very coarse grids fail completely to calculate some of the smallest features of the waves.

- Coarser grids produce waves with greater wave length.

- Thin hulls with small entrance angles and minimum flare of the bow bodyplan, tend to create particularly thin and elongated bow-wave hence require many panels in the transverse direction adjacent to the hull.

4.2 Numerical Experiments

- There is a considerable difference in the calculated values of C_W between the two potential solvers, in some extend attributed to the difference in the method of calculation of C_W.

- Both programs are in good agreement when it comes to determining the most efficient hull form.

- The wave resistance coefficient exhibits similar behavior when comparing the two potential solvers, with respect to the *Froude* number.

- Both programs predict the first hump of the wave resistance at $Fn \approx 0.20$, followed by a trough at $Fn \approx 0.23$-0.25.

- Both programs predict a rapid increase of C_W with a second hump at $Fn \approx 0.30$.

- At the partial displacement condition, both programs predict that the first hump is considerably higher, but after $Fn = 0.25$ the partial displacement condition exhibits lower values for C_W.

- In general *Shipflow* seems to shift the features of the curves at higher *Fn* and also seems to produce curves with considerably higher local extremes.

- Both programs are in better agreement regarding sinkage and trim.

- Both programs predict an almost linear increase of sinkage with *Fn*.

- Trim exhibits a different behavior. In the range $Fn \approx 0.15\text{-}0.25$, trim decreases almost linearly and after a local minimum at $Fn \approx 0.25\text{-}0.27$ it is gradually increased. After $Fn \approx 0.30$ trim seams to stabilize.

- Although most hull exhibit the abovementioned behavior, trim may have positive or negative values depending on the hull shape.

- Both programs agree that both sinkage and trim exhibit similar behavior in both loading conditions, and that sinkage has greater values in the case of condition A, while trim has smaller values in the case of condition A.

- The presence of the pod seat configuration does not have a considerable effect on C_W, sinkage or trim

- The hull with the pod seat exhibits higher values of C_W for $Fn < 0.25$ and lower values thereafter in both conditions.

- Trim has higher values for the hull with the pod seat, for $Fn < 0.25$ and lower values thereafter in both conditions.

- The wave pattern is very similar and the wave-cuts are identical for about 90% of the waterline length, after which the hull without the pod seat exhibits slightly higher waves.

- The potential solvers are inadequate for evaluating the effect on the resistance of the pod seat configuration, since it is located near the stern where viscous phenomena are known to play predominant role in both the formation of the waves and the total resistance.

- The hulls with the higher value of C_W are characterized by taller waves.

- Hulls of similar shape produce similar wave patterns.

- Both wave height and length increase with Fn.

- The prediction of the wave resistance is not accurate enough due mainly to the viscous effects at the stern of the ship.

- The prediction of the wave patterns is accurate except near and abaft the stern, were visous effects are dominant.

- Sinkage, trim and wetted surface can be accurately predicted even when using relatively coarse discretization.

- Potential solvers may be used in optimizing the hull shape with respect to the wave resistance.

REFERENCES

1. Hess, J.L. Smith, A.M.O., 1966. Calculations of potential flow about arbitrary bodies. *Prog. Aeraunaut. Sci.*, 8, 1-136.

2. Kellogg, O.D., 1929. *Foundations of Potential Theory*. Frederick Ungar Publishing Co., New York.

3. von Kerczek, C., Tuck, E.O., 1969. The Representation of ship hulls by conformal mapping functions. *Journal of Ship Research*, 19, 284–298.

4. von Kerczek, C., Stern, F., 1983. The representation of ship hulls by conformal mapping functions: Fractional maps. *Journal of Ship Research*, 27, 158-159.

5. Tzabiras, G.D., Dimas, A., Loukakis, T.A., 1986. A numerical method for the calculation of incompressible, steady, separated flows around aerofoils. *International Journal for Numerical Methods in Fluids*, 6, 789-809.

6. Tzabiras, G.D., Prifti, A.C., Grigoropoulos, G.J., Loukakis, T.A., 1995. An advanced CFD method for predicting the propulsive performance of traditional fishing vessels. *Proc. CADAP-95 RINA conference*, 17.1-17.16.

7. Tzabiras, G.D., 1996. Numerical study of the viscous flow past a ship's model with asymmetric stern. *Proc. MARIND-96 conference*, III.41-III.57.

8. Tzabiras, G.D., 1997. Numerical calculation of 2D free surface flows. *Proc. Computational methods and experimental measurements*, VIII, 361-370.

9. Tzabiras, G.D., 1997. Numerical evaluation of Reynolds scale effects on the resistance and propulsion characteristics of ships. In: Schmitt, H. (editor). *Flows at large Reynolds numbers, advances in fluid mech. series*. CMEM pub, 251-290.

10. Tzabiras, G.D., Prifti, A.C., 2001. Numerical simulation of the separated, turbulent flow past the stern of traditional fishing vessels. In: Tzabiras, G.D. (editor). *Calculation of complex turbulent flows, advances in fluid mech. series*. CMEM pub, 131-66.

11. Tzabiras, G.D. 2004. Resistance and self-propulsion simulations for a Series-60, C_B=0.6 hull at model and full scale. *Ship Technology Research*, 51, 21-34.

12. Tzabiras, G.D. 2008. A method for predicting the influence of an additive bulb on ship resistance. *Proc. 8th International conference on hydrodynamics*, 53-60.

13. Tzabiras, G. D., Kontogiannis, K., 2009. An integrated method for predicting the hydrodynamic resistance of low- C_B ships. *JCAD*, 1568, 1-16.

14. Zaraphonitis, G., Papanikolaou, A., Mourkoyiannis, D., 2003. Hull form optimization of high speed vessels with respect to wash and powering. *Proc. 8th International Marine Design Conference*.

APPENDIX A:

Main Input Variables of *Catamaran.f*

APPENDIX A: Main Input Variables of *Catamaran.f*

The computer program *catamaran* reads the necessary input data from three files. The geometry of the outer and inner halves of the hull is read from files *file*1 and *file*2 respectively. The above files are binary and are generated by the program *conformal.f*. The variables concerning all other aspects of the execution of the program are input through the text file *dinp*. The variables in *dinp* are formatted and arranged in rows. Every row is proceeded by a dummy row (the program ignores it) that contains the name of each variable. To facilitate the correct use of *dinp*, the columns reserved for each variable are indicated by the columns of the preceding line, that are occupied by the variable's name and the following underscores. All dimensions refer to the input coordinates' system (Fig. A.1). The origin point of the above system is located at the fore perpendicular, at the height of the main deck. The *z*-axis coincides with the longitudinal direction and the *z*-values increase towards the stern. The *y*-axis coincides with the vertical direction and the *y*-values increase with height. Finally the *x*-axis completes a left-handed coordinates system. An exemplar *dinp* file is given in Table A.1, while a list of the most important variables of *dinp*, their type and meaning, are given in Table A.2.

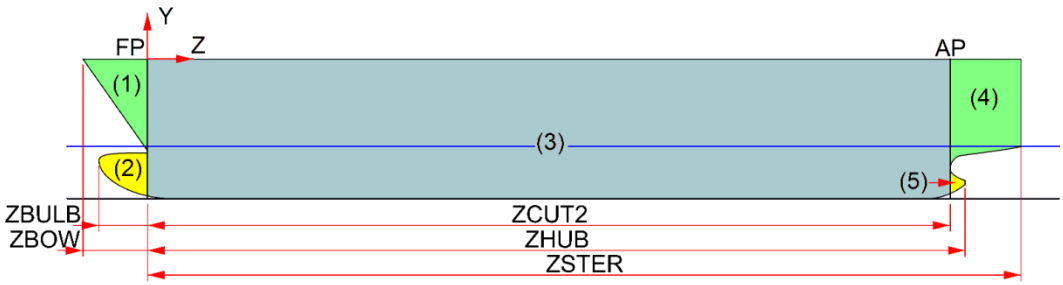

Figure A.1 Definition of the data input coordinates' system and the main dimensions.

Table A.1. Input file, *dinp*.

```
SDC_D354_a15
-----------------------GENERAL DATA--------------------------------
IWIT_KCRT_IVIS_NGRI_MAD7_
0     01
VELIN_____FROUDE____DENSIT____GRAV______
-15.0                  997.      9.81
VISCOS
1.e-6
SCALEL____XLWL______UCROSS____CROSFL____URFV______
0.00       77.000     +20.
XGRAV_____YGRAV_____ZGRAV_____
35.840       -6.955    -6.0
EXALA_____TRIM______URSINK____URTRIM____SINKLIM___TRIMLIM___
8.260      0.200     0.5        0.5
DZWMIN____DZWMAX____DSURF_____DYGMIN____
0.01       0.1       +0.01
FREBO_____FRELAS____
30.
```

```
ISYM_MAST_MASG_MASW_MASY_
1     2000 050  050   040

ISUR_NSUR_ISPL_LAGR_ISU3_ICAU_
+2     1    00   00  +1
IDOB_NONO_MODG_ISUT_IS3T_ICAU_
       1    01   +1   +0   +00
IBUL_IHUB_LTRA_NCAT_ISUC_
2     2    -2   03    +0
NKBL_NKHB_NPKL_LABA_ISUB_ITRL_
10    05    00
IVER_JUPA_IASC_ICON_ITRV_
+1     0   -4
JSUR_NOWC_KSCO_KGBC_MODE_
 -02  +01  00  +000
ISIN_ITRI_KSIN_KTRI_
200   200  025  025
NK1M_NK2M_N3BM_N3SM_NK4M_NK5M_
70    10    40   40  30   90
NK1S_NK2S_N3BS_N3SS_NK4S_NK5S_
35    05    20   20  15   45
NK1F_NK2F_N3BF_N3SF_NK4F_NK5F_
0
NI1M_NI1S_NI1F_
20    10
NI2M_NI2S_NI2F_
20    10
NJ1M_NJ1S_NJ1F_
45    30
NJ2M_NJ2S_NJ2F_
20    10
DSURMA____DSURMI____TANEPT____TANEPL____TANBOD____TANTRA____YMINWA____
0.010      0.0010                          +45.                 -8.5
DELTAT____YCOREC____DXSCOB____DXSCOS____DXSCOR____COSMAT____TANZG_____
-0.000      -0.0        0.       -00.0       0.    10000.      00.
URFVS_____URFTIM____URFSUR____URFBEM____URFLEM____BERNOUL___URFPS_____
1.0         -0.0      -0.0       -0.0      0.00                -1.0
ZBULB_____ZBOW______ZCUT1_____ZCUT2_____ZCUT3_____ZSTER_____
-3.532    -5.682     0.0       70.568    70.568    82.968
ZG1_______ZMID______ZG4_______ZG34______ZTRANS____
-120.00     45.      260.00     0.0000
DZBULB____DZBOWM1___DZBOWP1___DZKB1M1___DZSTERM1__DZSTERP1__
+0.15       +0.3000  0.00000     0.3      0.3        0.3
OM3B______DZKF1_____ZPAR1_____ZPAR2_____Z1KEEL____Z2KEEL____
1.5           0.400     0.         0.000
APLUS_____BPLUSB____BPLUSS____DZHULL____
0.200        0.300       0.50
ZHUB______DZHUB_____
71.877       0.400
IVDH_MAXH_NST__
0     030    +4
```

```
ISAV_ISAF_ISAM_MODF_
-2     00  0000
RR1_______RR2_______RR3_______SORMH_____
0.           0.           00.     0.0001
CONFOR*************************************************************
ICU1_ICU2_ICU3_ICB1_ICB2_
0     0     0
KVDU_IPRK_IPR2_IPRB_IPLO_
-0     0    +0  +0   +0
ZCUB1_____ZCUB2_____ZCUBB1____ZCUBB2____DABAX_____
0.00           00.
GRID***************************************************************
NISO_IXCO_KVDU_ITRB_IKB1_
                +1
NI1__NI2__NI3__NI4__NI5__NIBU_
10    10   20   20   20   10
IAB3_IAM3_IAS3_ISPS_ITRA_
3       3    3        +0
DRINV_____ANJY______EXPA3Y___DAR1______DAR2______DAR3______DAR4______
0.01
EXPAB_____EXPAD_____EXPA2B____EXPA2S____EXPA3S____
0.
DEXFIR____DEXLAS____BCANAL____BCANALD___DCANAL____
120.0       150.0      1.0        1.0      0.50
NKB__NJB__NJD__IADB_
                 -0
```

Table A.2. List of variables of input file *dinp*.

Row	Name	Type	Value	Meaning
1	NAME	80A1		Ship's name or the code of the run.
3	VELIN	F10.6	>0.	Ship's speed [m/s].
			<0.	abs(VELIN) = The ship's speed [kn].
	FROUDE		>0.	Froude Number.
	DENSIT		>0.	Water density [kg/m^3].
	GRAV		>0.	Gravitational acceleration [m/s^2].
4	VISCOS	*	>0.	Kinematic viscosity [m^2/s].
5	SCALEL	F10.6	>0.	Scale.
			<0.	1/abs(SCALEL) = Scale.
	XLWL		>0.	Indicative waterline length [m].
6	XGRAV	F10.6	>0.	Longitudinal position of the center of gravity [m].
	YGRAV		<0.	Transverse position of the centerline of a demi-hull [m].
	ZGRAV		<0.	Vertical position of the center of gravity [m].

7	EXALA	F10.6	>0.	Static freeboard [m].
	TRIM			Static trim [deg], (+) by stern.
	URSINK		>0.	Dynamic sinkage underelaxation factor.
	URTRIM		>0.	Dynamic trim underelaxation factor.
	SINKLIM			Maximum allowable value for sinkage [m].
	TRIMLIM			Maximum allowable value for trim [deg].
8	DZWMIN	F10.6	>0.	Minimum value of the minimum allowable length of the free surface panels [m].
	DZUMAX		>0.	Maximum value of the minimum allowable length of the free surface panels [m].
	DSURF		>0.	Height δz* of the control volume for the calculation of u_z* [m]
	DYGMIN		>0.	Minimum allowable correction of the free surface [m].
9	FREBO	F10.6	>0.	Length of the free surface astern ZG1 that the free surface is kept flat [m].
	FRELAS		>0.	Length of the free surface in front of ZG4 that the free surface is kept flat [m].
10	ISYM	I5	>0	Number of symetry planes (for ships ISYM = 1).
	MAST		>0	Maximum number of steps.
	MASG		>0	Step at which the number of panels is increased.
	MASW		>0	Number of steps during which the minimum allowable length of the free surface panels is DZWMAX. After MASW steps, the minimum allowable length of the free surface panels is DZWMIN.
	MASY		>0	Number of steps during which the maximum allowable correction of the free surface panels is DSURMA. After MASY steps, the maximum allowable correction of the free surface panels is DSURMI.
13	IBUL	I5	0	Ship without bow bulb.
			2	Ship with bow bulb.
	IHUB		0	Ship without stern bulb.
			2	Ship with stern bulb.
	LTRA		0 or -2	Cruiser type stern leading to a single point.
			-1	Cruiser type stern leading to a vertical line.
			+1	"Dry" transom stern.
			+2	"Wetted" transom stern.
	NCAT		1	The ship is considered a monohull.
			>1	The ship is considered a catamaran.
14	NKBL	I5	>0	Number of longitudinal sections on the bow bulb (see accompanying figure).
	NKHB		>0	Number of longitudinal sections on the stern bulb.

15	IASC	I5	-4	Variable concerning the input of the hull geometry.
17	ISIN	I5	>0	Steps before the sinkage calculations start.
	ITRI		>0	Steps before the trim calculations start.
	KSIN		>0	Steps between two consecutive sinkage calculations.
	KTRI		>0	Steps between two consecutive trim calculations.
18	NK1M	I5	>0	Maximum value of NK1, the number of panels in the longitudinal direction, in front of min(ZBOW,ZBULB) (see accompanying figure).
	NK2M		>0	Maximum value of NK2, the number of panels in the longitudinal direction, between max(ZBOW,ZBULB) and ZCUT1 (see accompanying figure).
	N3BM		>0	Maximum value of NK3B, the number of panels in the longitudinal direction, between ZCUT1 and ZMID (see accompanying figure).
	N3SM		>0	Maximum value of NK3S, the number of panels in the longitudinal direction, between ZMID and ZCUT3 (see accompanying figure).
	NK4M		>0	Maximum value of NK4, the number of panels in the longitudinal direction, between ZCUT3 and ZSTER (see accompanying figure).
	NK5M		>0	Maximum value of NK5, the number of panels in the longitudinal direction, astern ZSTER (see accompanying figure).
19	NK1S	I5	≥0	Increment of NK1 (if =0 then NK1S=NK1M).
	NK2S		≥0	Increment of NK2 (if =0 then NK2S=NK2M).
	N3BS		≥0	Increment of NK3B (if =0 then NK3bS=NK3BM).
	N3SS		≥0	Increment of NK3S (if =0 then NK3SS=NK3SM).
	NK4S		≥0	Increment of NK4 (if =0 then NK4S=NK4M).
	NK5S		≥0	Increment of NK5 (if =0 then NK5S=NK5M).
20	NK1F	I5	≥0	Initial value of NK1 (if =0 then NK1F=NK1S).
	NK2F		≥0	Initial value of NK2 (if =0 then NK2F=NK2S).
	N3BF		≥0	Initial value of NK3B (if =0 then NK3BF=NK3BS).
	N3SF		≥0	Initial value of NK3S (if =0 then NK3SF=NK3SS).
	NK4F		≥0	Initial value of NK4 (if =0 then NK4F=NK4S).
	NK5F		≥0	Initial value of NK5 (if =0 then NK1F=NK5S).
21	NI1M	I5	>0	Maximum value of NI1, the number of panels in the circumferential direction, on the outer half of the hull (see accompanying figure).
	NI1S		≥0	Increment of NI1 (if =0 then NI1S=NI1M).
	NI1F		≥0	Initial value of NI1 (if =0 then NI1F=NI1S).

22	NI2M	I5	>0	Maximum value of NI2, the number of panels in the circumferential direction, on the inner half of the hull (see accompanying figure).
	NI2S		≥0	Increment of NI2 (if =0 then NI2S=NI2M).
	NI2F		≥0	Initial value of NI2 (if =0 then NI2F=NI2S).
23	NJ1M	I5	>0	Maximum value of NJ1, the number of panels in the transverse direction, on the outer half of the water surface (see accompanying figure).
	NJ1S		≥0	Increment of NJ1 (if =0 then NJ1S=NJ1M).
	NJ1F		≥0	Initial value of NJ1 (if =0 then NJ1F=NJ1S).
24	NJ2M	I5	>0	Maximum value of NJ2, the number of panels in the transverse direction, on the inner half of the water surface (see accompanying figure).
	NJ2S		≥0	Increment of NJ2 (if =0 then NJ2S=NJ2M).
	NJ2F		≥0	Initial value of NJ2 (if =0 then NJ2F=NJ2S).
25	DSURMA	F10.6	>0.	Maximum allowable correction of the free surface panels for NSTEP<MASY.
	DSURMI		>0.	Maximum allowable correction of the free surface panels for NSTEP>MASY.
	TANBOD		≥0.	Maximum allowable angle in the transverse direction, between the first panel and the horizontal plane [deg]
	TANTRA		≥0.	Maximum allowable angle in the longitudinal direction, between the first panel aft the transom and the horizontal plane [deg]
	YMINWA		<0.	Maximum allowable depth of a wave trough [m].
27	URFVS	F10.6		Underelaxation factor for the renewal of the free surface.
	BERNOUL			Maximum allowable height of a wave crest [m].
	URFPS			Underelaxation factor for the pressure in the renewal of the free surface.
28	ZBULB	F10.6	<0.	Longitudinal position of the bow bulb tip [m].
	ZBOW		<0.	Longitudinal position of the bow [m].
	ZCUT1			Longitudinal position of fore perpendicular [m].
	ZCUT2		>0.	Longitudinal position of the 2nd cutting point[m].
	ZCUT3		>0.	Longitudinal position of aft perpendicular [m].
	ZSTER		>0.	Longitudinal position of the stern [m].
29	ZG1	F10.6	<0.	Longitudinal position of the first row of points [m].
	ZMID		>0.	Longitudinal position of interchange between NK3B and NK3S [m].
	ZG4		>0.	Longitudinal position of the last row of points [m].
	ZG34		≥0.	Height of skeg [m].

29	ZTRANS	F10.6	≥0.	Longitudinal position of the transom [m] (If ZTRANS = 0 and LTRA>0, the program finds at every step the rearmost partially submerged section K and sets ZTRANS = Z(K+1)).
30	DZBULB	F10.6	>0.	Length of the first panel of the bow bulb (z>ZBULB) [m].
	DZBOWM1		>0.	Length of the first panel of in front of the bow (z<min(ZBOW,ZBULB)) [m].
	DZBOWP1		>0.	Length of the first panel of aft the bow (z>min(ZBOW,ZBULB)) [m].
	DZKB1M1		>0.	Length of the last panel before ZCUT2 [m].
	DZSTERM1		>0.	Length of the first panel of in front of the stern [m].
	DZSTERP1		>0.	Length of the first panel of aft the stern [m].
31	DZKF1	F10.6	>0.	Length of the first panel of aft ZCUT1 [m].
32	APLUS	F10.6	>0.	Breadth of the first panel at the bow [m].
	BPLUS		>0.	Breadth of the first panel at ZMID [m].
	BPLUSS		>0.	Breadth of the first panel at the stern [m].
33	ZHUB	F10.6	>0.	Longitudinal position of the stern bulb tip [m].
	DZHUB		>0.	Length of the first panel of the stern bulb (z<ZHUB) [m].
35	ISAV	I5	+1	
			-2	All matrices are kept in the RAM.
40	ITRB	I5	1	The bow ends at a single point.
			2	The bow ends at a vertical line.
41	NI1	I5	>0	Maximum overall number of point in the circumferential direction, on the hull section (1)
	NI2		>0	Maximum overall number of point in the circumferential direction, on the hull section 2)
	NI3		>0	Maximum overall number of point in the circumferential direction, on the hull section (3)
	NI4		>0	Maximum overall number of point in the circumferential direction, on the hull section (4)
	NI5		>0	Maximum overall number of point in the circumferential direction, on the hull section (5)
	NIBU		≥0	Number of sections linearly interpolated between the first and second section on the bow bulb.
42	INTR	I5	>0	Number of panels on the radial direction, on the transom for LTRA=+2.
45	DEXFIR	F10.6	>0.	The half-breadth of the domain at the first row of points.
	DEXLAS		>0.	The half-breadth of the domain at the last row of points.
			0	DEXLAS = DEXFIR + tan(39.5^{o}) x (ZG1+ZG4).

APPENDIX B:

Output Files of *Catamaran.f*

APPENDIX B: Output Files of *Catamaran.f*

The computer program *catamaran.f* upon execution creates up to 35 files in which stores both output data and data needed for the execution. The later are data used in case not all variables are kept in the RAM (variable ISAVE, see Appendix A) or data necessary for restarting the program say in case of an unintentional termination. When the user wants to start an execution from the beginning, within a folder containing results of a previous run, he must make sure that the files *osurf* and *osurft* are deleted. A list of all the files and their type is given in Table B.1. As a rule all files with names ending in *t*, refer to the panels abaft the transom and are generated only when LTRA>0 (see Appendix A).

The most important output files are: ***cptec.dat, filegrsur, filegrsurt, hestec.dat, ohesp, osurf, osurft, sinkage*** and ***vtec.dat***.

The output files *filegrsur* and *filegrsurt* are binary files containing the free-surface geometry. They can be used as input files for the execution of the program *wlogp.exe* that generates a wave-cut at a transverse distance from the maximum beam, input upon execution through the keyboard. Two new text files are then created, *modelw.dat* and *plotlongex*. The former contains the intersection of the hull center plane and the hull itself with the water surface. The later contains the intersection of the water surface with a longitudinal, vertical plane located at the prescribed by the used distance from the maximum beam. In both files, the wave-cuts are given as *x*-*h* coordinates, were *x* is the longitudinal distance from the upstream end of the flow field in meters and *h* is the water elevation with respect to the calm water also in meters. The program *wlogp.exe* may be executed with only *filegrsur* as input, in that case an empty *filegrsurt* file is created.

The output text files *cptec.dat* and *vtec.dat* contain the pressure on the hull surface and the speed components on both hull and water surface respectively. The data are formatted in a suitable way to be used as a data files for *Tecplot*.

The output text file *hestec.dat* contains the coordinates of the hull and free-surface panels formatted in a suitable way to be used as a data file for *Tecplot*. By then using an appropriate **.lay* file, the user may plot the panels and the water elevation contour.

The output file *ohesp* is a text file containing hydrostatic and resistance data, such as *Wetted Surface Area, LCB, KB,* C_P, R_W, R_F (*ITTC* and *ATTC*), C_W, C_F, C_T and other. An exemplar *ohesp* file is presented in Table B.2.

Output text files *osurf* and *osurft* contain the convergence history of the potential solution (see chapter 2). When LTRA≤0 (no transom), file *osurft* is not created and file *osurf* contains the data for the hole field. When LTRA>0, file *osurf* contains the data for the portion of the field in front of the transom while file *osurft* contains the data for the portion of the field abaft the transom. The contained data are arranged in columns, Table B.3. Part of an *osurf* file is presented in Table B.4.

The output text file *sinkage* contains the convergence history of the free-surface solution (see 2.3). The contained data are arranged in columns, Table B.5. Part of a *sinkage* file is presented in Table B.6.

Table B.1. List of output files.

Name	Type	Description
cptec.dat	text	Pressure on the hull surface panels, formatted for Tecplot
filegrsur	binary	Free-surface geometry
filegrsurt	binary	Respective data of *filegrsur*, for the water surface astern the transom, when LTRA>0
hestec.dat	text	Hull and free-surface panel coordinates, formatted for Tecplot
ohesp	text	Resistance data
osurf	text	Convergence data of C_W and *dz*
osurft	text	Respective data of *osurf*, for the water surface astern the transom, when LTRA>0
sinkage	text	Convergence data of sinkage and trim
vtec.dat	text	Speed components on the hull and water surface, formatted for Tecplot
screen/ nohup.out	text	Contains the data normally printed on the system default output device (usually the screen), when execututing in UNIX/Linux and using the command: ./NAME_OF_EXECUTABLE> screen& or nohup ./NAME_OF_EXECUTABLE&
Other text files:		*dhess22, dhess22l, filecpot, filecpotl, fileprog, filez1, filez2, filezk, oconfor, ogridl, ogrids, ohess*
Other binary files:		*filecon1, filegrsul, filegrsult, fileh2g, fileh2s, fileh21, fileh22, fileprou, filersul, filersult, filersur, filersurt*

Table B.2. Output file, *ohesp*, run d354a15a.

```
*************************************************************************
          TOTAL PRESSURE COEFFICIENTS= CP/(0.5*S*V**2)
          -------------------------------------------------
                        CPX=  5.9047E-04
                        CPGX=  8.4487E-05
                        CPT=  6.7495E-04
                        CPY=  1.7594E-03
                        CPZ=  4.8632E-01
                        CPGZ=  1.5598E+00
                        AREA=  1.7294E+03

FX(Nt)=  3.0311E+04
FY(Nt)=  4.5158E+04
FZ(Nt)=  2.4965E+07
BOYANCY(Nt)=  2.6383E+07
X-F(m)=  3.5841E+01
Z-F(m)= -1.7713E+00
LCB(m)=  3.5673E+01
KB(m)= -1.8853E+00


FRICTION RES.    =  8.3220E+04 Nt    ITTC
FRICTION RES.    =  8.3192E+04 Nt    ATTC
RPRESSURE RES.   =  3.0311E+04 Nt
TOTAL RES.       =  1.1353E+05 Nt   ITTC
TOTAL RES.       =  1.1350E+05 Nt   ATTC

CW =  5.9047E-04
CF-ITTC =  1.6211E-03
CF-ATTC =  1.6206E-03

CT-ITTC =  2.2116E-03
CT-ATTC =  2.2110E-03
CW/CT =  2.6699E-01 IITC
CW/CT =  2.6705E-01 ATTC
CW/CF =  3.6423E-01 IITC
CW/CF =  3.6435E-01 ATTC


Xlwl =  7.7000E+01
Xrey =  8.2101E+01


Cpmax=    0.993244
Cpmin=   -0.313292
```

Table B.3. Output file, *osurf*, list of variables.

Column	Name	Description
1	IT	Iteration of the potential solution
2	RESM	Mass residual (dimensionless)
3	$\overline{\lvert\delta h\rvert}$	Mean free-surface correction (dimensionless), the mean value of the absolute vertical shift of all surface panels, divided by the reference length times the total number of surface elements
4	R_W	Wave resistance [Nt]
5	WS	Actual wetted surface [m^2]
6	C_W	Wave resistance coefficients
7	$\overline{\lvert\delta z\rvert}$	Pressure residual, the mean value of the absolute difference between the calculated and the ideal hydrostatic pressure at the control points of all surface panels, transformed in [m]

Table B.4. Output file, *osurf*, run d354a15a.

1	7.83532E-01	1.07220E-09	-1.75124E+04	1.68344E+03	-3.50449E-04	5.46406E-02
2	6.82608E-01	1.08665E-09	-1.71435E+04	1.68677E+03	-3.42388E-04	5.22458E-02
3	6.02777E-01	1.09684E-09	-1.65401E+04	1.69011E+03	-3.29686E-04	5.02412E-02
4	5.02789E-01	1.10209E-09	-1.57642E+04	1.69344E+03	-3.13601E-04	4.87186E-02
5	4.30084E-01	1.10110E-09	-1.49904E+04	1.69678E+03	-2.97621E-04	4.80164E-02
6	3.31679E-01	1.09671E-09	-1.40286E+04	1.70011E+03	-2.77979E-04	4.69080E-02
7	2.67271E-01	1.11347E-09	-1.28615E+04	1.70287E+03	-2.54440E-04	4.67489E-02
8	1.81965E-01	1.09323E-09	-1.15036E+04	1.70545E+03	-2.27233E-04	4.58438E-02
9	1.49609E-01	1.11403E-09	-9.73115E+03	1.70699E+03	-1.92048E-04	4.59312E-02
10	1.24529E-01	1.09590E-09	-7.95161E+03	1.70839E+03	-1.56799E-04	4.54115E-02
			…			
1920	1.15975E-02	2.75442E-11	3.03084E+04	1.72936E+03	5.90411E-04	1.64110E-02
1921	1.26787E-02	2.75483E-11	3.03118E+04	1.72969E+03	5.90362E-04	1.63140E-02
1922	1.15986E-02	2.75438E-11	3.03092E+04	1.72936E+03	5.90427E-04	1.64105E-02
1923	1.26746E-02	2.75487E-11	3.03122E+04	1.72969E+03	5.90370E-04	1.63133E-02
1924	1.16090E-02	2.75431E-11	3.03097E+04	1.72935E+03	5.90437E-04	1.64096E-02
1925	1.26818E-02	2.75470E-11	3.03143E+04	1.72969E+03	5.90412E-04	1.63125E-02
1926	1.15706E-02	2.75436E-11	3.03112E+04	1.72936E+03	5.90465E-04	1.64093E-02

Table B.5. Output file, *sinkage*, list of variables.

Column	Name	Description
1	IT_sink	Iteration of the sinkage/trim solution
2	IT	Iteration of the potential solution
3	F_X	Longitudinal force [Nt]
4	F_Z	Vertical force [Nt]
5	R_T	Total resistance [Nt]
6	BOYANCY	Buoyancy of the wave system [Nt]
7	x_{PF}	Longitudinal position of the center of buoyancy with respect to the water surface coordinates' system [m]
8	x_g	Longitudinal position of the center of gravity with respect to the water surface coordinates' system [m]
9	SINKAGE	Sinkage at x=0 [m]
10	TRIM	Trim [deg], (+) by stern

Table B.6. Output file, *sinkage*, run d354a15a.

```
 0  199     22831.367  23672924.000    103473.938  24965380.000 35.9603 35.8477  0.0000  0.2000
 1  200     22845.869  23673366.000    103466.844  25067168.000 35.9604 35.8477  0.0822  0.1686
 2  225     23529.430  24139202.000    105003.406  25543066.000 35.9646 35.8463  0.1345  0.1361
 3  250     24889.955  24370066.000    106781.188  25778064.000 35.9408 35.8450  0.1721  0.1100
 4  275     25853.453  24522738.000    108121.078  25931440.000 35.9177 35.8439  0.2000  0.0900
 5  300     27092.291  24632142.000    109587.297  26041684.000 35.8967 35.8432  0.2210  0.0756
 6  325     28032.869  24717234.000    110738.156  26126812.000 35.8817 35.8427  0.2366  0.0651
 7  350     28726.814  24781176.000    111566.250  26191324.000 35.8706 35.8423  0.2482  0.0575
 8  375     28979.383  24829208.000    111929.195  26241512.000 35.8633 35.8420  0.2567  0.0518
 9  400     29351.822  24864826.000    112364.742  26278010.000 35.8574 35.8418  0.2630  0.0476
10  425     29452.617  24890932.000    112535.250  26305068.000 35.8531 35.8416  0.2677  0.0446
                                                 ...
65 1800     30357.811  24964970.000    113574.773  26382940.000 35.8413 35.8413  0.2799  0.0373
66 1825     30334.920  24964670.000    113569.461  26382662.000 35.8414 35.8413  0.2799  0.0373
67 1850     30335.867  24964978.000    113554.461  26382846.000 35.8414 35.8413  0.2799  0.0373
68 1875     30335.424  24964716.000    113570.430  26382666.000 35.8415 35.8413  0.2799  0.0372
69 1900     30306.973  24964476.000    113524.828  26382294.000 35.8412 35.8413  0.2800  0.0372
70 1925     30314.348  24964958.000    113550.016  26382920.000 35.8414 35.8413  0.2800  0.0372
```

APPENDIX C:

Main Input Variables of *Conformal.f*, Files *data1*, *data2* & *data3*

APPENDIX C: Main Input Variables of *Conformal.f*, Files *data1, data2* & *data3*

The computer program *conformal* reads the necessary input data from text files *data1*, *data2* and *data3*. The variables concerning the execution of the program are input through the file *data1*, while the geometry of the hull is read from files *data2* and *data3*. The variables in the input files are formatted and arranged in rows. Every row is proceeded by a dummy row (the program ignores it) that contains the name of each variable. To facilitate the correct use of *data1*, the columns reserved for each variable are indicated by the columns of the preceding line, that are occupied by the variable's name and the following underscores. All dimensions refer to the input coordinates' system (Fig. C.1). The origin point of the above system is located at the fore perpendicular, at the height of the main deck. The *z*-axis coincides with the longitudinal direction and the *z*-values increase towards the stern. The *y*-axis coincides with the vertical direction and the *y*-values increase with height. Finally the *x*-axis completes a left-handed coordinates system.

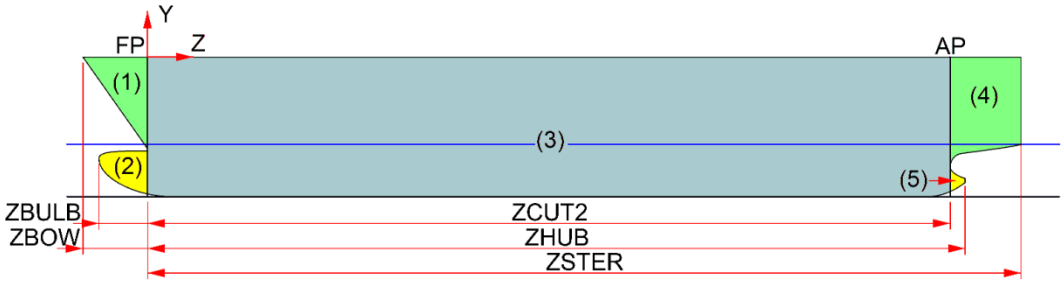

Figure C.1 Definition of the hull regions, the data input coordinates' system and the main dimensions.

In order for the program to be able to handle the complicated and varying hull shapes of modern ships, the hull surface is subdivided in five regions (Fig. C.1). The first region is the portion of the hull, in front of the fore perpendicular (*FP*) and above the bulb. The fore perpendicular is defined here as the vertical line tangential to the hull's centerline at the bow of the ship, near the intersection of the centerline with the water line. The second region is the bow bulb, defined as the portion of the hull, in front of the fore perpendicular and below the first region.

The fourth region contains the stern and is the portion of the hull, astern the aft perpendicular (*AP*) and above the bulb (when there is one). When the stern of the ship features a stern bulb, the aft perpendicular is defined as the vertical line tangential to the centerline, near the stern of the ship and the intersection of the centerline with the water line. In all other cases the location of the aft perpendicular is arbitrary. The fifth region is the stern bulb, defined as the portion of the hull, astern the aft perpendicular and below the fourth region. Finally the third region is the portion of the hull, astern the fore perpendicular and in front of the aft perpendicular. Regions (1) and (2) form the longitudinal section (A), region (3) forms the longitudinal section (B) and finally Regions (4) and (5) form the longitudinal section (C). The third region is the only requisite region in order for the program to be executed.

The regions (1), (3) and (4) are input through *data2*, while regions (2) and (5) are input through *data3*. If a ship does not have regions (2) and (5), *data3* may be neglected.

The geometry of each region is input through a set number of 2D transverse sections. Each section is input through the coordinates of a set number of points. The sections of each region must be sorted; starting with the foremost while the points describing each section must be sorted, staring with the uppermost. When two neighboring regions are described in *data1* (say (1) and (3)), the intersection of the regions is called a discontinuity section and must be input twice or else the fact must be declared to the program (see list of variables). When three regions from two neighboring longitudinal sections exist (say (1), (2) –section (A) – and (3) –section (B) –, Fig. C.1) then the last section of (1) and (2) and the first section of (3) must be the portion of the discontinuity section that is part of them. In our example whole the discontinuity section must be included in region (3) while region (1) must include the upper half and region (2) the lower half. The same applies in the case that the edge of one region is part of the edge of its neighboring region. For example regions (3) and (4) of Figure C.1 if region (5) did not exist.

The coordinates of the points of each section are input in the following manner. First the *z*-coordinate is given followed in the next row by the number of points (say K). Then K rows follow where the *x* and *y*-coordinates are given. The above are repeated for every section. Notice in Table C.2 the fact that a discontinuity section at the fore of the aft end of a region may be described by a single point.

Exemplar *data1, data2* and *data3* files are given in Tables C.1 & C.2, while lists of their most important the variables, their type and meaning, are given in Tables C.3-C.5.

In order to reduce the effort required to prepare the input data for *conformal.f*, a new software called *sorting.f90* was developed. This program reads unsorted coordinates from text files and prepares the input files *data2* & *data3*. For more details on *sorting.f90* see Appendix D.

Table C.1. Input file, *data1*.

```
1     SDC_D354
JOB__KREG_KRE1_KRE2_
+1     3    1    3
KJ0__KPRE_KJOB_KPRB_
           7     1
FAIR_MAX1_MAX2_NEXT_LASA_ICAL_IST1_  I5
0     300  300  -000  +3   +4   +01
IBUL_LEQU_ICAB_LAO__NEXB_LASB_IST2_
0     00    +4  +1   000  +01   +01
KVDU_IPR1_IPR2_IPLO_IPLB_
00     1    1    01   01
SCALE_____DEPTH_____ZCUT2_____ZCUB1_____ZCUB2_____DERROR____
            -13.5
DFO_______DFMIN_____DFMAX_____URFA______ANGIN_____DRINV_____URFAB_____
0.1         0.1                  +0.                              -0.5
KST__NAN__ITRE_ISTR_IANG_IERO_IFOU_NRM1_  KREG TIMES
08    050  +0   +0         +1   01
08    050  +0   +0         +1   01
50    100  +0   +0         +1   01
0
31    100  +0   +0         +1   01
8     050  +0   +0         +1   01
IPA1_IPA2_LIN1_LIN2_
0
ICU1_ICU2_ICU3_
0
IHES_NROW_
0     31
KNEW_IDEF_MINT_NINT_ITRM_
0     1   00   100   -0
0.25        -1.
```

Table C.2. Input files, *data2* & *data3.*

```
   -5.682300
    1
    0.000000    0.000000
   -4.870500
   50
    1.088100    0.000000
    1.072100   -0.030972
    1.056000   -0.061891
    1.039800   -0.092753
    1.023500   -0.123550
    1.007100   -0.154290
    0.990560   -0.184960
    0.973890   -0.215570
    …
```

Table C.3. List of variables of *data1*.

Row	Name	Type	Value	Meaning
1	IWIT	I5	0	Do not print input data on file ocondor.
			1	Print input data on file ocondor
	ZZ1	70A1		Ship's name.
2	JOB	I5	-2	Calculate conformal mapping coefficients & interpolate sections.
			-1	Only interpolate sections.
			+1	Only calculate conformal mapping coefficients.
	KREG		≥1	Number of hull regions in the longitudinal direction (see accompanying figure).
7	SCALE	F10.6		Scale factor for uniform scale.
	DEPT		>0.	Depth.
9A	KST(K)	I5	≥0	Number of input sections for region K.
	NAN(K)		≥0	Maximum number of coefficients per station.
	NREGM1(K)		≥0	Number of stations of K-1 region that are used in K region (no discontinuity section is required).
9B	KSTB(K)	I5	≥0	Number of input sections of the for the lower region K.
	NANB(K)		≥0	Maximum number of coefficients per station.
Rows 9A and 9B are read KREG times.				
Row 9B is always read but must contain non-zero values only for doubly connected sections.				
13	KNEW	I5		Number of new sections.
14	ZNEW(KN)	F10.6		z-coordinate of new section KN=1,KNEW.
Row 14 is read when JOBX=2, KNEW times.				
15	KNEWB	I5		Number of new sections.
Row 15 is read when KNEW/=0, KNEW times.				
16	ZNEWB(KN)	F10.6		z-coordinate of new section KN=1,KNEWB.
Row 16 is read when JOBX=2, KNEWB times.				

Table C.4. List of variables of *data2*.

Row	Name	Type	Value	Meaning
The following rows are read KST(K), K=1,KREG times.				
1	Z(K)	F12.6		*z*-coordinate of section K.
2	NPK	I5		Number of points describing section K.
3	XP(I,K)			*x*-coordinate of I-th point of section K.
	YP(I,K)			*y*-coordinate of I-th point of section K.
	NOP(I,K)			
Row 3 is read NPK times.				

Table C.5. List of variables of *data3.*

Row	Name	Type	Value	Meaning
The following rows are read KSTB(K), K=1,KREG times.				
1	ZB(K)	F12.6		*z*-coordinate of section K.
2	NPK	I5		Number of points describing section K.
3	XPB(I,K)			*x*-coordinate of I-th point of section K.
	YPB(I,K)			*y*-coordinate of I-th point of section K.
	NOPB(I,K)			
Row 3 is read NPK times.				

APPENDIX D:

A Guide to *Sorting.f90*

APPENDIX D: A Guide to *Sorting.f90*

The computer program *SORTING_DATA_FOR_CONDOR* realized by means of the *Fortran* source code *sorting.f90* reads the coordinates of points and after sorting them, creates the input files *data2* & *data3* for the conformal mapping program *conformal.f*. Additionally it may apply linear transformations such as scaling or increase of depth. Alternatively it can read the input files of the program *conformal.f* and create new after applying a linear transformation. The program *conformal.f* applies the conformal mapping at points that describe a 2D section of a ship's hull (see Appendix C). The input points for *conformal.f* must be sorted, beginning from the uppermost point.

The program *sorting.f90* needs two sets of data. The first is the coordinates (*x*,*y*,*z*) of the points. The second set consists of variables of the program. These variables are read from the input data file *dsort*. The coordinates (*x*,*y*,*z*) of the points refer to a system where *x* is the longitudinal direction and *y* and *z* are the transverse and vertical directions respectively. The origin point must be located correctly (see Fig. D.1) and the *x*-axis must have the same direction as the *z*-axis of the potential solver. The program will then automatically rotate the coordinates' system and inverse the new *x*-axis so that the new points refer to the input coordinates' system of *conformal.f* and the potential solver *catamaran.f*. The points are input from files, separately for each region (see below), or from input files of *conformal.f*. In the later case the points are considered already sorted.

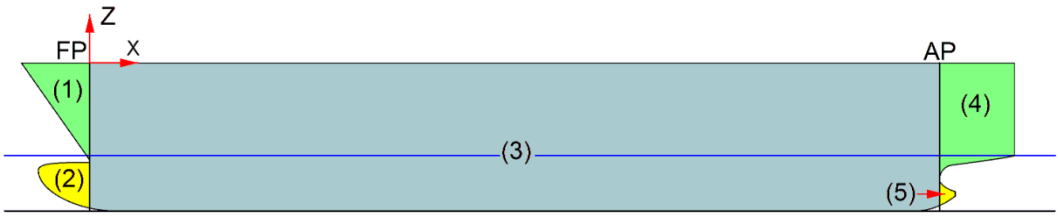

Figure D.1 Definition of the hull regions and the data input coordinates' system (for the program *sorting*).

In order for the potential solver *catamaran.f* to be able to handle the complicated and varying hull shapes of modern ships, the hull surface is subdivided in five regions (Fig. D.1). The first region is the portion of the hull, in front of the fore perpendicular (*FP*) and above the bulb. The fore perpendicular is defined here as the vertical line tangential to the hull's centerline at the bow of the ship, near the intersection of the centerline with the water line. The second region is the bow bulb, defined as the portion of the hull, in front of the fore perpendicular and below the first region.

The fourth region contains the stern and is the portion of the hull, astern the aft perpendicular (*AP*) and above the bulb (when there is one). When the stern of the ship features a stern bulb, the aft perpendicular is defined as the vertical line tangential to the centerline, near the stern of the ship and the intersection of the centerline with the water line. In all other cases the location of the aft perpendicular is arbitrary. The fifth region is the stern bulb, defined as the portion of the hull, astern the aft perpendicular and below the fourth region. Finally the third region is the portion of the hull, astern

the fore perpendicular and in front of the aft perpendicular. The third region is the only requisite region in order for *sorting* to be executed.

Originally the geometry of each region is input through a separate points files as set number of 2D transverse sections. Each section is input through the coordinates of a set number of points, as coordinates (*x*,*y*,*z*) of the input coordinates' system (Fig. D.1). Coordinates are unformatted and separated with "," while the program automatically finds their number.

Once the program reads the coordinates of the points of a region, it automatically sorts them by *x* (longitudinally) and groups them into sections. Then the sections are sorted staring with the foremost. Then the points of each section are sorted in the vertical direction. That may be done in four different ways. Firstly the points may be sorted in the *y*-direction (vertical) that is, starting from the one with the highest value of *y*-coordinate and ending with the one with the smallest value of *y*-coordinate. This method works for stations without propeller tunnel. Secondly the points may be sorted in the *x*-direction (transverse), that is, starting from the one with the highest value of *x*-coordinate and ending with the one with the smallest value of *x*-coordinate. This method does not work for bulbous stations. In the third method, the uppermost point if found followed by the one which is the closest. This method works for all reasonable section forms. In the last method, all points are rotated about *z*-axis and then sorted by the new *y*-axis.

Alternatively the points may be input from files *data3* & *data3*. In that case the program considers them already sorted so the sorting stage is skipped. Before proceeding with the linear transformations though, the program separates the points into groups according to the hull region they describe.

The program is able to apply linear transformations to the points. These transformations are scaling in the three directions as well as increase of the freeboard. In the later case the points are shifted downwards and a linear section is added above to increase the freeboard without otherwise altering the shape of the stations.

The second set of input data consists of the program variables. These variables are read from the text file *dsort* and are formatted and arranged in rows. Every row is proceeded by a dummy row (the program ignores it) that contains the name of each variable. To facilitate the correct use of *dsort*, the columns reserved for each variable are indicated by the columns of the preceding line, that are occupied by the variable's name and the following underscores. All dimensions refer to the input coordinates' system (Fig. D.1). An exemplar *dsort* file is given in Table D.1, while a list of all the variables of *dsort* as well as their type, possible values and meaning are given in Table D.2.

Table D.1. Input file, *dsort.*

```
Data for Sorting-----------------------------------------------------
Ship's_Name----------------------------------------------------------
INAME_
0
NAME
c427
Sorting_Options------------------------------------------------------
ABCDE
11111
SORT1_SORT2_SORT3_SORT4_SORT5_
 1     1     1     1     1
ANGL1_______ANGL2_______ANGL3_______ANGL4_______ANGL5_______
0.            0.            0.           0.           0.
Scaling_Options------------------------------------------------------
ZXYF
0000
SCALEZ______SCALEX______SCALEY______SCALEFB_____
+0.000         +0.000       +0.000    +0.000
```

Table D.2. List of variables of *dsort.*

Row	Variable Name	Variable name in program	Type	Value	Meaning
1	INAME	INAME	I6		Input option of variable NAME
				0	The program reads the value of the variable NAME form the keyboard.
				1	The program reads the value of the variable NAME from this file.
2	NAME	NAME	A*4		Ship's name (maximum 4 characters).
3	A,B,C, D,E	ISORT(M) M=1,…,5	5I1		Input and sorting option for the points:
				0	The program does not read or sort the points of the corresponding region.
				1	The program reads the value of the variable CAS(M) from this file.
				2	The program reads the value of the variable CAS(M) form the keyboard.
If ISORT(1)=ISORT(2)=ISORT(3)=ISORT(4)=ISORT(5)=0, then the program will seek points from files dcondor2 & dcondor3 and will proceed with the linear transformations.					
4	SORTi	CAS(M) M=1,…,5	5I6		Sorting option for the points of M-region:
				1	Sorting by ds.
				2	Sorting by X (simple stations).
				3	Sorting by Y (stations without propeller tunnel).
				4	Rotation about Z-axis by PHI(M)& sorting by Yn.
5	ANGLi	PHI(M) M=1,…,5	5F12.6		The angle [deg] of rotation about Z-axis, if PHI(M)=0. Then the program assumes that PHI(M)=45. (this line is always read).
6	XYZF	ISCALE(L) L=1,…,4	4I1		Transformation option:
				0	The points are not transformed.
				1	The program read the values of the variables SCALEF(L) from this file.
				2	The program read the values of the variables SCALEF(L) form the keyboard.
7	SCALEi	SCALEF(L) L=1,…,4	4F12.6		Scale factor along Z,X,Y directions:
				>0	The value of the scale factor.
				<0	ABS(SCALEF(1))= new length of section (3).
					ABS(SCALEF(2))= new beam.
					ABS(SCALEF(3))= new depth.
	SCALEFB				Scale factor for freeboard:
				>0	Increase of freeboard.
				<0	ABS(SCALEF(4))*DEPTH= Increase of freeboard.

APPENDIX E:

Input Files for the Test Cases

APPENDIX E: Input Files for the Test Cases

As mentioned in Appendix A, the program reads all necessary variables from file *dinp*. Tables E.1 – E.13 contain the input files for each test case, at condition A and V_S=15 kn. For runs at the same condition but different speed, variables NAME and VELIN were properly adjusted. For runs at condition B, the variables that had different values were XGRAV, ZGRAV, EXALA & TRIM.

E.1 Initial Designs

Table E.1. Input file for hull *A*.

```
A_a15n
----------------------GENERAL DATA--------------------------------
IWIT_KCRT_IVIS_NGRI_MAD7_
0     01
VELIN_____FROUDE____DENSIT____GRAV______
7.717                  997.      9.81
VISCOS
0.
SCALEL____XLWL______UCROSS____CROSFL____URFV______
0.00      80.000     +20.
XGRAV_____YGRAV_____ZGRAV_____
35.928       -7.75     -4.5
EXALA_____TRIM______URSINK____URTRIM____SINKLIM___TRIMLIM___
4.725      0.0        0.0         0.0
DZWMIN____DZWMAX____DSURF_____DYGMIN____
0.01       0.1        +0.01
FREBO_____FRELAS____
30.
ISYM_MAST_MASG_MASW_MASY_
1     2000 050  050   040
ISUR_NSUR_ISPL_LAGR_ISU3_ICAU_
+2     1    00   00  +1
IDOB_NONO_MODG_ISUT_IS3T_ICAU_
       1    01   +1   +0   +00
IBUL_IHUB_LTRA_NCAT_ISUC_
0     2    -2   02    +0
NKBL_NKHB_NPKL_LABA_ISUB_ITRL_
00    10    00
IVER_JUPA_IASC_ICON_ITRV_
+1     0   -4
JSUR_NOWC_KSCO_KGBC_MODE_
 -02  +01  00  +000
ISIN_ITRI_KSIN_KTRI_
000   000  000  000
NK1M_NK2M_N3BM_N3SM_NK4M_NK5M_
70    00    40   40  10   90
NK1S_NK2S_N3BS_N3SS_NK4S_NK5S_
35    00    20   20   05   45
NK1F_NK2F_N3BF_N3SF_NK4F_NK5F_
0
NI1M_NI1S_NI1F_
20    10
```

```
NI2M_NI2S_NI2F_
10
NJ1M_NJ1S_NJ1F_
45    30
NJ2M_NJ2S_NJ2F_
20    10
DSURMA____DSURMI____TANEPT____TANEPL____TANBOD____TANTRA____YMINWA____
0.010      0.0010                                                -8.5
DELTAT____YCOREC____DXSCOB____DXSCOS____DXSCOR____COSMAT____TANZG_____
-0.000      -0.0        0.       -00.0       0.    10000.      00.
URFVS_____URFTIM____URFSUR____URFBEM____URFLEM____BERNOUL___URFPS_____
1.0          -0.0      -0.0       -0.0      0.00                -1.0
ZBULB_____ZBOW______ZCUT1_____ZCUT2_____ZCUT3_____ZSTER_____
-0.0      -0.0        0.0       75.5      75.5       80.0
ZG1_______ZMID______ZG4_______ZG34______ZTRANS____
-120.00     40.       260.00     0.0000
DZBULB____DZBOWM1___DZBOWP1___DZKB1M1___DZSTERM1__DZSTERP1__
0.15        +0.3000  0.00000     0.3       0.3       0.3
OM3B______DZKF1_____ZPAR1_____ZPAR2_____Z1KEEL____Z2KEEL____
1.5           0.400     0.         0.000
APLUS_____BPLUSB____BPLUSS____DZHULL____
0.200         0.300       0.50
ZHUB______DZHUB_____
76.900        0.400
IVDH_MAXH_NST__
0     030    +4
ISAV_ISAF_ISAM_MODF_
-2     00  0000
RR1_______RR2_______RR3_______SORMH_____
0.          0.          00.     0.0001
CONFOR*****************************************************************
ICU1_ICU2_ICU3_ICB1_ICB2_
0     0     0
KVDU_IPRK_IPR2_IPRB_IPLO_
-0     0    +0  +0   +0
ZCUB1_____ZCUB2_____ZCUBB1____ZCUBB2____DABAX_____
0.00           00.
GRID*******************************************************************
NISO_IXCO_KVDU_ITRB_IKB1_
                +2
NI1__NI2__NI3__NI4__NI5__NIBU_
 0    00   20   20   20   0
IAB3_IAM3_IAS3_ISPS_ITRA_
3       3    3        +0
DRINV_____ANJY______EXPA3Y___DAR1______DAR2______DAR3______DAR4______
0.01
EXPAB_____EXPAD_____EXPA2B____EXPA2S____EXPA3S____
0.
DEXFIR____DEXLAS____BCANAL____BCANALD___DCANAL____
120.0       150.0      1.0        1.0      0.50
NKB__NJB__NJD__IADB_
                -0
```

Table E.2. Input file for hull *B*.

```
B_a15
----------------------GENERAL DATA-------------------------------
IWIT_KCRT_IVIS_NGRI_MAD7_
0     01
VELIN_____FROUDE____DENSIT____GRAV______
7.717                 997.      9.81
VISCOS
0.
SCALEL____XLWL______UCROSS____CROSFL____URFV______
0.00      80.000     +20.
XGRAV_____YGRAV_____ZGRAV_____
35.712       -7.75     -4.5
EXALA_____TRIM______URSINK____URTRIM____SINKLIM___TRIMLIM___
4.400      0.0        0.5       0.5
DZWMIN____DZWMAX____DSURF_____DYGMIN____
0.01       0.1       +0.01
FREBO_____FRELAS____
30.
ISYM_MAST_MASG_MASW_MASY_
1     2000 050  050   040
ISUR_NSUR_ISPL_LAGR_ISU3_ICAU_
+2     1    00   00  +1
IDOB_NONO_MODG_ISUT_IS3T_ICAU_
       1    01   +1   +0   +00
IBUL_IHUB_LTRA_NCAT_ISUC_
0     0    +1   01    +0
NKBL_NKHB_NPKL_LABA_ISUB_ITRL_
00    00    00
IVER_JUPA_IASC_ICON_ITRV_
+1     0   -4
JSUR_NOWC_KSCO_KGBC_MODE_
 -02  +01  00  +000
ISIN_ITRI_KSIN_KTRI_
200   200  050  050
NK1M_NK2M_N3BM_N3SM_NK4M_NK5M_
70    00    40   40  00   90
NK1S_NK2S_N3BS_N3SS_NK4S_NK5S_
0
NK1F_NK2F_N3BF_N3SF_NK4F_NK5F_
0
NI1M_NI1S_NI1F_
20
NI2M_NI2S_NI2F_

NJ1M_NJ1S_NJ1F_
45    30
NJ2M_NJ2S_NJ2F_
20    10
DSURMA____DSURMI____TANEPT____TANEPL____TANBOD____TANTRA____YMINWA____
0.010      0.0010                                              -8.5
```

```
DELTAT____YCOREC____DXSCOB____DXSCOS____DXSCOR____COSMAT____TANZG_____
-0.000      -0.0        0.       -00.0       0.    10000.      00.
URFVS_____URFTIM____URFSUR____URFBEM____URFLEM____BERNOUL___URFPS_____
1.0         -0.0      -0.0       -0.0      0.00                -1.0
ZBULB_____ZBOW______ZCUT1_____ZCUT2_____ZCUT3_____ZSTER_____
-0.0      -0.0       0.0       72.026    72.026     72.026
ZG1_______ZMID______ZG4_______ZG34______ZTRANS____
-120.00     40.      260.00     0.0000
DZBULB____DZBOWM1___DZBOWP1___DZKB1M1___DZSTERM1__DZSTERP1__
0.00        +0.3000  0.00000     0.3      0.3      0.3
OM3B______DZKF1_____ZPAR1_____ZPAR2_____Z1KEEL____Z2KEEL____
1.5           0.400     0.        0.000
APLUS_____BPLUSB____BPLUSS____DZHULL____
0.200        0.300       0.50
ZHUB______DZHUB_____
0.000       0.000
IVDH_MAXH_NST__
0     030    +4
ISAV_ISAF_ISAM_MODF_
+1     00  0000
RR1_______RR2_______RR3_______SORMH_____
0.          0.          00.     0.0001
CONFOR**********************************************************************
*********
ICU1_ICU2_ICU3_ICB1_ICB2_
0     0     0
KVDU_IPRK_IPR2_IPRB_IPLO_
-0     0    +0  +0   +0
ZCUB1_____ZCUB2_____ZCUBB1____ZCUBB2____DABAX_____
0.00           00.
GRID************************************************************************
********
NISO_IXCO_KVDU_ITRB_IKB1_
                +2
NI1__NI2__NI3__NI4__NI5__NIBU_
05    20   20   20   20   0
IAB3_IAM3_IAS3_ISPS_ITRA_
3       3    3        +0
DRINV_____ANJY______EXPA3Y___DAR1______DAR2______DAR3______DAR4______
0.01
EXPAB_____EXPAD_____EXPA2B____EXPA2S____EXPA3S____
0.
DEXFIR____DEXLAS____BCANAL____BCANALD___DCANAL____
120.0       150.0      1.0        1.0      0.50
NKB__NJB__NJD__IADB_
                -0
```

Table E.3. Input file for hull *C*.

```
C_a15
----------------------GENERAL DATA-------------------------------
IWIT_KCRT_IVIS_NGRI_MAD7_
0     01
VELIN_____FROUDE____DENSIT____GRAV______
7.717                 997.      9.81
VISCOS
0.
SCALEL____XLWL______UCROSS____CROSFL____URFV______
0.00      92.000     +20.
XGRAV_____YGRAV_____ZGRAV_____
48.453       -6.60     -4.5
EXALA_____TRIM______URSINK____URTRIM____SINKLIM___TRIMLIM___
5.230      0.0          0.5       0.5
DZWMIN____DZWMAX____DSURF_____DYGMIN____
0.01       0.1       +0.01
FREBO_____FRELAS____
30.
ISYM_MAST_MASG_MASW_MASY_
1     3000 050  050   040
ISUR_NSUR_ISPL_LAGR_ISU3_ICAU_
+2     1    00   00  +1
IDOB_NONO_MODG_ISUT_IS3T_ICAU_
       1    01   +1   +0   +00
IBUL_IHUB_LTRA_NCAT_ISUC_
0     2    -2   02    +0
NKBL_NKHB_NPKL_LABA_ISUB_ITRL_
00    10    00
IVER_JUPA_IASC_ICON_ITRV_
+1     0   -4
JSUR_NOWC_KSCO_KGBC_MODE_
 -02  +01  00  +000
ISIN_ITRI_KSIN_KTRI_
200   200  025  025
NK1M_NK2M_N3BM_N3SM_NK4M_NK5M_
70    00    40   40  10   90
NK1S_NK2S_N3BS_N3SS_NK4S_NK5S_
0
NK1F_NK2F_N3BF_N3SF_NK4F_NK5F_
0
NI1M_NI1S_NI1F_
20
NI2M_NI2S_NI2F_

NJ1M_NJ1S_NJ1F_
45    30
NJ2M_NJ2S_NJ2F_
20    10
DSURMA____DSURMI____TANEPT____TANEPL____TANBOD____TANTRA____YMINWA____
0.010      0.0010                                              -8.5
```

```
DELTAT____YCOREC____DXSCOB____DXSCOS____DXSCOR____COSMAT____TANZG_____
-0.000      -0.0        0.       -00.0       0.    10000.      00.
URFVS_____URFTIM____URFSUR____URFBEM____URFLEM____BERNOUL___URFPS_____
1.0         -0.0       -0.0       -0.0      0.00                -1.0
ZBULB_____ZBOW______ZCUT1_____ZCUT2_____ZCUT3_____ZSTER_____
-0.0      -0.0        0.0        87.5      87.5       92.0
ZG1_______ZMID______ZG4_______ZG34______ZTRANS____
-120.00     40.       260.00     0.0000
DZBULB____DZBOWM1___DZBOWP1___DZKB1M1___DZSTERM1__DZSTERP1__
0.15        +0.3000  0.00000     0.3       0.3       0.3
OM3B______DZKF1_____ZPAR1_____ZPAR2_____Z1KEEL____Z2KEEL____
1.5           0.400     0.         0.000
APLUS_____BPLUSB____BPLUSS____DZHULL____
0.200        0.300       0.50
ZHUB______DZHUB_____
88.900       0.400
IVDH_MAXH_NST__
0     030    +4
ISAV_ISAF_ISAM_MODF_
-2     00  0000
RR1_______RR2_______RR3_______SORMH_____
0.          0.          00.     0.0001
CONFOR*************************************************************
ICU1_ICU2_ICU3_ICB1_ICB2_
0     0     0
KVDU_IPRK_IPR2_IPRB_IPLO_
-0     0    +0  +0   +0
ZCUB1_____ZCUB2_____ZCUBB1____ZCUBB2____DABAX_____
0.00           00.
GRID***************************************************************
NISO_IXCO_KVDU_ITRB_IKB1_
                +2
NI1__NI2__NI3__NI4__NI5__NIBU_
 0    00   20   20   20   0
IAB3_IAM3_IAS3_ISPS_ITRA_
3       3    3        +0
DRINV_____ANJY______EXPA3Y___DAR1______DAR2______DAR3______DAR4______
0.01
EXPAB_____EXPAD_____EXPA2B____EXPA2S____EXPA3S____
0.
DEXFIR____DEXLAS____BCANAL____BCANALD___DCANAL____
120.0       150.0      1.0        1.0      0.50
NKB__NJB__NJD__IADB_
                -0
```

Table E.4. Input file for hull *D.*

```
D_a15n
----------------------GENERAL DATA-------------------------------
IWIT_KCRT_IVIS_NGRI_MAD7_
0     01
VELIN_____FROUDE____DENSIT____GRAV______
7.717                 997.      9.81
VISCOS
0.
SCALEL____XLWL______UCROSS____CROSFL____URFV______
0.00      92.000     +20.
XGRAV_____YGRAV_____ZGRAV_____
44.396       -6.60     -4.5
EXALA_____TRIM______URSINK____URTRIM____SINKLIM___TRIMLIM___
4.690      0.0        0.5       0.5
DZWMIN____DZWMAX____DSURF_____DYGMIN____
0.01       0.1       +0.01
FREBO_____FRELAS____
30.
ISYM_MAST_MASG_MASW_MASY_
1     2000 050  050   040
ISUR_NSUR_ISPL_LAGR_ISU3_ICAU_
+2     1    00   00  +1
IDOB_NONO_MODG_ISUT_IS3T_ICAU_
       1    01   +1   +0   +00
IBUL_IHUB_LTRA_NCAT_ISUC_
0     0    +1   01    +0
NKBL_NKHB_NPKL_LABA_ISUB_ITRL_
00    00    00
IVER_JUPA_IASC_ICON_ITRV_
+1     0   -4
JSUR_NOWC_KSCO_KGBC_MODE_
 -02  +01  00  +000
ISIN_ITRI_KSIN_KTRI_
200   200  025  025
NK1M_NK2M_N3BM_N3SM_NK4M_NK5M_
70    00    40   40  00   90
NK1S_NK2S_N3BS_N3SS_NK4S_NK5S_
35    00    20   20  00   45
NK1F_NK2F_N3BF_N3SF_NK4F_NK5F_
0
NI1M_NI1S_NI1F_
20    10
NI2M_NI2S_NI2F_

NJ1M_NJ1S_NJ1F_
45    30
NJ2M_NJ2S_NJ2F_
20    10
DSURMA____DSURMI____TANEPT____TANEPL____TANBOD____TANTRA____YMINWA____
0.010      0.0010                                              -8.5
```

```
DELTAT____YCOREC____DXSCOB____DXSCOS____DXSCOR____COSMAT____TANZG_____
-0.000      -0.0        0.       -00.0       0.    10000.       00.
URFVS_____URFTIM____URFSUR____URFBEM____URFLEM____BERNOUL___URFPS_____
1.0         -0.0       -0.0       -0.0      0.00                -1.0
ZBULB_____ZBOW______ZCUT1_____ZCUT2_____ZCUT3_____ZSTER_____
-0.0      -0.0        0.0        92.000    92.000     92.000
ZG1_______ZMID______ZG4_______ZG34______ZTRANS____
-120.00     46.       260.00     0.0000
DZBULB____DZBOWM1___DZBOWP1___DZKB1M1___DZSTERM1__DZSTERP1__
0.00        +0.3000  0.00000     0.3       0.3       0.3
OM3B______DZKF1_____ZPAR1_____ZPAR2_____Z1KEEL____Z2KEEL____
1.5           0.400     0.         0.000
APLUS_____BPLUSB____BPLUSS____DZHULL____
0.200        0.300       0.50
ZHUB______DZHUB_____
0.000       0.000
IVDH_MAXH_NST__
0     030    +4
ISAV_ISAF_ISAM_MODF_
-2     00  0000
RR1_______RR2_______RR3_______SORMH_____
0.          0.          00.     0.0001
CONFOR*************************************************************
ICU1_ICU2_ICU3_ICB1_ICB2_
0     0     0
KVDU_IPRK_IPR2_IPRB_IPLO_
-0     0    +0  +0   +0
ZCUB1_____ZCUB2_____ZCUBB1____ZCUBB2____DABAX_____
0.00           00.
GRID***************************************************************
NISO_IXCO_KVDU_ITRB_IKB1_
                +2
NI1__NI2__NI3__NI4__NI5__NIBU_
05    20   20   20   20   0
IAB3_IAM3_IAS3_ISPS_ITRA_
3       3    3        +0
DRINV_____ANJY______EXPA3Y___DAR1______DAR2______DAR3______DAR4______
0.01
EXPAB_____EXPAD_____EXPA2B____EXPA2S____EXPA3S____
0.
DEXFIR____DEXLAS____BCANAL____BCANALD___DCANAL____
120.0       150.0      1.0        1.0      0.50
NKB__NJB__NJD__IADB_
                -0
```

Table E.5. Input file for hull *E*.

```
E_a15
----------------------GENERAL DATA-------------------------------
IWIT_KCRT_IVIS_NGRI_MAD7_
0     01
VELIN_____FROUDE____DENSIT____GRAV______
7.717                 997.      9.81
VISCOS
0.
SCALEL____XLWL______UCROSS____CROSFL____URFV______
0.00      80.000     +20.
XGRAV_____YGRAV_____ZGRAV_____
40.         -8.00     -4.5
EXALA_____TRIM______URSINK____URTRIM____SINKLIM___TRIMLIM___
5.280      0.0        0.5        0.5
DZWMIN____DZWMAX____DSURF_____DYGMIN____
0.01       0.1       +0.01
FREBO_____FRELAS____
30.
ISYM_MAST_MASG_MASW_MASY_
1     2000 050  050   040
ISUR_NSUR_ISPL_LAGR_ISU3_ICAU_
+2     1    00   00  +1
IDOB_NONO_MODG_ISUT_IS3T_ICAU_
       1    01   +1   +0   +00
IBUL_IHUB_LTRA_NCAT_ISUC_
0     0    -2   01    +0
NKBL_NKHB_NPKL_LABA_ISUB_ITRL_
00    00    00
IVER_JUPA_IASC_ICON_ITRV_
+1     0   -4
JSUR_NOWC_KSCO_KGBC_MODE_
 -02  +01  00  +000
ISIN_ITRI_KSIN_KTRI_
200   200  050  050
NK1M_NK2M_N3BM_N3SM_NK4M_NK5M_
70    00    40   40  00   90
NK1S_NK2S_N3BS_N3SS_NK4S_NK5S_
0
NK1F_NK2F_N3BF_N3SF_NK4F_NK5F_
0
NI1M_NI1S_NI1F_
20
NI2M_NI2S_NI2F_

NJ1M_NJ1S_NJ1F_
45    30
NJ2M_NJ2S_NJ2F_
20    10
DSURMA____DSURMI____TANEPT____TANEPL____TANBOD____TANTRA____YMINWA____
0.010      0.0010                                              -8.5
```

```
DELTAT____YCOREC____DXSCOB____DXSCOS____DXSCOR____COSMAT____TANZG_____
-0.000      -0.0        0.       -00.0       0.    10000.      00.
URFVS_____URFTIM____URFSUR____URFBEM____URFLEM____BERNOUL___URFPS_____
1.0         -0.0       -0.0       -0.0      0.00                -1.0
ZBULB_____ZBOW______ZCUT1_____ZCUT2_____ZCUT3_____ZSTER_____
-0.0       -0.0        0.0        80.0      80.0       80.0
ZG1_______ZMID______ZG4_______ZG34______ZTRANS____
-120.00     40.       260.00     0.0000
DZBULB____DZBOWM1___DZBOWP1___DZKB1M1___DZSTERM1__DZSTERP1__
0.0         +0.3000  0.00000     0.3       0.3       0.3
OM3B______DZKF1_____ZPAR1_____ZPAR2_____Z1KEEL____Z2KEEL____
1.5           0.400     0.         0.000
APLUS_____BPLUSB____BPLUSS____DZHULL____
0.200        0.300       0.50
ZHUB______DZHUB_____

IVDH_MAXH_NST__
0     030    +4
ISAV_ISAF_ISAM_MODF_
-2     00  0000
RR1_______RR2_______RR3_______SORMH_____
0.          0.          00.     0.0001
CONFOR*************************************************************
ICU1_ICU2_ICU3_ICB1_ICB2_
0     0     0
KVDU_IPRK_IPR2_IPRB_IPLO_
-0     0    +0  +0   +0
ZCUB1_____ZCUB2_____ZCUBB1____ZCUBB2____DABAX_____
0.00           00.
GRID***************************************************************
NISO_IXCO_KVDU_ITRB_IKB1_
                +2
NI1__NI2__NI3__NI4__NI5__NIBU_
05    20   20   20   20   0
IAB3_IAM3_IAS3_ISPS_ITRA_
3       3    3        +0
DRINV_____ANJY______EXPA3Y___DAR1______DAR2______DAR3______DAR4______
0.01
EXPAB_____EXPAD_____EXPA2B____EXPA2S____EXPA3S____
0.
DEXFIR____DEXLAS____BCANAL____BCANALD___DCANAL____
120.0       150.0      1.0        1.0      0.50
NKB__NJB__NJD__IADB_
                -0
```

E.2 First Optimization

Table E.6. Input file for hull *B377*.

```
B377_a15
----------------------GENERAL DATA-------------------------------
IWIT_KCRT_IVIS_NGRI_MAD7_
0     01
VELIN_____FROUDE____DENSIT____GRAV______
7.717                 997.      9.81
VISCOS
0.
SCALEL____XLWL______UCROSS____CROSFL____URFV______
0.00      80.000     +20.
XGRAV_____YGRAV_____ZGRAV_____
37.743       -7.190    -5.1
EXALA_____TRIM______URSINK____URTRIM____SINKLIM___TRIMLIM___
6.800      0.0        0.5        0.5
DZWMIN____DZWMAX____DSURF_____DYGMIN____
0.01       0.1       +0.01
FREBO_____FRELAS____
30.
ISYM_MAST_MASG_MASW_MASY_
1     2000 050  050   040
ISUR_NSUR_ISPL_LAGR_ISU3_ICAU_
+2     1    00   00  +1
IDOB_NONO_MODG_ISUT_IS3T_ICAU_
       1    01   +1   +0   +00
IBUL_IHUB_LTRA_NCAT_ISUC_
2     0    -2   03    +0
NKBL_NKHB_NPKL_LABA_ISUB_ITRL_
10    00    00
IVER_JUPA_IASC_ICON_ITRV_
+1     0   -4
JSUR_NOWC_KSCO_KGBC_MODE_
 -02  +01  00  +000
ISIN_ITRI_KSIN_KTRI_
200   200  025  025
NK1M_NK2M_N3BM_N3SM_NK4M_NK5M_
70    10    40   40  20   90
NK1S_NK2S_N3BS_N3SS_NK4S_NK5S_
35    05    20   20  10   45
NK1F_NK2F_N3BF_N3SF_NK4F_NK5F_
0
NI1M_NI1S_NI1F_
20    10
NI2M_NI2S_NI2F_
20    10
NJ1M_NJ1S_NJ1F_
45    30
NJ2M_NJ2S_NJ2F_
20    10
```

```
DSURMA____DSURMI____TANEPT____TANEPL____TANBOD____TANTRA____YMINWA____
0.010      0.0010                                                -8.5
DELTAT____YCOREC____DXSCOB____DXSCOS____DXSCOR____COSMAT____TANZG_____
-0.000      -0.0        0.       -00.0       0.    10000.      00.
URFVS_____URFTIM____URFSUR____URFBEM____URFLEM____BERNOUL___URFPS_____
1.0         -0.0       -0.0       -0.0      0.00                -1.0
ZBULB_____ZBOW______ZCUT1_____ZCUT2_____ZCUT3_____ZSTER_____
-2.720    -6.470     0.0        70.509    70.509    83.400
ZG1_______ZMID______ZG4_______ZG34______ZTRANS____
-120.00     40.      260.00     0.0000
DZBULB____DZBOWM1___DZBOWP1___DZKB1M1___DZSTERM1__DZSTERP1__
0.15        +0.3000  0.00000     0.3       0.3       0.3
OM3B______DZKF1_____ZPAR1_____ZPAR2_____Z1KEEL____Z2KEEL____
1.5           0.400     0.         0.000
APLUS_____BPLUSB____BPLUSS____DZHULL____
0.200        0.300       0.50
ZHUB______DZHUB_____
0.000       0.400
IVDH_MAXH_NST__
0     030    +4
ISAV_ISAF_ISAM_MODF_
-2     00  0000
RR1_______RR2_______RR3_______SORMH_____
0.          0.          00.     0.0001
CONFOR*************************************************************
ICU1_ICU2_ICU3_ICB1_ICB2_
0     0     0
KVDU_IPRK_IPR2_IPRB_IPLO_
-0     0    +0  +0   +0
ZCUB1_____ZCUB2_____ZCUBB1____ZCUBB2____DABAX_____
0.00           00.
GRID***************************************************************
NISO_IXCO_KVDU_ITRB_IKB1_
                +1
NI1__NI2__NI3__NI4__NI5__NIBU_
10    10   20   20   00   10
IAB3_IAM3_IAS3_ISPS_ITRA_
3       3    3        +0
DRINV_____ANJY______EXPA3Y___DAR1______DAR2______DAR3______DAR4______
0.01
EXPAB_____EXPAD_____EXPA2B____EXPA2S____EXPA3S____
0.
DEXFIR____DEXLAS____BCANAL____BCANALD___DCANAL____
120.0       150.0      1.0        1.0      0.50
NKB__NJB__NJD__IADB_
                -0
```

Table E.7. Input file for hull *B401*.

```
B401_a15
----------------------GENERAL DATA-------------------------------
IWIT_KCRT_IVIS_NGRI_MAD7_
0     01
VELIN_____FROUDE____DENSIT____GRAV______
7.717                 997.      9.81
VISCOS
0.
SCALEL____XLWL______UCROSS____CROSFL____URFV______
0.00      90.000     +20.
XGRAV_____YGRAV_____ZGRAV_____
41.665       -5.915    -4.5
EXALA_____TRIM______URSINK____URTRIM____SINKLIM___TRIMLIM___
6.800      0.0        0.5         0.5
DZWMIN____DZWMAX____DSURF_____DYGMIN____
0.01       0.1        +0.01
FREBO_____FRELAS____
30.
ISYM_MAST_MASG_MASW_MASY_
1     2000 050  050   040
ISUR_NSUR_ISPL_LAGR_ISU3_ICAU_
+2     1    00   00  +1
IDOB_NONO_MODG_ISUT_IS3T_ICAU_
       1    01   +1   +0   +00
IBUL_IHUB_LTRA_NCAT_ISUC_
2     0    -2   03    +0
NKBL_NKHB_NPKL_LABA_ISUB_ITRL_
10    00    00
IVER_JUPA_IASC_ICON_ITRV_
+1     0   -4
JSUR_NOWC_KSCO_KGBC_MODE_
 -02  +01  00  +000
ISIN_ITRI_KSIN_KTRI_
200   200  025  025
NK1M_NK2M_N3BM_N3SM_NK4M_NK5M_
70    10    40   40  20   90
NK1S_NK2S_N3BS_N3SS_NK4S_NK5S_
35    05    20   20  10   45
NK1F_NK2F_N3BF_N3SF_NK4F_NK5F_
0
NI1M_NI1S_NI1F_
20    10
NI2M_NI2S_NI2F_
20    10
NJ1M_NJ1S_NJ1F_
45    30
NJ2M_NJ2S_NJ2F_
20    10
DSURMA____DSURMI____TANEPT____TANEPL____TANBOD____TANTRA____YMINWA____
0.010      0.0010                                              -8.5
```

```
DELTAT____YCOREC____DXSCOB____DXSCOS____DXSCOR____COSMAT____TANZG_____
-0.000      -0.0        0.       -00.0       0.    10000.      00.
URFVS_____URFTIM____URFSUR____URFBEM____URFLEM____BERNOUL___URFPS_____
1.0         -0.0       -0.0       -0.0      0.00                -1.0
ZBULB_____ZBOW______ZCUT1_____ZCUT2_____ZCUT3_____ZSTER_____
-3.060    -6.470     0.0       78.982    78.982    93.400
ZG1_______ZMID______ZG4_______ZG34______ZTRANS____
-120.00     40.       260.00     0.0000
DZBULB____DZBOWM1___DZBOWP1___DZKB1M1___DZSTERM1__DZSTERP1__
0.15        +0.3000  0.00000     0.3       0.3       0.3
OM3B______DZKF1_____ZPAR1_____ZPAR2_____Z1KEEL____Z2KEEL____
1.5           0.400     0.        0.000
APLUS_____BPLUSB____BPLUSS____DZHULL____
0.200        0.300       0.50
ZHUB______DZHUB_____
0.000       0.400
IVDH_MAXH_NST__
0     030    +4
ISAV_ISAF_ISAM_MODF_
-2     00  0000
RR1_______RR2_______RR3_______SORMH_____
0.          0.          00.     0.0001
CONFOR*************************************************************
ICU1_ICU2_ICU3_ICB1_ICB2_
0     0     0
KVDU_IPRK_IPR2_IPRB_IPLO_
-0     0    +0  +0   +0
ZCUB1_____ZCUB2_____ZCUBB1____ZCUBB2____DABAX_____
0.00           00.
GRID***************************************************************
NISO_IXCO_KVDU_ITRB_IKB1_
                +1
NI1__NI2__NI3__NI4__NI5__NIBU_
10    10   20   20   00   10
IAB3_IAM3_IAS3_ISPS_ITRA_
3       3    3        +0
DRINV_____ANJY______EXPA3Y___DAR1______DAR2______DAR3______DAR4______
0.01
EXPAB_____EXPAD_____EXPA2B____EXPA2S____EXPA3S____
0.
DEXFIR____DEXLAS____BCANAL____BCANALD___DCANAL____
120.0       150.0      1.0        1.0      0.50
NKB__NJB__NJD__IADB_
                -0
```

Table E.8. Input file for hull *B422.*

```
B422_a15
----------------------GENERAL DATA-------------------------------
IWIT_KCRT_IVIS_NGRI_MAD7_
0     01
VELIN_____FROUDE____DENSIT____GRAV______
7.717                 997.      9.81
VISCOS
0.
SCALEL____XLWL______UCROSS____CROSFL____URFV______
0.00      80.000     +20.
XGRAV_____YGRAV_____ZGRAV_____
37.635       -7.245    -5.1
EXALA_____TRIM______URSINK____URTRIM____SINKLIM___TRIMLIM___
6.800      0.0        0.5        0.5
DZWMIN____DZWMAX____DSURF_____DYGMIN____
0.01       0.1       +0.01
FREBO_____FRELAS____
30.
ISYM_MAST_MASG_MASW_MASY_
1     2000 050  050   040
ISUR_NSUR_ISPL_LAGR_ISU3_ICAU_
+2     1    00   00  +1
IDOB_NONO_MODG_ISUT_IS3T_ICAU_
       1    01   +1   +0   +00
IBUL_IHUB_LTRA_NCAT_ISUC_
2     0    -2   03    +0
NKBL_NKHB_NPKL_LABA_ISUB_ITRL_
10    00    00
IVER_JUPA_IASC_ICON_ITRV_
+1     0   -4
JSUR_NOWC_KSCO_KGBC_MODE_
 -02  +01  00  +000
ISIN_ITRI_KSIN_KTRI_
200   200  025  025
NK1M_NK2M_N3BM_N3SM_NK4M_NK5M_
70    10    40   40  20   90
NK1S_NK2S_N3BS_N3SS_NK4S_NK5S_
35    05    20   20  10   45
NK1F_NK2F_N3BF_N3SF_NK4F_NK5F_
0
NI1M_NI1S_NI1F_
20    10
NI2M_NI2S_NI2F_
20    10
NJ1M_NJ1S_NJ1F_
45    30
NJ2M_NJ2S_NJ2F_
20    10
DSURMA____DSURMI____TANEPT____TANEPL____TANBOD____TANTRA____YMINWA____
0.010      0.0010                                              -8.5
```

```
DELTAT____YCOREC____DXSCOB____DXSCOS____DXSCOR____COSMAT____TANZG_____
-0.000      -0.0        0.       -00.0       0.    10000.      00.
URFVS_____URFTIM____URFSUR____URFBEM____URFLEM____BERNOUL___URFPS_____
1.0         -0.0       -0.0       -0.0      0.00                -1.0
ZBULB_____ZBOW______ZCUT1_____ZCUT2_____ZCUT3_____ZSTER_____
-2.210    -6.538     0.0       70.534    70.534    83.400
ZG1_______ZMID______ZG4_______ZG34______ZTRANS____
-120.00     40.       260.00     0.0000
DZBULB____DZBOWM1___DZBOWP1___DZKB1M1___DZSTERM1__DZSTERP1__
0.15        +0.3000  0.00000     0.3       0.3       0.3
OM3B______DZKF1_____ZPAR1_____ZPAR2_____Z1KEEL____Z2KEEL____
1.5           0.400     0.        0.000
APLUS_____BPLUSB____BPLUSS____DZHULL____
0.200        0.300       0.50
ZHUB______DZHUB_____
0.000       0.400
IVDH_MAXH_NST__
0     030    +4
ISAV_ISAF_ISAM_MODF_
-2     00  0000
RR1_______RR2_______RR3_______SORMH_____
0.          0.          00.     0.0001
CONFOR*************************************************************
ICU1_ICU2_ICU3_ICB1_ICB2_
0     0     0
KVDU_IPRK_IPR2_IPRB_IPLO_
-0     0    +0  +0   +0
ZCUB1_____ZCUB2_____ZCUBB1____ZCUBB2____DABAX_____
0.00           00.
GRID***************************************************************
NISO_IXCO_KVDU_ITRB_IKB1_
                +1
NI1__NI2__NI3__NI4__NI5__NIBU_
10    10   20   20   00   10
IAB3_IAM3_IAS3_ISPS_ITRA_
3       3    3        +0
DRINV_____ANJY______EXPA3Y___DAR1______DAR2______DAR3______DAR4______
0.01
EXPAB_____EXPAD_____EXPA2B____EXPA2S____EXPA3S____
0.
DEXFIR____DEXLAS____BCANAL____BCANALD___DCANAL____
120.0       150.0      1.0        1.0      0.50
NKB__NJB__NJD__IADB_
                -0
```

Table E.9. Input file for hull *B428.*

```
B428_a15
----------------------GENERAL DATA-------------------------------
IWIT_KCRT_IVIS_NGRI_MAD7_
0     01
VELIN_____FROUDE____DENSIT____GRAV______
7.717                 997.      9.81
VISCOS
0.
SCALEL____XLWL______UCROSS____CROSFL____URFV______
0.00      90.000     +20.
XGRAV_____YGRAV_____ZGRAV_____
42.169       -6.060    -5.25
EXALA_____TRIM______URSINK____URTRIM____SINKLIM___TRIMLIM___
7.000      0.0       0.5        0.5
DZWMIN____DZWMAX____DSURF_____DYGMIN____
0.01       0.1       +0.01
FREBO_____FRELAS____
30.
ISYM_MAST_MASG_MASW_MASY_
1     2000 050  050   040
ISUR_NSUR_ISPL_LAGR_ISU3_ICAU_
+2     1    00   00  +1
IDOB_NONO_MODG_ISUT_IS3T_ICAU_
       1    01   +1   +0   +00
IBUL_IHUB_LTRA_NCAT_ISUC_
2     0    -2   03    +0
NKBL_NKHB_NPKL_LABA_ISUB_ITRL_
10    00    00
IVER_JUPA_IASC_ICON_ITRV_
+1     0   -4
JSUR_NOWC_KSCO_KGBC_MODE_
 -02  +01  00  +000
ISIN_ITRI_KSIN_KTRI_
200   200  025  025
NK1M_NK2M_N3BM_N3SM_NK4M_NK5M_
70    10    40   40  20   90
NK1S_NK2S_N3BS_N3SS_NK4S_NK5S_
35    05    20   20  10   45
NK1F_NK2F_N3BF_N3SF_NK4F_NK5F_
0
NI1M_NI1S_NI1F_
20    10
NI2M_NI2S_NI2F_
20    10
NJ1M_NJ1S_NJ1F_
45    30
NJ2M_NJ2S_NJ2F_
20    10
DSURMA____DSURMI____TANEPT____TANEPL____TANBOD____TANTRA____YMINWA____
0.010      0.0010                                              -8.5
```

```
DELTAT____YCOREC____DXSCOB____DXSCOS____DXSCOR____COSMAT____TANZG_____
-0.000      -0.0        0.       -00.0       0.    10000.      00.
URFVS_____URFTIM____URFSUR____URFBEM____URFLEM____BERNOUL___URFPS_____
1.0         -0.0       -0.0       -0.0      0.00                -1.0
ZBULB_____ZBOW______ZCUT1_____ZCUT2_____ZCUT3_____ZSTER_____
-3.328    -6.660     0.0       79.129    79.129    93.500
ZG1_______ZMID______ZG4_______ZG34______ZTRANS____
-120.00     50.       260.00     0.0000
DZBULB____DZBOWM1___DZBOWP1___DZKB1M1___DZSTERM1__DZSTERP1__
0.15        +0.3000  0.00000     0.3       0.3       0.3
OM3B______DZKF1_____ZPAR1_____ZPAR2_____Z1KEEL____Z2KEEL____
1.5           0.400     0.        0.000
APLUS_____BPLUSB____BPLUSS____DZHULL____
0.200        0.300       0.50
ZHUB______DZHUB_____
0.000       0.400
IVDH_MAXH_NST__
0     030    +4
ISAV_ISAF_ISAM_MODF_
-2     00  0000
RR1_______RR2_______RR3_______SORMH_____
0.          0.          00.     0.0001
CONFOR*************************************************************
ICU1_ICU2_ICU3_ICB1_ICB2_
0     0     0
KVDU_IPRK_IPR2_IPRB_IPLO_
-0     0    +0  +0   +0
ZCUB1_____ZCUB2_____ZCUBB1____ZCUBB2____DABAX_____
0.00           00.
GRID***************************************************************
NISO_IXCO_KVDU_ITRB_IKB1_
                +1
NI1__NI2__NI3__NI4__NI5__NIBU_
10    10   20   20   00   10
IAB3_IAM3_IAS3_ISPS_ITRA_
3       3    3        +0
DRINV_____ANJY______EXPA3Y___DAR1______DAR2______DAR3______DAR4______
0.01
EXPAB_____EXPAD_____EXPA2B____EXPA2S____EXPA3S____
0.
DEXFIR____DEXLAS____BCANAL____BCANALD___DCANAL____
120.0       150.0      1.0        1.0      0.50
NKB__NJB__NJD__IADB_
                -0
```

E.3 Second & Third Optimization

Table E.10. Input file for hull *C247*.

```
C247_a15
----------------------GENERAL DATA-------------------------------
IWIT_KCRT_IVIS_NGRI_MAD7_
0     01
VELIN_____FROUDE____DENSIT____GRAV______
-15.0                  997.      9.81
VISCOS
1.e-6
SCALEL____XLWL______UCROSS____CROSFL____URFV______
0.00      80.000     +20.
XGRAV_____YGRAV_____ZGRAV_____
36.099       -7.460    -6.0
EXALA_____TRIM______URSINK____URTRIM____SINKLIM___TRIMLIM___
9.360      0.517     0.5        0.5
DZWMIN____DZWMAX____DSURF_____DYGMIN____
0.01       0.1       +0.01
FREBO_____FRELAS____
30.
ISYM_MAST_MASG_MASW_MASY_
1     2000 050  050   040
ISUR_NSUR_ISPL_LAGR_ISU3_ICAU_
+2     1    00   00  +1
IDOB_NONO_MODG_ISUT_IS3T_ICAU_
       1    01   +1   +0   +00
IBUL_IHUB_LTRA_NCAT_ISUC_
2     2    -2   03    +0
NKBL_NKHB_NPKL_LABA_ISUB_ITRL_
10    05    00
IVER_JUPA_IASC_ICON_ITRV_
+1     0   -4
JSUR_NOWC_KSCO_KGBC_MODE_
 -02  +01  00  +000
ISIN_ITRI_KSIN_KTRI_
200   200  025  025
NK1M_NK2M_N3BM_N3SM_NK4M_NK5M_
70    10    40   40  30   90
NK1S_NK2S_N3BS_N3SS_NK4S_NK5S_
35    05    20   20  15   45
NK1F_NK2F_N3BF_N3SF_NK4F_NK5F_
0
NI1M_NI1S_NI1F_
20    10
NI2M_NI2S_NI2F_
20    10
NJ1M_NJ1S_NJ1F_
45    30
NJ2M_NJ2S_NJ2F_
20    10
```

```
DSURMA____DSURMI____TANEPT____TANEPL____TANBOD____TANTRA____YMINWA____
0.010      0.0010                          +45.                 -8.5
DELTAT____YCOREC____DXSCOB____DXSCOS____DXSCOR____COSMAT____TANZG_____
-0.000      -0.0        0.       -00.0       0.    10000.      00.
URFVS_____URFTIM____URFSUR____URFBEM____URFLEM____BERNOUL___URFPS_____
1.0         -0.0       -0.0       -0.0      0.00                -1.0
ZBULB_____ZBOW______ZCUT1_____ZCUT2_____ZCUT3_____ZSTER_____
-3.150    -5.611     0.0        70.950    70.950    84.175
ZG1_______ZMID______ZG4_______ZG34______ZTRANS____
-120.00     45.       260.00     0.0000
DZBULB____DZBOWM1___DZBOWP1___DZKB1M1___DZSTERM1__DZSTERP1__
0.15        +0.3000  0.00000     0.3       0.3        0.3
OM3B______DZKF1_____ZPAR1_____ZPAR2_____Z1KEEL____Z2KEEL____
1.5           0.400     0.         0.000
APLUS_____BPLUSB____BPLUSS____DZHULL____
0.200        0.300       0.50
ZHUB______DZHUB_____
72.260       0.400
IVDH_MAXH_NST__
0     030    +4
ISAV_ISAF_ISAM_MODF_
-2     00  0000
RR1_______RR2_______RR3_______SORMH_____
0.          0.          00.     0.0001
CONFOR*************************************************************
ICU1_ICU2_ICU3_ICB1_ICB2_
0     0     0
KVDU_IPRK_IPR2_IPRB_IPLO_
-0     0    +0  +0   +0
ZCUB1_____ZCUB2_____ZCUBB1____ZCUBB2____DABAX_____
0.00           00.
GRID***************************************************************
NISO_IXCO_KVDU_ITRB_IKB1_
                -1
NI1__NI2__NI3__NI4__NI5__NIBU_
10    10   20   20   20   10
IAB3_IAM3_IAS3_ISPS_ITRA_
3       3    3        +0
DRINV_____ANJY______EXPA3Y___DAR1______DAR2______DAR3______DAR4______
0.01
EXPAB_____EXPAD_____EXPA2B____EXPA2S____EXPA3S____
0.
DEXFIR____DEXLAS____BCANAL____BCANALD___DCANAL____
120.0       150.0      1.0        1.0      0.50
NKB__NJB__NJD__IADB_
                -0
```

Table E.11. Input file for hull *C423.*

```
C423_a15
----------------------GENERAL DATA-------------------------------
IWIT_KCRT_IVIS_NGRI_MAD7_
0     01
VELIN_____FROUDE____DENSIT____GRAV______
-15.0                 997.      9.81
VISCOS
1.e-6
SCALEL____XLWL______UCROSS____CROSFL____URFV______
0.00      80.000     +20.
XGRAV_____YGRAV_____ZGRAV_____
35.797       -7.365    -6.0
EXALA_____TRIM______URSINK____URTRIM____SINKLIM___TRIMLIM___
9.070      0.396     0.5        0.5
DZWMIN____DZWMAX____DSURF_____DYGMIN____
0.01       0.1       +0.01
FREBO_____FRELAS____
30.
ISYM_MAST_MASG_MASW_MASY_
1     2000 050  050   040
ISUR_NSUR_ISPL_LAGR_ISU3_ICAU_
+2     1    00   00  +1
IDOB_NONO_MODG_ISUT_IS3T_ICAU_
       1    01   +1   +0   +00
IBUL_IHUB_LTRA_NCAT_ISUC_
2     2    -2   03    +0
NKBL_NKHB_NPKL_LABA_ISUB_ITRL_
10    05    00
IVER_JUPA_IASC_ICON_ITRV_
+1     0   -4
JSUR_NOWC_KSCO_KGBC_MODE_
 -02  +01  00  +000
ISIN_ITRI_KSIN_KTRI_
200   200  025  025
NK1M_NK2M_N3BM_N3SM_NK4M_NK5M_
70    10    40   40  30   90
NK1S_NK2S_N3BS_N3SS_NK4S_NK5S_
35    05    20   20  15   45
NK1F_NK2F_N3BF_N3SF_NK4F_NK5F_
0
NI1M_NI1S_NI1F_
20    10
NI2M_NI2S_NI2F_
20    10
NJ1M_NJ1S_NJ1F_
45    30
NJ2M_NJ2S_NJ2F_
20    10
DSURMA____DSURMI____TANEPT____TANEPL____TANBOD____TANTRA____YMINWA____
0.010      0.0010                          +45.                  -8.5
```

```
DELTAT____YCOREC____DXSCOB____DXSCOS____DXSCOR____COSMAT____TANZG_____
-0.000      -0.0        0.       -00.0       0.    10000.      00.
URFVS_____URFTIM____URFSUR____URFBEM____URFLEM____BERNOUL___URFPS_____
1.0         -0.0       -0.0       -0.0      0.00                -1.0
ZBULB_____ZBOW______ZCUT1_____ZCUT2_____ZCUT3_____ZSTER_____
-3.520    -6.050     0.0       70.580    70.580    83.618
ZG1_______ZMID______ZG4_______ZG34______ZTRANS____
-120.00     45.       260.00     0.0000
DZBULB____DZBOWM1___DZBOWP1___DZKB1M1___DZSTERM1__DZSTERP1__
0.15        +0.3000  0.00000     0.3       0.3        0.3
OM3B______DZKF1_____ZPAR1_____ZPAR2_____Z1KEEL____Z2KEEL____
1.5           0.400     0.        0.000
APLUS_____BPLUSB____BPLUSS____DZHULL____
0.200        0.300       0.50
ZHUB______DZHUB_____
71.890       0.400
IVDH_MAXH_NST__
0     030    +4
ISAV_ISAF_ISAM_MODF_
-2     00  0000
RR1_______RR2_______RR3_______SORMH_____
0.          0.          00.     0.0001
CONFOR*************************************************************
ICU1_ICU2_ICU3_ICB1_ICB2_
0     0     0
KVDU_IPRK_IPR2_IPRB_IPLO_
-0     0    +0  +0   +0
ZCUB1_____ZCUB2_____ZCUBB1____ZCUBB2____DABAX_____
0.00           00.
GRID***************************************************************
NISO_IXCO_KVDU_ITRB_IKB1_
                +1
NI1__NI2__NI3__NI4__NI5__NIBU_
10    10   20   20   20   10
IAB3_IAM3_IAS3_ISPS_ITRA_
3       3    3        +0
DRINV_____ANJY______EXPA3Y___DAR1______DAR2______DAR3______DAR4______
0.01
EXPAB_____EXPAD_____EXPA2B____EXPA2S____EXPA3S____
0.
DEXFIR____DEXLAS____BCANAL____BCANALD___DCANAL____
120.0       150.0      1.0        1.0      0.50
NKB__NJB__NJD__IADB_
                -0
```

Table E.12. Input file for hull *C427*.

```
C427_a15
----------------------GENERAL DATA-------------------------------
IWIT_KCRT_IVIS_NGRI_MAD7_
0     01
VELIN_____FROUDE____DENSIT____GRAV______
-15.0                 997.      9.81
VISCOS
1.e-6
SCALEL____XLWL______UCROSS____CROSFL____URFV______
0.00      80.000     +20.
XGRAV_____YGRAV_____ZGRAV_____
36.050       -7.370    -6.0
EXALA_____TRIM______URSINK____URTRIM____SINKLIM___TRIMLIM___
8.970      0.240     0.5        0.5
DZWMIN____DZWMAX____DSURF_____DYGMIN____
0.01       0.1       +0.01
FREBO_____FRELAS____
30.
ISYM_MAST_MASG_MASW_MASY_
1     2000 050  050   040
ISUR_NSUR_ISPL_LAGR_ISU3_ICAU_
+2     1    00   00  +1
IDOB_NONO_MODG_ISUT_IS3T_ICAU_
       1    01   +1   +0   +00
IBUL_IHUB_LTRA_NCAT_ISUC_
2     2    -2   03    +0
NKBL_NKHB_NPKL_LABA_ISUB_ITRL_
10    05    00
IVER_JUPA_IASC_ICON_ITRV_
+1     0   -4
JSUR_NOWC_KSCO_KGBC_MODE_
 -02  +01  00  +000
ISIN_ITRI_KSIN_KTRI_
200   200  025  025
NK1M_NK2M_N3BM_N3SM_NK4M_NK5M_
70    10    40   40  30   90
NK1S_NK2S_N3BS_N3SS_NK4S_NK5S_
35    05    20   20  15   45
NK1F_NK2F_N3BF_N3SF_NK4F_NK5F_
0
NI1M_NI1S_NI1F_
20    10
NI2M_NI2S_NI2F_
20    10
NJ1M_NJ1S_NJ1F_
45    30
NJ2M_NJ2S_NJ2F_
20    10
DSURMA____DSURMI____TANEPT____TANEPL____TANBOD____TANTRA____YMINWA____
0.010      0.0010                          +45.                  -8.5
```

```
DELTAT____YCOREC____DXSCOB____DXSCOS____DXSCOR____COSMAT____TANZG_____
-0.000      -0.0        0.       -00.0       0.    10000.      00.
URFVS_____URFTIM____URFSUR____URFBEM____URFLEM____BERNOUL___URFPS_____
1.0         -0.0       -0.0       -0.0      0.00                -1.0
ZBULB_____ZBOW______ZCUT1_____ZCUT2_____ZCUT3_____ZSTER_____
-3.300    -5.751     0.0       70.800    70.800    83.837
ZG1_______ZMID______ZG4_______ZG34______ZTRANS____
-120.00     45.       260.00     0.0000
DZBULB____DZBOWM1___DZBOWP1___DZKB1M1___DZSTERM1__DZSTERP1__
0.15        +0.3000  0.00000     0.3       0.3        0.3
OM3B______DZKF1_____ZPAR1_____ZPAR2_____Z1KEEL____Z2KEEL____
1.5           0.400     0.        0.000
APLUS_____BPLUSB____BPLUSS____DZHULL____
0.200        0.300       0.50
ZHUB______DZHUB_____
72.110       0.400
IVDH_MAXH_NST__
0     030    +4
ISAV_ISAF_ISAM_MODF_
-2     00  0000
RR1_______RR2_______RR3_______SORMH_____
0.          0.          00.     0.0001
CONFOR*************************************************************
ICU1_ICU2_ICU3_ICB1_ICB2_
0     0     0
KVDU_IPRK_IPR2_IPRB_IPLO_
-0     0    +0  +0   +0
ZCUB1_____ZCUB2_____ZCUBB1____ZCUBB2____DABAX_____
0.00           00.
GRID***************************************************************
NISO_IXCO_KVDU_ITRB_IKB1_
                -1
NI1__NI2__NI3__NI4__NI5__NIBU_
10    10   20   20   20   10
IAB3_IAM3_IAS3_ISPS_ITRA_
3       3    3        +0
DRINV_____ANJY______EXPA3Y___DAR1______DAR2______DAR3______DAR4______
0.01
EXPAB_____EXPAD_____EXPA2B____EXPA2S____EXPA3S____
0.
DEXFIR____DEXLAS____BCANAL____BCANALD___DCANAL____
120.0       150.0      1.0        1.0      0.50
NKB__NJB__NJD__IADB_
                -0
```

Table E.13. Input file for hull *D354*.

```
D354_a15a
----------------------GENERAL DATA-------------------------------
IWIT_KCRT_IVIS_NGRI_MAD7_
0     01
VELIN_____FROUDE____DENSIT____GRAV______
-15.0                 997.      9.81
VISCOS
1.e-6
SCALEL____XLWL______UCROSS____CROSFL____URFV______
0.00       77.000     +20.
XGRAV_____YGRAV_____ZGRAV_____
35.840       -6.955    -6.0
EXALA_____TRIM______URSINK____URTRIM____SINKLIM___TRIMLIM___
8.260      0.200     0.5         0.5
DZWMIN____DZWMAX____DSURF_____DYGMIN____
0.01       0.1       +0.01
FREBO_____FRELAS____
30.
ISYM_MAST_MASG_MASW_MASY_
1     2000 050  050   040
ISUR_NSUR_ISPL_LAGR_ISU3_ICAU_
+2     1    00   00  +1
IDOB_NONO_MODG_ISUT_IS3T_ICAU_
       1    01   +1   +0   +00
IBUL_IHUB_LTRA_NCAT_ISUC_
2     2    -2   03    +0
NKBL_NKHB_NPKL_LABA_ISUB_ITRL_
10    05    00
IVER_JUPA_IASC_ICON_ITRV_
+1     0   -4
JSUR_NOWC_KSCO_KGBC_MODE_
 -02  +01  00  +000
ISIN_ITRI_KSIN_KTRI_
200   200  025  025
NK1M_NK2M_N3BM_N3SM_NK4M_NK5M_
70    10    40   40  30   90
NK1S_NK2S_N3BS_N3SS_NK4S_NK5S_
35    05    20   20  15   45
NK1F_NK2F_N3BF_N3SF_NK4F_NK5F_
0
NI1M_NI1S_NI1F_
20    10
NI2M_NI2S_NI2F_
20    10
NJ1M_NJ1S_NJ1F_
45    30
NJ2M_NJ2S_NJ2F_
20    10
DSURMA____DSURMI____TANEPT____TANEPL____TANBOD____TANTRA____YMINWA____
0.010      0.0010                          +45.                  -8.5
```

```
DELTAT____YCOREC____DXSCOB____DXSCOS____DXSCOR____COSMAT____TANZG_____
-0.000      -0.0        0.       -00.0       0.    10000.      00.
URFVS_____URFTIM____URFSUR____URFBEM____URFLEM____BERNOUL___URFPS_____
1.0         -0.0       -0.0       -0.0      0.00                -1.0
ZBULB_____ZBOW______ZCUT1_____ZCUT2_____ZCUT3_____ZSTER_____
-3.532    -5.682     0.0       70.568    70.568    82.968
ZG1_______ZMID______ZG4_______ZG34______ZTRANS____
-120.00     45.       260.00     0.0000
DZBULB____DZBOWM1___DZBOWP1___DZKB1M1___DZSTERM1__DZSTERP1__
+0.15       +0.3000  0.00000     0.3       0.3        0.3
OM3B______DZKF1_____ZPAR1_____ZPAR2_____Z1KEEL____Z2KEEL____
1.5           0.400     0.        0.000
APLUS_____BPLUSB____BPLUSS____DZHULL____
0.200        0.300       0.50
ZHUB______DZHUB_____
71.877       0.400
IVDH_MAXH_NST__
0     030    +4
ISAV_ISAF_ISAM_MODF_
-2     00  0000
RR1_______RR2_______RR3_______SORMH_____
0.          0.          00.     0.0001
CONFOR*************************************************************
ICU1_ICU2_ICU3_ICB1_ICB2_
0     0     0
KVDU_IPRK_IPR2_IPRB_IPLO_
-0     0    +0  +0   +0
ZCUB1_____ZCUB2_____ZCUBB1____ZCUBB2____DABAX_____
0.00           00.
GRID***************************************************************
NISO_IXCO_KVDU_ITRB_IKB1_
                +1
NI1__NI2__NI3__NI4__NI5__NIBU_
10    10   20   20   20   10
IAB3_IAM3_IAS3_ISPS_ITRA_
3       3    3        +0
DRINV_____ANJY______EXPA3Y___DAR1______DAR2______DAR3______DAR4______
0.01
EXPAB_____EXPAD_____EXPA2B____EXPA2S____EXPA3S____
0.
DEXFIR____DEXLAS____BCANAL____BCANALD___DCANAL____
120.0       150.0      1.0        1.0      0.50
NKB__NJB__NJD__IADB_
                -0
```

APPENDIX F:

Tables of Numerical Results

F.1 Initial Designs

F.1.1 *Hull A*

Table F.1. Numerical Results, Hull *A*, Condition *A.*

Run	V_S		*Fn*	*Catamaran*			*Shipflow*		
	kn	m/s		C_W	*Sinkage* m	*Trim* deg	C_W	*Sinkage* m	*Trim* deg
CAA10	10.00	5.144	0.188	5.63E-04			3.27E-03		
CAA11	11.00	5.659	0.206	6.08E-04			2.77E-03		
CAA12	12.00	6.173	0.225	7.58E-04			2.32E-03		
CAA13	13.00	6.688	0.244	1.35E-03			2.27E-03		
CAA14	14.00	7.202	0.263	2.33E-03			3.33E-03		
CAA15	15.00	7.717	0.281	2.76E-03			4.84E-03		
CAA16	16.00	8.231	0.300	2.43E-03			4.21E-03		
CAA17	17.00	8.746	0.319	2.09E-03			3.10E-03		
CAA18	18.00	9.260	0.338	2.17E-03			2.06E-03		
CAA19	19.00	9.774	0.356	2.76E-03			1.87E-03		
CAA20	20.00	10.289	0.375	3.37E-03			2.47E-03		

Table F.2. Numerical Results, Hull *A*, Condition *B.*

Run	V_S		*Fn*	*Catamaran*			*Shipflow*		
	kn	m/s		C_W	*Sinkage* m	*Trim* deg	C_W	*Sinkage* m	*Trim* deg
	10.00	5.144	0.189				2.80E-03		
	11.00	5.659	0.208				2.27E-03		
	12.00	6.173	0.226				2.02E-03		
	13.00	6.688	0.245				2.23E-03		
	14.00	7.202	0.264				3.26E-03		
CAB15	15.00	7.717	0.283	1.18E-03	3.578	-4.704	3.82E-03		
	16.00	8.231	0.302				3.19E-03		
	17.00	8.746	0.321				2.31E-03		
	18.00	9.260	0.340				1.83E-03		
	19.00	9.774	0.359				2.01E-03		
	20.00	10.289	0.377				2.67E-03		

F.1.2 *Hull B*

Table F.3. Numerical Results, Hull *B*, Condition *A*.

Run	V_S		*Fn*	*Catamaran*			*Shipflow*		
				C_W	*Sinkage*	*Trim*	C_W	*Sinkage*	*Trim*
	kn	m/s			m	deg		m	deg
CBA10	10.00	5.144	0.194	2.97E-04	0.102	-0.096	4.91E-04		
CBA11	11.00	5.659	0.213	3.44E-04	0.136	-0.126	6.92E-04		
CBA12	12.00	6.173	0.232	5.48E-04	0.188	-0.172	5.76E-04		
CBA13	13.00	6.688	0.252	8.95E-04	0.232	-0.206	1.34E-03		
CBA14	14.00	7.202	0.271	2.36E-03	0.234	-0.085	3.02E-03		
CBA15	15.00	7.717	0.290	2.68E-03	0.276	-0.082			
CBA16	16.00	8.231	0.310	2.58E-03	0.253	-0.029			
CBA17	17.00	8.746	0.329	2.44E-03	0.321	-0.097	1.30E-03		
CBA18	18.00	9.260	0.348	3.33E-03	0.179	0.163	1.70E-03		
CBA19	19.00	9.774	0.368	2.93E-03	0.368	-0.155			
CBA20	20.00	10.289	0.387	3.26E-03	0.483	-0.273			

Table F.4. Numerical Results, Hull *B*, Condition *B*.

Run	V_S		*Fn*	*Catamaran*			*Shipflow*		
				C_W	*Sinkage*	*Trim*	C_W	*Sinkage*	*Trim*
	kn	m/s			m	deg		m	deg
	10.00	5.144	0.199				9.31E-04		
	11.00	5.659	0.219				1.24E-03		
	12.00	6.173	0.239				1.08E-03		
	13.00	6.688	0.259				2.24E-03		
	14.00	7.202	0.279				3.72E-03		
CBB15	15.00	7.717	0.299	2.66E-03	0.174	0.027			
	16.00	8.231	0.319				2.10E-03		
	17.00	8.746	0.339				1.70E-03		
	18.00	9.260	0.358				1.90E-03		
	19.00	9.774	0.378						
	20.00	10.289	0.398						

F.1.3 *Hull C*

Table F.5. Numerical Results, Hull *C*, Condition *A*.

Run	V_S		*Fn*	*Catamaran*			*Shipflow*		
	kn	m/s		C_W	*Sinkage* m	*Trim* deg	C_W	*Sinkage* m	*Trim* deg
CCA10	10.00	5.144	0.175	6.37E-04	0.012	0.052	2.71E-03		
CCA11	11.00	5.659	0.193	7.58E-04	0.010	0.070	2.60E-03		
CCA12	12.00	6.173	0.210	8.97E-04	0.007	0.093	2.20E-03		
CCA13	13.00	6.688	0.228	1.07E-03	0.001	0.121	2.32E-03		
CCA14	14.00	7.202	0.245	1.34E-03	-0.008	0.158	2.55E-03		
CCA15	15.00	7.717	0.263	1.81E-03	-0.025	0.208	2.20E-03		
CCA16	16.00	8.231	0.280	2.19E-03	-0.029	0.241	2.80E-03		
CCA17	17.00	8.746	0.298	2.22E-03	-0.012	0.244			
CCA18	18.00	9.260	0.315	2.09E-03	-0.002	0.258			
CCA19	19.00	9.774	0.333	2.04E-03	-0.014	0.304			
CCA20	20.00	10.289	0.350	2.06E-03	-0.060	0.392	1.93E-03		

Table F.6. Numerical Results, Hull *C*, Condition *B*.

Run	V_S		*Fn*	*Catamaran*			*Shipflow*		
	kn	m/s		C_W	*Sinkage* m	*Trim* deg	C_W	*Sinkage* m	*Trim* deg
	10.00	5.144	0.176				2.43E-03		
	11.00	5.659	0.193				2.24E-03		
	12.00	6.173	0.211				1.83E-03		
	13.00	6.688	0.228				2.07E-03		
	14.00	7.202	0.246				1.93E-03		
CCB15	15.00	7.717	0.263	-1.17E-03	0.043	0.091	1.88E-03		
	16.00	8.231	0.281				2.37E-03		
	17.00	8.746	0.299						
	18.00	9.260	0.316						
	19.00	9.774	0.334				1.85E-03		
	20.00	10.289	0.351				1.59E-03		

F.1.4 *Hull D*

Table F.7. Numerical Results, Hull *D*, Condition *A.*

Run	V_S		*Fn*	*Catamaran*			*Shipflow*		
	kn	m/s		C_W	*Sinkage* m	*Trim* deg	C_W	*Sinkage* m	*Trim* deg
CDA10	10.00	5.144	0.179	1.60E-04	0.044	-0.032	5.99E-04		
CDA11	11.00	5.659	0.197	1.90E-04	0.068	-0.048	6.20E-04		
CDA12	12.00	6.173	0.215	2.40E-04	0.092	-0.060	7.21E-04		
CDA13	13.00	6.688	0.233	3.04E-04	0.117	-0.074	1.01E-03		
CDA14	14.00	7.202	0.251	4.75E-04	0.132	-0.070	8.92E-04		
CDA15	15.00	7.717	0.269	6.59E-04	0.229	-0.157	1.28E-03		
CDA16	16.00	8.231	0.287	1.15E-03	0.123	0.025	1.95E-03		
CDA17	17.00	8.746	0.305	1.29E-03	0.130	0.053	2.01E-03		
CDA18	18.00	9.260	0.323	1.48E-03	0.094	0.127	1.60E-03		
CDA19	19.00	9.774	0.341	1.57E-03	0.109	0.146	1.17E-03		
CDA20	20.00	10.289	0.359	1.79E-03	0.086	0.210	1.29E-03		

Table F.8. Numerical Results, Hull *D*, Condition *B.*

Run	V_S		*Fn*	*Catamaran*			*Shipflow*		
	kn	m/s		C_W	*Sinkage* m	*Trim* deg	C_W	*Sinkage* m	*Trim* deg
	10.00	5.144	0.183				5.19E-04		
	11.00	5.659	0.202				5.08E-04		
	12.00	6.173	0.220				9.45E-04		
	13.00	6.688	0.238				1.05E-03		
	14.00	7.202	0.256				1.03E-03		
CDB15	15.00	7.717	0.275	1.62E-03	0.062	0.124	1.67E-03		
	16.00	8.231	0.293				2.09E-03		
	17.00	8.746	0.311						
	18.00	9.260	0.330						
	19.00	9.774	0.348				1.24E-03		
	20.00	10.289	0.366				1.65E-03		

F.1.5 *Hull E*

Table F.9. Numerical Results, Hull *E*, Condition *A.*

Run	V_S		*Fn*	*Catamaran*			*Shipflow*		
	kn	m/s		C_W	*Sinkage* m	*Trim* deg	C_W	*Sinkage* m	*Trim* deg
CEA10	10.00	5.144	0.184	9.33E-04	0.051	-0.002	1.30E-03		
CEA11	11.00	5.659	0.202	1.74E-03	0.070	-0.003	8.80E-04		
CEA12	12.00	6.173	0.220	3.60E-03	0.112	-0.006	3.09E-03		
CEA13	13.00	6.688	0.239	3.61E-03	0.112	-0.007	4.80E-03		
CEA14	14.00	7.202	0.257	3.96E-03	0.136	0.021	2.35E-03		
CEA15	15.00	7.717	0.276	5.47E-03	0.122	0.090	3.07E-03		
CEA16	16.00	8.231	0.294	6.70E-03	0.155	0.066	6.11E-03		
CEA17	17.00	8.746	0.312	6.70E-03	0.155	0.066	7.63E-03		
CEA18	18.00	9.260	0.331	4.73E-03	0.264	-0.113			
CEA19	19.00	9.774	0.349	3.74E-03	0.259	-0.064	5.47E-03		
CEA20	20.00	10.289	0.367	3.35E-03	0.187	0.108	3.64E-03		

Table F.10. Numerical Results, Hull *E*, Condition *B.*

Run	V_S		*Fn*	*Catamaran*			*Shipflow*		
	kn	m/s		C_W	*Sinkage* m	*Trim* deg	C_W	*Sinkage* m	*Trim* deg
	10.00	5.144	0.184				1.18E-03		
	11.00	5.659	0.202				8.49E-04		
	12.00	6.173	0.220				2.69E-03		
	13.00	6.688	0.239				4.22E-03		
	14.00	7.202	0.257				2.26E-03		
CEB15	15.00	7.717	0.276	4.52E-03	0.107	0.079			
	16.00	8.231	0.294						
	17.00	8.746	0.312						
	18.00	9.260	0.331						
	19.00	9.774	0.349						
	20.00	10.289	0.367						

F.2 First Optimization

F.2.1 *Hull B377*

Table F.11. Numerical Results, Hull *B377*, Condition *A.*

Run	V_S		*Fn*	*Catamaran*			*Shipflow*		
	kn	m/s		C_W	*Sinkage* m	*Trim* deg	C_W	*Sinkage* m	*Trim* deg
	10.00	5.144	0.184						
	11.00	5.659	0.202						
	12.00	6.173	0.220						
	13.00	6.688	0.239						
b377a14	14.00	7.202	0.257	1.09E-03	0.262	-0.202			
b377a15	15.00	7.717	0.276	1.83E-03	0.258	-0.149	1.93E-04		
	16.00	8.231	0.294						
	17.00	8.746	0.312						
	18.00	9.260	0.331						
	19.00	9.774	0.349						
	20.00	10.289	0.367						

Table F.12. Numerical Results, Hull *B377*, Condition *B.*

Run	V_S		*Fn*	*Catamaran*			*Shipflow*		
	kn	m/s		C_W	*Sinkage* m	*Trim* deg	C_W	*Sinkage* m	*Trim* deg
	10.00	5.144	0.185						
	11.00	5.659	0.204						
	12.00	6.173	0.222						
	13.00	6.688	0.241						
b377b14	14.00	7.202	0.259	9.76E-04	0.215	-0.144			
b377b15	15.00	7.717	0.278	1.67E-03	0.217	-0.103	1.59E-03		
	16.00	8.231	0.296						
	17.00	8.746	0.315						
	18.00	9.260	0.333						
	19.00	9.774	0.352						
	20.00	10.289	0.370						

F.2.2 *Hull B401*

Table F.13. Numerical Results, Hull *B401*, Condition *A.*

Run	V_S		*Fn*	*Catamaran*			*Shipflow*		
	kn	m/s		C_W	*Sinkage* m	*Trim* deg	C_W	*Sinkage* m	*Trim* deg
b401a10	10.00	5.144	0.173	8.72E-05	0.078	-0.058	1.44E-04	0.048	-0.031
b401a11	11.00	5.659	0.190	1.43E-04	0.103	-0.074	1.41E-04	0.058	-0.044
b401a12	12.00	6.173	0.208	1.66E-04	0.133	-0.095	2.17E-04	0.071	-0.054
b401a13	13.00	6.688	0.225	1.31E-04	0.176	-0.129	1.93E-04	0.083	-0.090
b401a14	14.00	7.202	0.242	1.74E-04	0.219	-0.160	1.53E-04	0.101	-0.104
b401a15	15.00	7.717	0.260	3.06E-04	0.258	-0.182	1.96E-04	0.119	-0.130
b401a16	16.00	8.231	0.277	5.27E-04	0.282	-0.182	4.85E-04	0.136	-0.166
b401a17	17.00	8.746	0.294	6.90E-04	0.285	-0.157	8.51E-04	0.158	-0.164
b401a18	18.00	9.260	0.312	7.25E-04	0.302	-0.149	1.07E-03	0.188	-0.079
b401a19	19.00	9.774	0.329	9.56E-04	0.306	-0.126	1.11E-03	0.222	0.012
b401a20	20.00	10.289	0.346	1.13E-03	0.310	-0.099	1.01E-03	0.243	0.041

Table F.14. Numerical Results, Hull *B401*, Condition *B.*

Run	V_S		*Fn*	*Catamaran*			*Shipflow*		
	kn	m/s		C_W	*Sinkage* m	*Trim* deg	C_W	*Sinkage* m	*Trim* deg
b401a10	10.00	5.144	0.174	2.06E-04	0.049	-0.024	1.25E-04	0.045	-0.008
b401b11	11.00	5.659	0.191	2.64E-04	0.065	-0.031	1.65E-04	0.056	-0.014
b401b12	12.00	6.173	0.209	2.84E-04	0.087	-0.044	2.46E-04	0.063	-0.024
b401b13	13.00	6.688	0.226	2.59E-04	0.118	-0.063	2.89E-04	0.074	-0.048
b401b14	14.00	7.202	0.244	2.01E-04	0.158	-0.091	2.61E-04	0.098	-0.067
b401b15	15.00	7.717	0.261	2.91E-04	0.192	-0.107	2.10E-04	0.117	-0.085
b401b16	16.00	8.231	0.279	4.33E-04	0.214	-0.105	4.10E-04	0.136	-0.109
b401b17	17.00	8.746	0.296	5.84E-04	0.226	-0.090	7.36E-04	0.159	-0.110
b401b18	18.00	9.260	0.313	6.35E-04	0.239	-0.081	9.17E-04	0.188	-0.057
b401b19	19.00	9.774	0.331	7.52E-04	0.252	-0.069	9.17E-04	0.217	0.006
b401b20	20.00	10.289	0.348	9.52E-04	0.225	0.004	8.67E-04	0.242	0.045

F.2.3 *Hull B422*

Table F.15. Numerical Results, Hull *B422*, Condition *A.*

Run	V_S		*Fn*	*Catamaran*			*Shipflow*		
	kn	m/s		C_W	*Sinkage* m	*Trim* deg	C_W	*Sinkage* m	*Trim* deg
	10.00	5.144	0.184						
	11.00	5.659	0.202						
	12.00	6.173	0.220						
	13.00	6.688	0.239						
b422a14	14.00	7.202	0.257	1.24E-03	0.263	-0.206			
b422a15	15.00	7.717	0.275	2.16E-03	0.248	-0.132	2.26E-04		
	16.00	8.231	0.294						
	17.00	8.746	0.312						
	18.00	9.260	0.331						
	19.00	9.774	0.349						
	20.00	10.289	0.367						

Table F.16. Numerical Results, Hull *B422*, Condition *B.*

Run	V_S		*Fn*	*Catamaran*			*Shipflow*		
	kn	m/s		C_W	*Sinkage* m	*Trim* deg	C_W	*Sinkage* m	*Trim* deg
	10.00	5.144	0.186						
	11.00	5.659	0.204						
	12.00	6.173	0.223						
	13.00	6.688	0.241						
b422b14	14.00	7.202	0.260	1.14E-03	0.136	-0.031			
b422b15	15.00	7.717	0.278	1.95E-03	0.129	0.027	1.94E-03		
	16.00	8.231	0.297						
	17.00	8.746	0.316						
	18.00	9.260	0.334						
	19.00	9.774	0.353						
	20.00	10.289	0.371						

F.2.4 *Hull B428*

Table F.17. Numerical Results, Hull *B428*, Condition *A.*

Run	V_S		*Fn*	*Catamaran*			*Shipflow*		
	kn	m/s		C_W	*Sinkage* m	*Trim* deg	C_W	*Sinkage* m	*Trim* deg
		5.144	0.173						
		5.659	0.190						
		6.173	0.208						
		6.688	0.225						
		7.202	0.242						
b428a15	15.00	7.717	0.260	3.01E-04	0.243	-0.166	1.79E-04		
		8.231	0.277						
		8.746	0.294						
		9.260	0.312						
		9.774	0.329						
		10.289	0.346						

Table F.18. Numerical Results, Hull *B428*, Condition *B.*

Run	V_S		*Fn*	*Catamaran*			*Shipflow*		
	kn	m/s		C_W	*Sinkage* m	*Trim* deg	C_W	*Sinkage* m	*Trim* deg
		5.144	0.174						
		5.659	0.191						
		6.173	0.209						
		6.688	0.226						
		7.202	0.243						
b428b15	15.00	7.717	0.261	3.06E-04	0.178	-0.093	2.32E-04		
		8.231	0.278						
		8.746	0.295						
		9.260	0.313						
		9.774	0.330						
		10.289	0.348						

F.3 Second Optimization

F.3.1 *Hull C247*

Table F.19. Numerical Results, Hull *C247*, Condition *A.*

Run	V_S		*Fn*	*Catamaran*				*Shipflow*			
	kn	m/s		C_W	*Sinkage* m	*Trim* deg	*WS* m^2	C_W	*Sinkage* m	*Trim* deg	*WS* m^2
c247a10	10.00	5.144	0.185	1.62E-04	0.105	0.421	1758.4	4.50E-04			1762.3
c247a11	11.00	5.659	0.204	1.23E-04	0.140	0.392	1761.7	5.53E-04			1765.0
c247a12	12.00	6.173	0.222	6.59E-05	0.186	0.352	1766.8	4.42E-04			1771.0
c247a13	13.00	6.688	0.241	1.97E-04	0.236	0.311	1772.7	3.03E-04			1775.4
c247a14	14.00	7.202	0.259	5.09E-04	0.278	0.290	1779.7	4.18E-04			1783.8
c247a15	15.00	7.717	0.278	8.76E-04	0.299	0.305	1781.5	9.52E-04			1787.8
c247a16	16.00	8.231	0.297	9.87E-04	0.326	0.309	1785.0	1.36E-03			1788.6
	17.00	8.746	0.309					1.16E-03			1794.1
	18.00	9.260	0.328					7.37E-04			1806.3
	19.00	9.774	0.346					6.36E-04			1820.3

Table F.20. Numerical Results, Hull *C247*, Condition *B.*

Run	V_S		*Fn*	*Catamaran*				*Shipflow*			
	kn	m/s		C_W	*Sinkage* m	*Trim* deg	*WS* m^2	C_W	*Sinkage* m	*Trim* deg	*WS* m^2
c247b10	10.00	5.144	0.182	6.42E-04	0.036	1.168	1566.9	7.26E-04			1565.2
c247b11	11.00	5.659	0.200	6.86E-04	0.048	1.166	1572.0	8.72E-04			1567.7
	12.00	6.173	0.218					9.20E-04			1572.3
c247b13	13.00	6.688	0.237	4.02E-04	0.109	1.124	1584.0	7.08E-04			1578.9
c247b14	14.00	7.202	0.255	4.11E-04	0.145	1.105	1589.8	4.12E-04			1595.6
c247b15	15.00	7.717	0.273	6.21E-04	0.165	1.118	1593.9	5.16E-04			1592.3
c247b16	16.00	8.231	0.291	6.61E-04	0.184	1.133	1597.9	9.62E-04			1595.4
	17.00	8.746	0.309					1.11E-03			1597.9
	18.00	9.260	0.328					8.51E-04			1605.0
	19.00	9.774	0.346					6.67E-04			1615.5

Table F.21. Numerical Results, Hull *C247*, Condition *A*, with and without the pod seat arrangement.

Run	V_S		*Fn*	*Without pod seat*				*Difference* [%]			
	kn	m/s		C_W	*Sinkage* m	*Trim* deg	*WS* m^2	C_W	*Sinkage*	*Trim*	*WS*
c247a10	10.00	5.144	0.185	9.42E-05	0.106	0.419	1747.8	-41.95	0.19	-0.45	-0.60
c247a11	11.00	5.659	0.204	3.60E-05	0.139	0.392	1751.2	-70.75	-0.50	0.00	-0.60
	12.00	6.173	0.222								
c247a13	13.00	6.688	0.241	1.09E-04	0.236	0.311	1761.9	-44.52	-0.25	0.03	-0.61
c247a14	14.00	7.202	0.259	5.13E-04	0.278	0.287	1769.1	0.82	0.18	-0.73	-0.60
c247a15	15.00	7.717	0.278	9.18E-04	0.291	0.309	1769.3	4.80	-2.61	1.28	-0.68
c247a16	16.00	8.231	0.297	1.03E-03	0.325	0.310	1774.1	4.17	-0.34	0.39	-0.61

Table F.22. Numerical Results, Hull *C247*, Condition *B*, with and without the pod seat arrangement.

Run	V_S		*Fn*	*Without pod seat*				*Difference* [%]			
	kn	m/s		C_W	*Sinkage* m	*Trim* deg	*WS* m^2	C_W	*Sinkage*	*Trim*	*WS*
c247b10	10.00	5.144	0.182	5.62E-04	0.038	1.164	1557.2	-12.40	5.25	-0.39	-0.62
c247b11	11.00	5.659	0.200	5.61E-04	0.038	1.164	1556.8	-18.19	-21.16	-0.23	-0.97
	12.00	6.173	0.218								
c247b13	13.00	6.688	0.237	3.21E-04	0.108	1.125	1573.1	-20.14	-0.55	0.04	-0.69
c247b14	14.00	7.202	0.255	3.38E-04	0.144	1.106	1578.5	-17.82	-0.41	0.07	-0.71
c247b15	15.00	7.717	0.273	6.45E-04	0.165	1.116	1582.7	4.00	0.24	-0.19	-0.70
c247b16	16.00	8.231	0.291	6.98E-04	0.184	1.131	1586.1	5.55	0.05	-0.15	-0.74

F.3.2 *Hull C423.*

Table F.23. Numerical Results, Hull *C423*, Condition *A.*

Run	V_S		*Fn*	*Catamaran*				*Shipflow*			
	kn	m/s		C_W	*Sinkage* m	*Trim* deg	*WS* m^2	C_W	*Sinkage* m	*Trim* deg	*WS* m^2
c423a10	10.00	5.144	0.186	1.22E-04	0.086	0.333	1758.0	3.17E-04			1776.2
c423a11	11.00	5.659	0.204	1.34E-04	0.120	0.306	1762.2	4.51E-04			1778.7
c423a12	12.00	6.173	0.223	1.37E-04	0.166	0.264	1767.5	3.93E-04			1784.4
c423a13	13.00	6.688	0.241	2.47E-04	0.214	0.225	1773.9	3.73E-04			1790.7
c423a14	14.00	7.202	0.260	5.13E-04	0.252	0.208	1779.6	5.90E-04			1798.1
c423a15	15.00	7.717	0.279	7.57E-04	0.276	0.215	1783.3	9.98E-04			1802.0
c423a16	16.00	8.231	0.297	9.81E-04	0.304	0.218	1789.9	1.14E-03			1803.8
	17.00	8.746	0.316					8.55E-04			1810.4
	18.00	9.260	0.334					5.81E-04			1823.6
	19.00	9.774	0.353					7.67E-04			1837.2

Table F.24. Numerical Results, Hull *C423*, Condition *B.*

Run	V_S		*Fn*	*Catamaran*				*Shipflow*			
	kn	m/s		C_W	*Sinkage* m	*Trim* deg	*WS* m^2	C_W	*Sinkage* m	*Trim* deg	*WS* m^2
c423b10	10.00	5.144	0.182	5.06E-04	0.000	1.148	1569.0	5.02E-04			1581.7
c423b11	11.00	5.659	0.200	4.94E-04	0.020	1.138	1574.2	7.12E-04			1582.7
c423b12	12.00	6.173	0.218	3.63E-04	0.053	1.110	1579.4	7.50E-04			1586.8
c423b13	13.00	6.688	0.237	2.05E-04	0.093	1.081	1586.0	5.01E-04			1594.1
c423b14	14.00	7.202	0.255	2.50E-04	0.129	1.062	1591.5	3.45E-04			1599.5
c423b15	15.00	7.717	0.273	3.37E-04	0.158	1.060	1595.6	4.67E-04			1605.6
c423b16	16.00	8.231	0.291	4.11E-04	0.186	1.060	1601.6	6.73E-04			1611.3
	17.00	8.746	0.309					6.46E-04			1614.8
	18.00	9.260	0.328					4.99E-04			1622.5
	19.00	9.774	0.346					5.96E-04			1633.6

Table F.25. Numerical Results, Hull *C423*, Condition *A*, with and without the pod seat arrangement.

Run	V_S		*Fn*	*Without pod seat*				*Difference* [%]			
	kn	m/s		C_W	*Sinkage* m	*Trim* deg	*WS* m^2	C_W	*Sinkage*	*Trim*	*WS*
c423a10	10.00	5.144	0.186	5.02E-05	0.087	0.330	1748.0	-58.73	1.28	-1.02	-0.57
c423a11	11.00	5.659	0.204	5.73E-05	0.120	0.305	1751.8	-57.38	0.08	-0.23	-0.59
c423a12	12.00	6.173	0.223	4.64E-05	0.165	0.265	1756.8	-66.17	-0.30	0.19	-0.61
c423a13	13.00	6.688	0.241	1.52E-04	0.214	0.224	1763.5	-38.36	-0.05	-0.09	-0.59
c423a14	14.00	7.202	0.260	5.00E-04	0.252	0.207	1768.7	-2.69	0.04	-0.24	-0.61
c423a15	15.00	7.717	0.279	7.92E-04	0.275	0.216	1772.2	4.58	-0.62	0.75	-0.62
c423a16	16.00	8.231	0.297	9.87E-04	0.304	0.219	1779.0	0.66	0.03	0.09	-0.61

Table F.26. Numerical Results, Hull *C423*, Condition *B*, with and without the pod seat arrangement.

Run	V_S		*Fn*	*Without pod seat*				*Difference* [%]			
	kn	m/s		C_W	*Sinkage* m	*Trim* deg	*WS* m^2	C_W	*Sinkage*	*Trim*	*WS*
c423b10	10.00	5.144	0.182	4.18E-04	0.001	1.145	1558.8	-17.48		-0.21	-0.65
c423b11	11.00	5.659	0.200	4.09E-04	0.019	1.138	1563.4	-17.10	-1.03	0.02	-0.69
c423b12	12.00	6.173	0.218	2.75E-04	0.053	1.111	1568.7	-24.24	-1.69	0.14	-0.68
c423b13	13.00	6.688	0.237	1.33E-04	0.092	1.083	1575.2	-35.34	-1.50	0.19	-0.68
c423b14	14.00	7.202	0.255	1.56E-04	0.129	1.064	1580.3	-37.74	-0.62	0.15	-0.70
c423b15	15.00	7.717	0.273	6.45E-04	0.165	1.116	1582.7	91.53	4.95	5.26	-0.81
c423b16	16.00	8.231	0.291	4.04E-04	0.184	1.063	1591.7	-1.74	-1.02	0.25	-0.62

F.3.3 *Hull C427.*

Table F.27. Numerical Results, Hull *C427*, Condition *A.*

Run	V_S		*Fn*	*Catamaran*				*Shipflow*			
	kn	m/s		C_W	*Sinkage* m	*Trim* deg	*WS* m^2	C_W	*Sinkage* m	*Trim* deg	*WS* m^2
c427a10	10.00	5.144	0.186	7.43E-05	0.074	0.194	1745.8	3.86E-04			1762.3
c427a11	11.00	5.659	0.204	8.31E-05	0.107	0.168	1748.9	4.71E-04			1765.0
c427a12	12.00	6.173	0.223	7.41E-05	0.151	0.130	1754.3	3.81E-04			1771.0
c427a13	13.00	6.688	0.241	4.92E-04	0.237	0.077	1767.5	2.83E-04			1775.4
c427a14	14.00	7.202	0.260	4.92E-04	0.237	0.077	1767.5	4.52E-04			1783.8
c427a15	15.00	7.717	0.278	8.35E-04	0.259	0.091	1771.0	9.99E-04			1787.8
c427a16	16.00	8.231	0.297	1.00E-03	0.287	0.096	1775.7	1.34E-03			1788.6
	17.00	8.746	0.316					1.11E-03			1794.1
	18.00	9.260	0.334					7.11E-04			1806.3
	19.00	9.774	0.353					6.96E-04			1820.3

Table F.28. Numerical Results, Hull *C427*, Condition *B.*

Run	V_S		*Fn*	*Catamaran*				*Shipflow*			
	kn	m/s		C_W	*Sinkage* m	*Trim* deg	*WS* m^2	C_W	*Sinkage* m	*Trim* deg	*WS* m^2
c427b10	10.00	5.144	0.182	5.43E-04	0.005	0.981	1559.2	5.75E-04			1565.2
c427b11	11.00	5.659	0.200	5.14E-04	0.022	0.974	1564.7	7.25E-04			1567.7
c427b12	12.00	6.173	0.219	4.39E-04	0.052	0.952	1570.2	7.87E-04			1572.3
c427b13	13.00	6.688	0.237	3.23E-04	0.088	0.930	1575.0	6.35E-04			1578.9
c427b14	14.00	7.202	0.255	3.36E-04	0.126	0.909	1581.9	3.63E-04			1595.6
c427b15	15.00	7.717	0.273	5.46E-04	0.148	0.918	1585.7	4.92E-04			1592.3
c427b16	16.00	8.231	0.292	5.69E-04	0.172	0.926	1590.6	8.64E-04			1595.4
	17.00	8.746	0.310					9.55E-04			1597.9
	18.00	9.260	0.328					7.55E-04			1605.0
	19.00	9.774	0.346					6.68E-04			1615.5

Table F.29. Numerical Results, Hull *C427*, Condition *A*, with and without the pod seat arrangement.

Run	V_S		*Fn*	*Without pod seat*				*Difference* [%]			
	kn	m/s		C_W	*Sinkage* m	*Trim* deg	*WS* m^2	C_W	*Sinkage*	*Trim*	*WS*
c427a10	10.00	5.144	0.186	1.23E-05	0.076	0.191	1734.7	-83.49	2.85	-1.96	-0.64
c427a11	11.00	5.659	0.204	2.57E-05	0.109	0.165	1737.9	-69.05	1.40	-1.55	-0.63
c427a12	12.00	6.173	0.223	7.65E-06	0.152	0.129	1742.9	-89.67	0.60	-1.00	-0.65
c427a13	13.00	6.688	0.241	1.37E-04	0.199	0.094	1750.0	-72.17	-16.16	21.50	-0.99
c427a14	14.00	7.202	0.260	5.01E-04	0.239	0.075	1756.7	1.84	0.76	-3.24	-0.61
c427a15	15.00	7.717	0.278	8.97E-04	0.260	0.090	1759.5	7.32	0.27	-0.77	-0.65
c427a16	16.00	8.231	0.297	1.05E-03	0.287	0.097	1764.2	4.60	-0.17	1.26	-0.65

Table F.30. Numerical Results, Hull *C427*, Condition *B*, with and without the pod seat arrangement.

Run	V_S		*Fn*	*Without pod seat*				*Difference* [%]			
	kn	m/s		C_W	*Sinkage* m	*Trim* deg	*WS* m^2	C_W	*Sinkage*	*Trim*	*WS*
c427b10	10.00	5.144	0.182	4.67E-04	0.007	0.978	1549.0	-14.05	26.42	-0.36	-0.65
c427b11	11.00	5.659	0.200	4.63E-04	0.022	0.973	1553.1	-9.83	0.90	-0.11	-0.74
c427b12	12.00	6.173	0.219	3.72E-04	0.052	0.952	1558.6	-15.21	0.00	-0.05	-0.74
c427b13	13.00	6.688	0.237	2.64E-04	0.087	0.930	1563.7	-18.41	-0.80	0.06	-0.72
c427b14	14.00	7.202	0.255	2.84E-04	0.125	0.910	1569.8	-15.61	-0.79	0.15	-0.76
c427b15	15.00	7.717	0.273	5.63E-04	0.148	0.918	1574.3	3.06	0.00	-0.01	-0.72
c427b16	16.00	8.231	0.292	6.07E-04	0.171	0.928	1579.3	6.77	-0.35	0.16	-0.71

F.4 Third Optimization

F.4.1 *Hull D354*

Table F.31. Numerical Results, Hull *D354*, Condition *A*.

Run	V_S		*Fn*	*Catamaran*				*Shipflow*			
				C_W	*Sinkage*	*Trim*	*WS*	C_W	*Sinkage*	*Trim*	*WS*
	kn	m/s			m	deg	m^2		m	deg	m^2
d354a10	10.00	5.144	0.186	1.04E-04	0.079	0.155	1695.7	3.16E-04			1714.3
d354a11	11.00	5.659	0.204	1.22E-04	0.113	0.130	1701.8	4.17E-04			1717.1
d354a12	12.00	6.173	0.223	9.26E-05	0.154	0.097	1707.1	3.26E-04			1724.0
d354a13	13.00	6.688	0.242	1.17E-04	0.203	0.061	1714.1	2.63E-04			1729.2
d354a14	14.00	7.202	0.260	2.99E-04	0.247	0.038	1722.7	3.14E-04			1738.0
d354a15	15.00	7.717	0.279	5.90E-04	0.280	0.037	1729.4	6.90E-04			1744.2
d354a16	16.00	8.231	0.297	9.11E-04	0.300	0.061	1738.3	1.16E-03			1746.2
	17.00	8.746	0.316					1.10E-03			1751.8
	18.00	9.260	0.334					8.05E-04			1764.7
	19.00	9.774	0.353					7.92E-04			1781.4

Table F.32. Numerical Results, Hull *D354*, Condition *B*.

Run	V_S		*Fn*	*Catamaran*				*Shipflow*			
				C_W	*Sinkage*	*Trim*	*WS*	C_W	*Sinkage*	*Trim*	*WS*
	kn	m/s			m	deg	m^2		m	deg	m^2
d354b10	10.00	5.144	0.182	6.71E-04	0.018	0.894	1523.2	3.79E-04			1537.1
d354b11	11.00	5.659	0.200	7.09E-04	0.033	0.891	1529.7	5.67E-04			1538.8
d354b12	12.00	6.173	0.219	6.42E-04	0.057	0.880	1532.8	4.45E-04			1545.3
d354b13	13.00	6.688	0.237	4.98E-04	0.091	0.861	1539.5	5.07E-04			1549.2
d354b14	14.00	7.202	0.255	3.72E-04	0.133	0.837	1546.7	3.19E-04			1555.2
d354b15	15.00	7.717	0.273	3.82E-04	0.172	0.823	1555.1	3.32E-04			1564.0
d354b16	16.00	8.231	0.292	4.87E-04	0.197	0.835	1561.4	8.01E-04			1568.4
	17.00	8.746	0.310					9.13E-04			1572.8
	18.00	9.260	0.328					7.50E-04			1582.7
	19.00	9.774	0.346					6.95E-04			1597.2

Table F.33. Numerical Results, Hull *D354*, Condition *A*, with and without the pod seat arrangement.

Run	V_S		*Fn*	*Without pod seat*				*Difference* [%]			
	kn	m/s		C_W	*Sinkage* m	*Trim* deg	*WS* m^2	C_W	*Sinkage*	*Trim*	*WS*
d354a10	10.00	5.144	0.186	7.76E-05	0.082	0.150	1686.4	-25.43	3.79	-3.04	-0.55
d354a11	11.00	5.659	0.204	1.17E-04	0.115	0.127	1691.9	-3.85	1.78	-2.24	-0.58
d354a12	12.00	6.173	0.223	9.02E-05	0.156	0.096	1697.7	-2.57	0.84	-1.44	-0.55
d354a13	13.00	6.688	0.242	9.57E-05	0.204	0.060	1704.5	-18.11	0.54	-1.80	-0.56
d354a14	14.00	7.202	0.260	3.34E-04	0.249	0.037	1712.8	11.61	0.44	-2.65	-0.57
d354a15	15.00	7.717	0.279	6.52E-04	0.279	0.039	1718.7	10.42	-0.21	5.91	-0.62
d354a16	16.00	8.231	0.297	9.39E-04	0.300	0.062	1727.0	3.04	-0.17	3.14	-0.65

Table F.34. Numerical Results, Hull *D354*, Condition *B*, with and without the pod seat arrangement.

Run	V_S		*Fn*	*Without pod seat*				*Difference* [%]			
	kn	m/s		C_W	*Sinkage* m	*Trim* deg	*WS* m^2	C_W	*Sinkage*	*Trim*	*WS*
d354b10	10.00	5.144	0.182	6.30E-04	0.020	0.891	1513.2	-6.13	13.07	-0.38	-0.66
d354b11	11.00	5.659	0.200	7.01E-04	0.034	0.888	1519.5	-1.03	5.52	-0.27	-0.67
d354b12	12.00	6.173	0.219	6.51E-04	0.058	0.878	1523.4	1.39	2.30	-0.14	-0.61
d354b13	13.00	6.688	0.237	5.03E-04	0.092	0.860	1528.4	1.01	1.32	-0.09	-0.72
d354b14	14.00	7.202	0.255	3.61E-04	0.133	0.838	1535.5	-3.03	0.23	0.07	-0.72
d354b15	15.00	7.717	0.273	4.34E-04	0.171	0.827	1544.3	13.84	-0.87	0.46	-0.69
d354b16	16.00	8.231	0.292	5.36E-04	0.195	0.839	1550.8	9.93	-0.71	0.46	-0.68

APPENDIX G:

The Effect of Variables URFPS & DSURMI

APPENDIX G: The Effect of Variable URFPS & DSURMI

As described in paragraph 2.2, the free surface is calculated by means of an iterative procedure. Assuming that at an intermediate step the free-surface geometry is known, the potential problem is solved, by setting the normal velocity on the control point of each panel equal to zero (kinematic condition) Then the inviscid momentum equation (2.2.1) for the vertical velocity component u_Z* is solved were the difference between the calculated the pressure p* and the sum of the ambient p_S (=0) plus the hydrostatic pressure ρgz, is introduced as a source term. Then the free surface is updated in two steps and the procedure is repeated until the dynamic boundary condition converges (Tzabiras, 2008).

The satisfaction of the dynamic boundary condition is tested through $\overline{|\delta z|}$ which is the mean value of the absolute difference between the calculated and the ideal hydrostatic pressure at the control points of all surface panels, transformed in [m]. Owing to the free-surface approximation with quadrilateral elements, this value decreases as the problem converges but exhibits a limiting behavior. Therefore, convergence with respect to $\overline{|\delta z|}$ is satisfied, when it becomes lower than a suitable value depending on both the Froude number and the scale. By definition, the smaller the limiting value of $\overline{|\delta z|}$, the more accurate the solution.

In the above described numerical method, a number of variables affect the accuracy and the convergence. As presented in 3.1.2 the discretization i.e. the number of panels used has a considerable effect on accuracy. Furthermore the height δz* of the control volume acts as an arbitrary parameter that controls the convergence of the procedure since it is involved in the convective terms A_i of (2.2.8), but essentially determines the influence of the pressure gradient. The input variables DSURMA and DSURMI are also important since they restrict the surface renewal in order to avoid convergence problems, hence decelerating convergence. The former is used during the first MASY iterations replaced then by the latter. Finally two underelaxation factors URFVS and URFPS are introduced also to stabilize the process.

A balance between the opposing demands for accuracy and speed must be found by calibrating the values of the abovementioned variables. During this investigation the effects of DSURMI and URFPS were systematically examined, throughout 84 test cases. The program used was the sister program of *catamaran.f, panel.f,* which adopts the same method for solving the potential free surface problem around monohulls. The hull used was that of a flat-water racing kayak. All numerical experiments were at the same displacement and at two speeds, $V_{S,1}$=2.005 m/s, Fn=0.284 and $V_{S,2}$=3.493 m/s, Fn=0.495.

The main particulars of the hull are given in Table G.1. The results for the test cases are presented in Tables G.2 and G.3, specifically the required number of iterations, the limiting value of $\overline{|\delta z|}$, wave resistance coefficient C_W, Wetted surface *WS*, *sinkage* and *trim*. Figures G.1-G.8 depict the values of $\overline{|\delta z|}$ and C_W, for the various values of DSURMI and URFPS.

Table G.1. Main Particulars.

Hull:			***Kayak***
Total Number of Elements:			**11,878**
Overall Length	L_{OA}	**m**	5.160
Calm Waterline Length	L_{WL}	**m**	5.076
Breadth	B_{OA}	**m**	0.410
Depth	D	**m**	0.410
Draft at Fore Perpendicullar	T_F	**m**	0.134
Freeboard at Fore Perpendicullar	FB_F	**m**	0.276
Trim at zero speed (positive by bow)	t	**deg**	0.000
Wetted Surface (at zero speed)	WSA	**m^2**	1.586
Displacement	Δ	**kg**	86.80
Volume of Displacement	V	**m^3**	8.68e-2
Longitudinal position of Center of Buoyancy	LCB	**m**	2.419
Longitudinal position of Center of Gravity	LCF	**m**	2.595

Table G.1. Results for $V_{S,1}$=2.005 m/s, Fn=0.284.

Run	**DSURMI**	**Iterations**	**URFPS**	***dz***	C_W	***Trim*** **deg**	***Sinkage*** **m**	***WS*** **m^2**
ca05g			**-2.00**	7.179E-04	1.881E-04	-0.0240	0.0035	1.6152
ca05h			**-1.90**	7.372E-04	1.867E-04	-0.0244	0.0035	1.6154
ca05i			**-1.80**	7.391E-04	1.848E-04	-0.0244	0.0035	1.6150
ca05j			**-1.70**	7.440E-04	1.687E-04	-0.0288	0.0037	1.6153
ca05k			**-1.60**	7.557E-04	1.768E-04	-0.0260	0.0036	1.6158
ca05a	**1E-04**	**2,000**	**-1.50**	7.811E-04	1.829E-04	-0.0258	0.0036	1.6158
ca05b			**-1.40**	7.834E-04	1.765E-04	-0.0256	0.0036	1.6161
ca05c			**-1.30**	7.954E-04	1.723E-04	-0.0260	0.0036	1.6164
ca05d			**-1.20**	8.122E-04	1.682E-04	-0.0261	0.0036	1.6162
ca05e			**-1.10**	8.373E-04	1.609E-04	-0.0259	0.0036	1.6178
ca05f			**-1.00**	8.686E-04	1.559E-04	-0.0262	0.0036	1.6177

ca05xa	**1E-05**	**2,000**	**5.00**	1.201E-03	1.400E-04	-0.0198	0.0034	1.6136
ca05xb			**10.00**	1.021E-03	1.333E-04	-0.0276	0.0037	1.6151
ca05xc			**20.00**	8.598E-04	1.515E-04	-0.0323	0.0039	1.6166
ca05xd			**50.00**	6.886E-04	1.836E-04	-0.0339	0.0039	1.6159
ca05xe			**100.00**	6.278E-04	1.811E-04	-0.0333	0.0039	1.6184
ca05xf			**200.00**	5.678E-04	1.919E-04	-0.0362	0.0040	1.6176
ca05xg			**500.00**	6.099E-04	1.929E-04	-0.0374	0.0040	1.6183
ca05xh			**1000.00**	1.470E-03	2.228E-04	-0.0365	0.0040	1.6243
ca05za	**1E-05**	**6,000**	**5.00**	1.004E-03	9.531E-05	-0.0291	0.0038	1.6146
ca05zb			**10.00**	7.682E-04	9.149E-05	-0.0326	0.0039	1.6144
ca05zc			**20.00**	5.926E-04	1.245E-04	-0.0321	0.0038	1.6145
ca05zd			**50.00**	3.979E-04	1.721E-04	-0.0305	0.0038	1.6160
ca05ze			**100.00**	2.919E-04	1.901E-04	-0.0305	0.0037	1.6158
ca05zf			**200.00**	2.164E-04	1.984E-04	-0.0317	0.0038	1.6150
ca05zg			**500.00**	3.307E-04	2.076E-04	-0.0314	0.0038	1.6160
ca05zh			**1000.00**	5.517E-04	2.002E-04	-0.0310	0.0038	1.6181
ca05ya	**1E-05**	**4,000**	**5.00**	1.087E-03	1.261E-04	-0.0214	0.0035	1.6127
ca05yb			**10.00**	8.486E-04	1.107E-04	-0.0309	0.0038	1.6146
ca05yc			**20.00**	6.587E-04	1.295E-04	-0.0339	0.0039	1.6138
ca05yd			**50.00**	5.012E-04	1.586E-04	-0.0332	0.0038	1.6152
ca05ye			**100.00**	4.486E-04	1.723E-04	-0.0334	0.0038	1.6145
ca05yf			**200.00**	5.024E-04	1.995E-04	-0.0311	0.0038	1.6151
ca05yg			**500.00**	1.010E-03	2.111E-04	-0.0316	0.0038	1.6357
ca05yh			**1000.00**	1.410E-03	1.882E-04	-0.0343	0.0039	1.6261
ca05wa	**2E-06**	**4,000**	**5.00**	1.002E-03	9.589E-05	-0.0289	0.0038	1.6149
ca05wb			**10.00**	7.805E-04	9.060E-05	-0.0326	0.0039	1.6145
ca05wc			**20.00**	6.045E-04	1.231E-04	-0.0322	0.0038	1.6146
ca05wd			**50.00**	3.985E-04	1.685E-04	-0.0304	0.0037	1.6148
ca05we			**100.00**	2.985E-04	1.893E-04	-0.0307	0.0038	1.6165
ca05wf			**200.00**	2.720E-04	2.005E-04	-0.0313	0.0038	1.6157
ca05wg			**500.00**	3.961E-04	2.067E-04	-0.0316	0.0038	1.6188
ca05wh			**1000.00**	6.177E-04	2.164E-04	-0.0297	0.0038	1.6219

Table G.2. Results for $V_{S,1}$=3.493 m/s, *Fn*=0.495.

Run	DSURMI	Iterations	URFPS	*dz*	C_W	*Trim* deg	*Sinkage* m	*WS* m^2
ca08j			**-2.00**	2.530E-03	9.525E-04	0.5744	-0.0163	1.6621
ca08x			**-1.60**	2.443E-03	9.286E-04	0.5735	-0.0157	1.6466
ca08w			**-1.50**	2.376E-03	9.240E-04	0.5653	-0.0155	1.6287
ca08v			**-1.40**	2.307E-03	9.171E-04	0.5707	-0.0155	1.6644
ca08u			**-1.30**	2.288E-03	9.083E-04	0.5616	-0.0151	1.6397
ca08s			**-1.20**	2.286E-03	8.987E-04	0.5526	-0.0153	1.6296
ca08t			**-1.10**	2.328E-03	8.897E-04	0.5576	-0.0151	1.6530
ca08i	**1E-04**	**2,000**	**-1.00**	2.338E-03	8.825E-04	0.5457	-0.0146	1.6257
ca08p			**-0.80**	2.434E-03	8.574E-04	0.5260	-0.0144	1.6231
ca08o			**-0.70**	2.577E-03	8.391E-04	0.5129	-0.0139	1.6293
ca08n			**-0.60**	2.776E-03	8.134E-04	0.4921	-0.0131	1.6218
ca08m			**-0.50**	2.935E-03	7.748E-04	0.4662	-0.0122	1.6320
ca08q			**-0.40**	3.213E-03	7.324E-04	0.4449	-0.0116	1.6422
ca08r			**-0.30**	4.162E-03	6.782E-04	0.4138	-0.0105	1.6430
ca08l			**-0.20**	5.438E-03	5.214E-04	0.3025	-0.0063	1.6484
ca08k			**0.00**	2.136E-03	1.017E-03	0.6172	-0.0172	1.6451
ca08za			**1.00**	5.285E-03	2.027E-04	0.0292	0.0047	1.6309
ca08zb			**2.00**	5.296E-03	4.822E-04	0.2316	-0.0032	1.5978
ca08zc			**3.00**	4.729E-03	6.464E-04	0.3545	-0.0079	1.6022
ca08zd			**4.00**	3.963E-03	7.347E-04	0.4257	-0.0105	1.6120
ca08ze			**5.00**	3.384E-03	7.811E-04	0.4628	-0.0118	1.6212
ca08zf			**6.00**	2.995E-03	8.094E-04	0.4846	-0.0126	1.6257
ca08zg			**7.00**	2.750E-03	8.322E-04	0.4980	-0.0131	1.6278
ca08zh	**1E-04**	**2,000**	**8.00**	2.577E-03	8.503E-04	0.5112	-0.0136	1.6289
ca08zi			**9.00**	2.440E-03	8.670E-04	0.5213	-0.0139	1.6292
ca08zj			**10.00**	2.327E-03	8.806E-04	0.5351	-0.0143	1.6314
ca08zk			**20.00**	1.812E-03	9.303E-04	0.5717	-0.0155	1.6414
ca08zl			**50.00**	1.715E-03	9.818E-04	0.6027	-0.0166	1.6472
ca08zm			**100.00**	2.094E-03	1.017E-03	0.6062	-0.0171	1.6449
ca08zn			**200.00**	3.115E-03	1.030E-03	0.6204	-0.0177	1.6476
ca08zx			**1000.00**	7.064E-03	2.583E-04	0.6498	-0.0192	1.8384

ca08zo	**1E-05**	**4,000**	**10.00**	2.126E-03	8.764E-04	0.5349	-0.0146	1.6287
ca08zp			**20.00**	1.522E-03	9.272E-04	0.5742	-0.0159	1.6389
ca08zq		**6,000**	**50.00**	9.816E-04	9.782E-04	0.6020	-0.0169	1.6421
ca08zr			**100.00**	7.875E-04	1.013E-03	0.6156	-0.0175	1.6412
ca08zs			**200.00**	6.750E-04	1.025E-03	0.6233	-0.0179	1.6451
ca08zt			**300.00**	9.577E-04	1.021E-03	0.6249	-0.0179	1.6456
ca08zu			**400.00**	9.271E-04	1.027E-03	0.6273	-0.0180	1.6421
ca08zv			**500.00**	1.235E-03	1.020E-03	0.6276	-0.0180	1.6430
ca08zw			**1000.00**	3.767E-03	1.029E-03	0.6353	-0.0182	1.6642
ca08zy	**1E-06**	**6,000**	**1000.00**	1.025E-02	1.685E-03	1.1507	-0.0411	

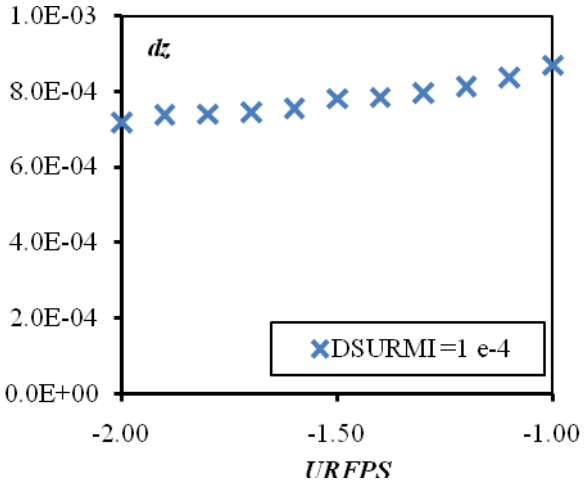

Figure G.1 Limiting values of $|\delta z|$ for DSURMI=1e-4, URFPS<0, V_S=2.005 m/s, *Fn*=0.284.

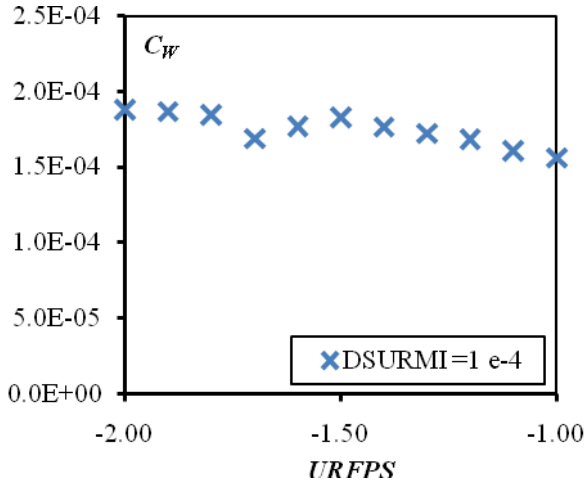

Figure G.2 Wave resistance coefficient C_W, for DSURMI=1e-4, URFPS<0, V_S=2.005 m/s, *Fn*=0.284.

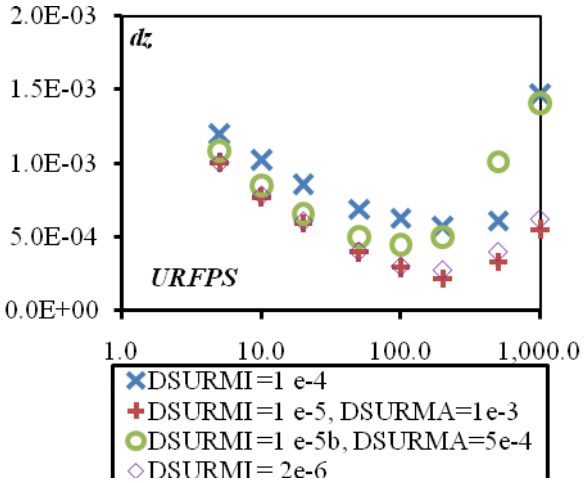

Figure G.3 Limiting values of $|\delta z|$, URFPS>0, V_S=2.005 m/s, *Fn*=0.284.

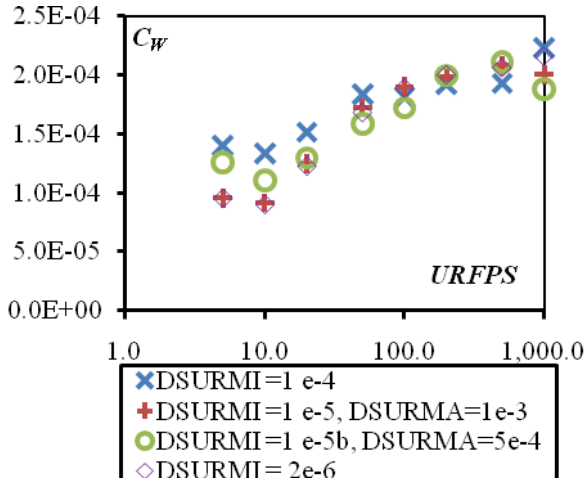

Figure G.4 Wave resistance coefficient C_W, URFPS>0, V_S=2.005 m/s, *Fn*=0.284.

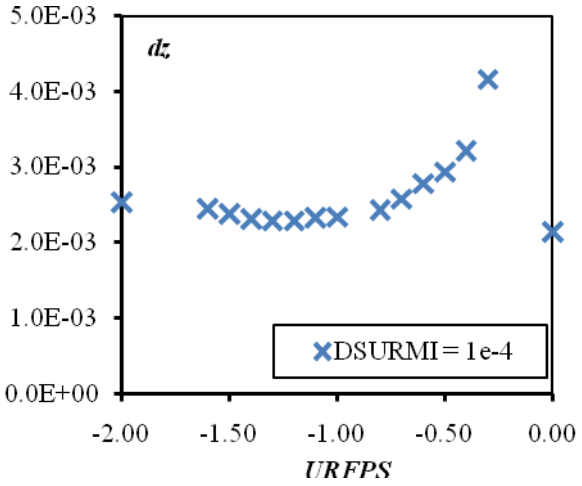

Figure G.5 Limiting values of $\overline{|\delta z|}$ for DSURMI=1e-4, URFPS<0, V_S=3.493 m/s, *Fn*=0.495.

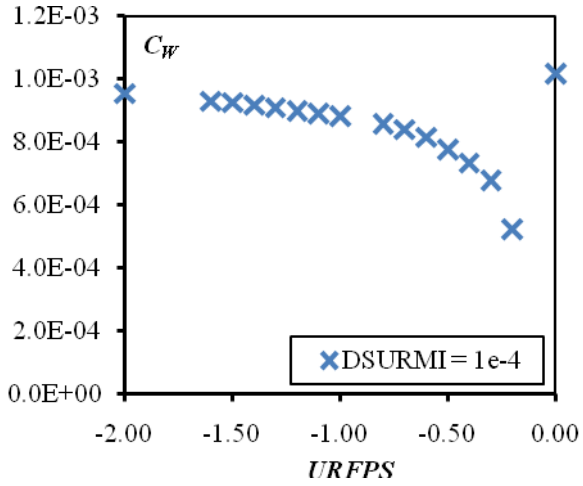

Figure G.6 Wave resistance coefficient C_W, for DSURMI=1e-4, URFPS<0, V_S=3.493 m/s, *Fn*=0.495.

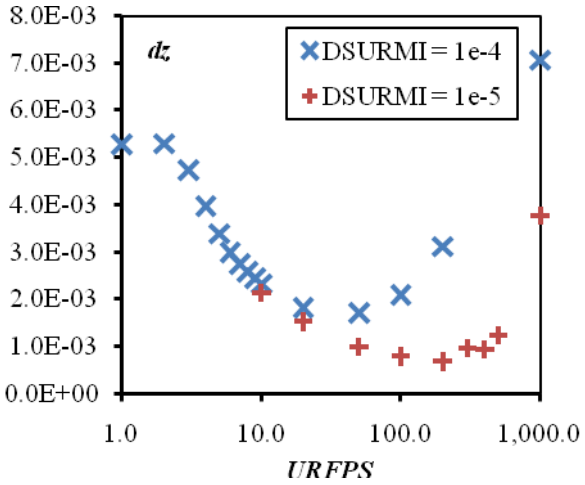

Figure G.7 Limiting values of $\overline{|\delta z|}$, URFPS>0, V_S=3.493 m/s, *Fn*=0.495.

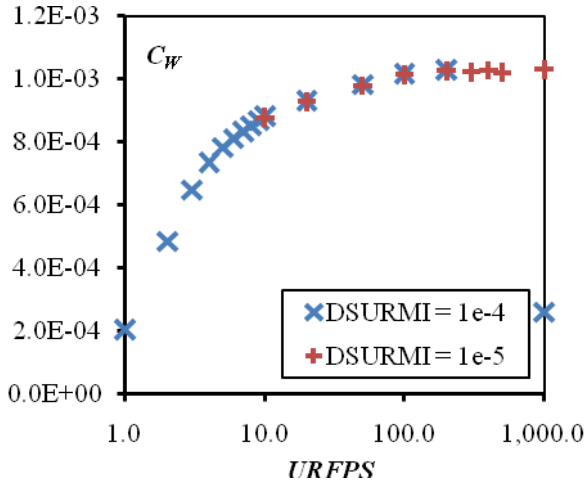

Figure G.8 Wave resistance coefficient C_W, URFPS>0, V_S=3.493 m/s, *Fn*=0.495.

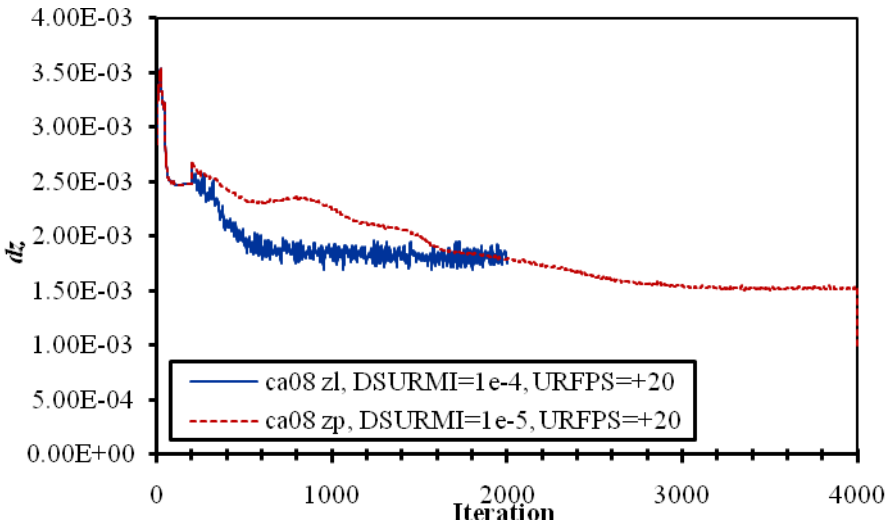

Figure G.9 Convergence history of $\overline{|\delta z|}$ for V_S=3.493 m/s, *Fn*=0.495.

From the above results we can confirm that the solution depends heavily on the values of the variables that control the execution of the algorithm. From figures G.1, G.3, G.5 and G.7 we see that $\overline{|\delta z|}$ is sensitive to changes of URFPS, both when negative and when positive. Furthermore in both areas there is a value of URFPS that minimizes $\overline{|\delta z|}$. As can be seen in Figs. G.3 and G.7 $\overline{|\delta z|}$ is also sensitive to changes of DSURMI and rather expectedly it is becoming smaller as DSURMI decreases. Unfortunately smaller values of DSURMI have the effect of slowing convergence substantially as can be seen in Tables G.1 and G.2 and Figure G.9.

The wave resistance coefficient is also sensitive to changes of URFPS and less in changes of DSURMI. With regard to URFPS, C_W seems to converge to two different values as the absolute value of URFPS becomes bigger.

Ultimately taking into account the computational time, it was decided to use in this investigation the following values: DSURMI=1e-3, URFPS=-1.